Master's Thesis:

Preparation and in vitro characterization of modified bio-degradable albumin-based nanoparticles for the efficient delivery of therapeutic drugs and genes in breast cancer applications

Sana Abbasi ©

Department of Biomedical Engineering

Faculty of Medicine

McGill University, Montreal

Supervisor: Dr. Satya Prakash

July, 2011 ©

A thesis submitted to McGill University in partial fulfillment of the Master's of Biomedical Engineering degree requirements.

ABSTRACT

Breast cancer is considered the second most commonly diagnosed type of cancer across the world. The common modes of treatment are limited by severe side-effects that hinder the efficacy of the drugs, compromise the patients' quality of life and often lead to other disorders. One of the main focuses of nanobiotechnology research is to develop novel anti-cancer drug delivery systems that improve the drug efficacy, limit harmful side effects and also allow for the delivery of developing therapeutics that are rapidly degraded in circulation, such as small interfering RNA (siRNA). Nano-carriers are helpful particularly in anti-cancer drug delivery due to the Enhanced Permeability and Retention (EPR) effect. In the current research study, we developed and investigated the use of surface modified HSA nanoparticles for the delivery of anti-cancer therapeutics in breast cancer applications. Results showed formation of modified HSA nanoparticles of sizes below 150 nm and contained a positive surface charge. The cellular uptake of the nanoparticles was higher in coated particles (average: ~70%) than uncoated particles. Furthermore, the cytotoxicity assessment of modified HSA nanoparticles suggested that empty particles are biocompatible and non-toxic to cells. Therefore, the presented PEI-enhanced and TAT-coated HSA nanoparticles form an appealing delivery system for anti-cancer therapeutics with a potential for clinical application.

RÉSUMÉ

Le cancer du sein est considéré comme le deuxième type de cancer le plus couramment diagnostiqué à travers le monde. La plupart des traitements sont characterisés par des effets secondaires nocifs qui limitent l'efficacité des médicaments, *compromettent* la qualité de vie des patients et conduisent souvent à d'autres troubles nocifs. L'un des principaux axes de recherche en nanobiotechnologie est de développer un nouveaux système de délivrance qui permet d'améliorer l'efficacité du médicament, de limiter les effets secondaires nocifs et aussi de permettre la livraison de molecules qui sont rapidement dégradées dans la circulation, tels que les petits ARN interférents (siRNA). Les nano-transporteurs sont utiles en particulier dans l'administration de médicaments anticancerigenes en raison de leur perméabilité accrue et de leur conservation (EPR). Dans l'étude de la recherche actuelle, nous avons développé et étudié l'utilisation de nanoparticules HSA à surface modifiée pour la livraison de médicaments anticancéreux dans les applications de cancer du sein. Les résultats ont montré la formation de nanoparticules HSA de tailles modifiées en dessous de 150 nm contenant une charge de surface positive. L'absorption cellulaire des nanoparticules est plus élevée dans les particules enrobées (moyenne: ~ 70%) que les particules non enrobée. Par ailleurs, l'évaluation de la cytotoxicité des nanoparticules HSA modifiées a suggéré que les particules vides sont biocompatibles et non toxiques pour les cellules. Par conséquent, les nanoparticules HSA revêtues de TAT et PEI-améliorée forment un système de prestation idéale pour les thérapies anti-cancereuses avec un potentiel d'application clinique.

ACKNOWLEDGEMENTS

I would like to graciously thank my co-authors, Arghya Paul, Afshan Khan, Wei Shao and Meenakshi Malhotra for their continuous assistance and support in conducting this research work. I am also extremely appreciative and thankful to my colleagues, Catherine Tomaro-Duchesneau, Shyamali Saha, Marc Fakhoury, Laetitia Poupoune and the rest at the Biomedical Technology and Cell Research Laboratory for being accommodating and helpful.

I am also grateful to my supervisor, Dr. Satya Prakash, for his guidance and support. I acknowledge the McGill Internal- - G. G. Harris Fellowship and the Ontario-Quebec Exchange Fellowship for financial support. I also acknowledge the research grant awarded to Dr. Satya Prakash from Canadian Institute of Health Research (CIHR), because of which this study was possible.

Finally, I would like to thank my family for their unconditional support, guidance and tolerance.

THESIS PREFACE

In accordance with the thesis preparation and submission guidelines, this thesis has been written in the form of a compilation of original research articles, presented in Chapters 3-5. Each research article consists of the following sections: Abstract, Introduction, Materials and Methods, Results, Discussion and Conclusions. A common Abstract, Introduction, Literature Review, General Discussion, Conclusions, Recommendations & Future Applications and References are included in this thesis as per the guidelines.

LIST OF ABBREVIATIONS

PEI	Poly(ethylenimine)
TAT	*Trans*-activating transcriptional activator peptide
s-TAT	Scrambled TAT sequence
HSA	Human Serum Albumin
BSA	Bovine Serum Albumin
siRNA	Small interfering RNA
ASO	Anti-sense oligonucleotides
RISC	RNA-induced silencing complex
EPR	Enhanced Permability and Retention effect
NPs	Nanoparticles
Dox	Doxorubicin
PTD	Protein transduction domain
CPPs	Cell Penetrating Peptides
PLGA	Poly(lactic-*co*-glycolic acid)
BMP-2	Bone morphogenetic protein-2
PEG	Poly(ethylene glycol)
PDI	Polydispersity index
SEM	Scanning Electron microscopy
TEM	Transmission Electron microscopy
AFM	Atomic Force microscopy
FBS	Fetal Bovine Serum
DMEM	Dulbecco's modified Eagle's Medium
DNA	Deoxy-RiboNucleic acid

M.W.	Molecular Weight
PBS	Phosphate Buffered Saline
gp60	60 kDa glycoprotein receptor
TdT	Terminal deoxynucelotidyl transferase
DAB	diaminobenzidine
FITC	Fluorescein isothiocyanate

TABLE OF CONTENTS

1.0 General Introduction

It has been estimated that approximately 12.7 million new cancer cases and 7.6 million deaths from cancer occurred in 2008. Breast cancer is considered as the second most commonly diagnosed type of cancer across the world [1]. After the diagnosis of cancer, the common modes of treatment include: surgery, radiotherapy and chemotherapy [2]. The patients have to suffer the symptoms of the disease as well as debilitating side-effects of the conventional treatment methods that compromise their quality of life. Common side-effects of cytotoxic anti-cancer drugs include neutropenia, peripheral neuropathy, hypersensitivity reactions, nausea, vomiting and diarrhea [3,4]. Specifically, doxorubicin is known to cause more serious effects: acute and late irreversible cardiotoxicity which may also lead to congestive heart failure [3].

One of the main focuses of nanobiotechnology research is to develop novel drug delivery systems that improve anti-cancer drug efficacy, limit their harmful side effects and also allow for the delivery of therapeutics that are rapidly degraded in circulation. Nano-carriers are helpful in anti-cancer drug delivery due to the Enhanced Permeability and Retention (EPR) effect [5,6]. In an active tumor, the vasculature differs from that in normal tissue as it is leaky, irregular with large gaps or fenestrations [7]. Furthermore, a poor lymphatic drainage and slow venous blood return with increased permeability of the tumor tissue results in an accumulation of nanoparticles and macromolecules (>50 kDa) within the tumor interstitium [8]. Thus, a suitable nano-carrier would be able to passively target cytotoxic anti-cancer drugs, such as doxorubicin, to tumour tissue.

In addition, small interfering RNA (siRNA) gene-silencing has shown the potential of developing into a potent cancer treatment; however, its application is limited by the highly unstable nature of siRNA. siRNA-mediated gene silencing involves post-transcriptional silencing of specific genes. [9]. siRNA interacts with a protein complex, known as RNA-induced silencing complex (RISC), and activates it. Upon activation, the RISC is directed to the target complementary strand of mRNA molecules, leading to sequence-specific cleavage of the target transcript [10]. By incorporating siRNA into nanoparticles, the gene silencing function of siRNA can be exploited to target cancer.

In this research study, we investigated the use of a biodegradable and biocompatible delivery system for anti-cancer drugs and siRNA. Human serum albumin (HSA) nanoparticles with cationic surface functionalization were developed and characterized in vitro for the enhanced delivery of anti-cancer drugs and siRNA. Surface coatings were added on the HSA nanoparticles to improve the cellular uptake of the drug-loaded nanoparticles to maximize the therapeutic efficacy of the drug.

1.1 Thesis Hypothesis

Do surface modified HSA nanoparticles enhance the delivery features of the drug and gene by increasing the stability, bioavailability and cellular uptake of the loaded therapeutics for breast cancer applications?

1.2 Research Objectives

1) To characterize and assess the efficacy of modified surface functionalized (polyethylenimine) siRNA-loaded HSA nanoparticles.

2) To investigate the potential of using polyethylenimine-coated HSA nanoparticles for the delivery of anti-cancer drugs, using doxorubicin as an example.

3) To design novel HIV 1 TAT peptide coated HSA nanoparticles for the delivery of therapeutics (siRNA) in breast cancer applications.

2.0 Literature Review

2.1 Introduction to breast cancer

Cancer is considered as one of the most pressing issues currently facing health care across the world. In 2008, there were an estimated 12.7 million new cancer cases and 7.6 million deaths due to cancer across the world [1]. As shown in Figure 1, prostate, lung/bronchus, colon/rectum cancers among men, while breast, lung/bronchus and colon/rectum cancers are the most common in women (in decreasing order) [11]. Breast cancer is the second most common diagnosed type of cancer, amounting to 1.38 million cases (10.9 % of total cases) worldwide [11]. However, the mortality rate of breast cancer has decreased in developed countries over the past decades, ranging to approximately 6-19 deaths per 100,000 [12].

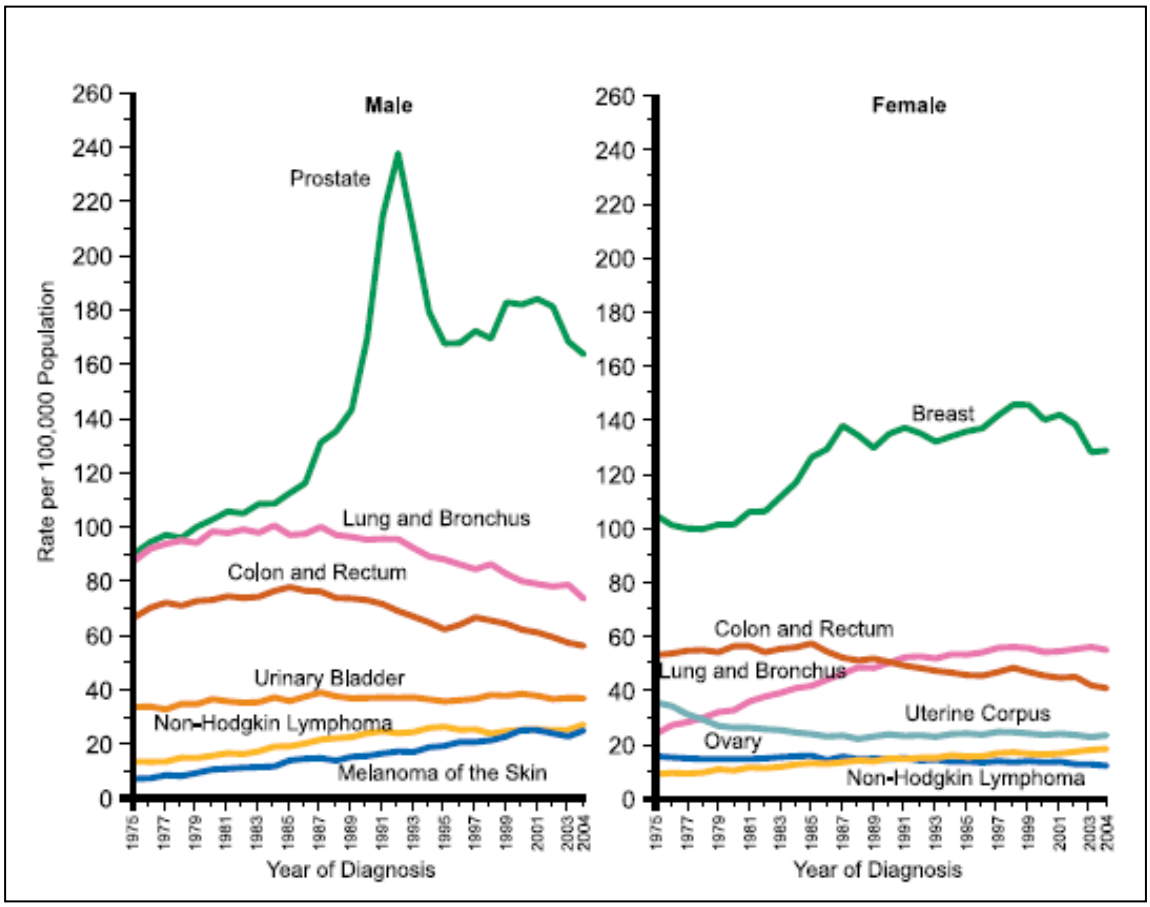

FIGURE 2.1: Annual age-adjusted incidence rates of different types of cancers from 1975 to 2004 for the U.S. standard population [11].

Breast cancer leads to the most number of deaths from cancer among women globally [11]. The decline in mortality could be because of increased awareness and improved cancer screening and treatment methods [13]. Similar to other types of cancers, breast cancer can also not be attributed to a single cause. There are several risk factors that have been found to play a role in the development of the disease, including age, reproductive history, exogenous hormone in-take, life style (alcohol consumption, diet, obesity, exercise), and genetic factors [13].

The growth of tumours is initiated by a single cancerous cell that replicates and divides at a higher rate than the surrounding healthy cells. Thus, the cancerous cell metabolizes at a higher rate, consuming more nutrients and releasing a greater amount of waste products [14]. Upon the formation of a small tumour mass, the healthy cells are deprived of an insufficient nutrient supply. The tumour mass will continue to proliferate and grow until it has completely displaced the healthy cells and reached a maximum size, beyond which it cannot grow with the existing normal nutrient and oxygen supply [14]. At this point, the tumour is at a steady state size. The cells towards the periphery of the tumour receive maximum nutrients and continue multiplying, while the cells on the inside are deprived of nutrients and proper elimination of waste products due to which they die, forming a necrotic core of the tumour. For the tumour to further grow, new vasculature must form to provide the required nutrients and removal of wastes [14].

2.2 Currently used methods for treating breast cancer and their limitations

An early diagnosis of the disease is the most important step towards its treatment. Regular clinical and self-examinations, ultrasonography and mammography are ways of detecting tumor growth in the breast. These practices together with greater public awareness of the disease have led to earlier diagnoses and a resultant decline in the breast cancer mortality rate [11,15,16]. There has been an estimated 24% of decline in mortality from breast cancer between 1990 and 2000 [17]. Biopsy, an invasive method of removing the tumor tissue for pathological examination, confirms the presence of cancerous cells. After the detection and diagnosis of breast cancer, it is classified into one of four stages, according to size, location and presence of metastasis [16]. For earlier stages of cancer, localized treatment is usually the initial mode of targeting the disease.

Localized treatment methods include surgery and radiotherapy. On the other hand, systemic therapy may also be used in combination with localized treatments for possible spread of potential tumor cells. This minimizes the chances of disseminated cancerous cells becoming a tumor at another location [18]. After the breast cancer tumor becomes metastatic, the disease cannot be "cured" or eradicated [19].

Systemic therapy, primarily, consists of two types: administration of hormones or chemotherapy. Hormone therapy is designed to target tumors that over express the estrogen receptor or progesterone receptor. On the other hand, chemotherapy is most effective against high-grade tumors that are rapidly proliferating [17,20]. Chemotherapeutics, by definition, are mostly inhibitors of proliferating cells that block different aspects of DNA synthesis or repair [18]. To do so, these compounds may be involved in the disruption of alkylation, inhibition of DNA topoisomerases, physical binding or intercalation of DNA or microtubules [21]. As the action of these chemotherapeutic agents is non-selective, it may affect healthy dividing cells as well, leading to serious adverse side effects. This lack of selectivity is one of the major limitations of anti-cancer chemotherapy. Common chemotherapeutic agents for breast cancer are anthracyclines, namely doxorubicin and epirubicin, and taxanes, including docetaxel and paclitaxel [22].

Taxanes are hydrophobic compounds that can be intravenously administered with the help of solvent-based delivery vehicles. Despite the potent anti-cancer effect of taxanes through mitotic arrest, their clinical efficacy has been hindered by toxicity caused by their solvent-based administration. The solvent-based vehicle used for paclitaxel consists of poly-ethoxylated castor oil (Cremophor® EL) and ethanol (Taxol®), CrEL-paxlitaxel. Side effects commonly associated with CrEL-paclitaxel include neutropenia, peripheral neuropathy, hypersensitivity reactions, nausea, vomiting and diarrhea [3,4]. Anthracyclines are known to cause short-term side effects, such as myelosuppression, vomiting, alopecia, and mucositis; more serious effects include acute and late irreversible cardiotoxicity which may also lead to congestive heart failure [3]. Anthracyclines lead to the generation of oxygen-based free radicals, which damage proteins, lipids and DNA molecules. The oxidative stress has shown to result in apoptosis of myocytes [23].

2.3 Upcoming strategies to treat breast cancer: using siRNA

Many researchers have been actively investigating new treatment methods in order to evade the side effects of conventional anti-cancer therapies. Drugs directed against angiogenesis in tumour development or other signalling pathways that are responsible for tumour growth are being studied [24]. In addition, efforts are being made towards developing a breast cancer vaccine that will enable T-cells to identify and eliminate tumour cells specifically [25]. Gene-based therapies are also being studied extensively in order to manipulate gene expression to suppress the growth of cancerous cells [26-28]. siRNA-based gene silencing has shown considerable promise for developing into an effective mode of treating cancers [29-32]. siRNA are about 20-25 base-pairs in length and upon entering cells, they bind and activate the RNA-induced silencing complexes (RISCs) that consist of an endoribonuclease. As illustrated in Figure 2, upon formation of the active RISCs, the siRNA strands direct the complex to the target complementary strand of mRNA and leads to the destruction of the target RNA molecule [33,34]. In this manner, the messenger RNA molecule of a particular gene can be destroyed specifically, thereby blocking protein expression of the gene of interest.

The ability of siRNA to alter gene expression is the key to employing siRNA-gene silencing in tumor cells for cancer therapy. The objective of siRNA therapy is to downregulate genes that lead to cancer malignancy and to make the tumour cells more susceptible to other modes of treatment [35]. The expression of receptor tyrosine kinases, along with other antiapoptotic genes, survival factors, growth factors, signalling molecules and genes required for cell division, can be suppressed, as detailed in Table 1. Global oncogenic transcription factors, such as Myc, or cell-type specific transcription factors may be targeted using siRNA therapy. Such selectivity would not be possible using conventional drug therapy. Furthermore, siRNA also has potential to target cancer stem cells, responsible for the recurrence of the disease, that are resistant to radio- and chemotherapy [35]. Another advantage of using siRNA gene silencing over conventional drugs is that the transporter proteins present in drug resistant tumour cells are unlikely to act upon RNA molecules. The dulation of siRNA gene silencing is dependent upon the distribution of siRNA bound to the RISCs that occurs between daughter cells as the cells

divide [35]. For rapidly dividing tumour cells, the duration of gene silencing can extend up to a week. Despite this limitation, sufficient gene silencing may have already occurred to bring about the desired tumor suppressive effect. Alternatively, continuous weekly administration of siRNA could be carried out to prolong the span of siRNA gene silencing [35]. Although siRNA-based gene silencing holds immense potential for developing into an effective anti-cancer therapy, the biggest hurdle is the unstable rapidly degradable nature of siRNA [36,37]. Many researchers have been attempting to develop a suitable delivery system for siRNA in order to protect its functional and structural integrity, while enhancing its cellular uptake [33,37].

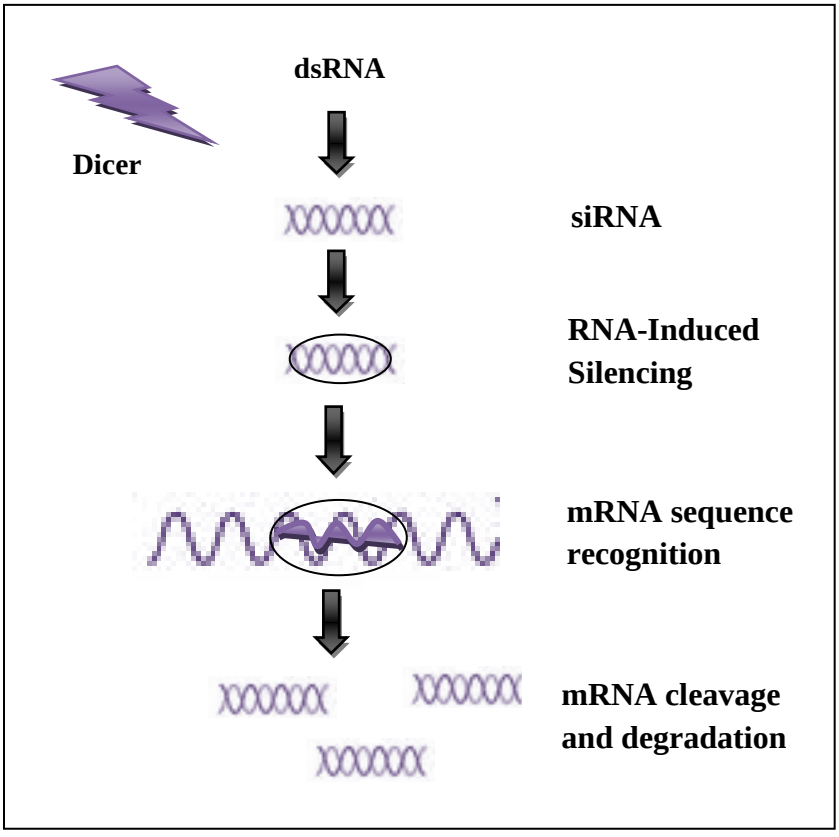

FIGURE 2.2: Schematic illustration of post-transcriptional gene silencing by siRNA that can be used for gene silencing in breast cancer [38].

TABLE 2.1: Examples of genes that have been targeted by siRNA gene silencing in breast cancer [39].

Target protein function	Gene(s) silenced	In vitro	In vivo	References
Estrogen receptor cofactor	NFAT3	✓	-	[40]
Estrogen induced protein	GREB2	✓	-	[41]
Receptor tyrosine kinase	ERBB2	✓	-	[42]
Cytosolic serine-threonine kinase	Raf-1	✓	✓	[43]
Rho GTPases	RhoA, RhoC	✓	✓	[44]
Antiapoptotic protein	XIAP	✓	✓	[45,46]
P-glycoprotein	MDR1	✓	-	[47,48]
Double strand break repair protein	RAD21	✓	-	[49]
Urokinase plasminogen activator	UPA	✓	-	[39]
Laminin adhesion receptor	α6β4 integrin	✓	-	[39,50]

2.4 Nanotechnology and breast cancer

The cancer-based research achievements over the past few decades have not resulted in similar advances in clinical applications. This is largely due to the lack of selectivity of anti-cancer therapeutics, which leads to toxicity of healthy cells. The survival rate of cancer patients and their quality of life is determined by the targeting ability of their cancer treatment [14]. A promising avenue that may help address this issue is of nanotechnology, which is an increasingly progressive field that promises innovative solutions for the treatment of numerous diseases. By definition, nanotechnological devices need to be man-made and of 1-1000 nm in at least one dimension [51]. Nano-technologies used for cancer diagnostics or therapy include nanovectors, designed to deliver therapeutics, and nano magnetic resonance imaging contrast agents [51]. The various nanovectors include nanoparticles, liposomes, quantum dots, carbon nanotubes, micelles and dendrimers [52]. An ideal therapeutic delivery system would be specific for

only tumour cells and be able to overcome barriers, such as the cell membrane and the blood-brain barrier, that stop it from reaching its target [51].

2.5 Polymeric nanoparticles- carriers for anti-cancer therapeutics

Various nanoparticle-based systems are being studied to achieve these goals of improving the efficacy of the therapeutics and also limiting harmful side effects of various cancer drugs. Polymeric nanoparticles may be defined as sub-cellular colloidal entities, composed of natural or synthetic polymers [53]. One of the objectives of a nanoparticle-based drug delivery system is targeted delivery to help reduce side-effects of various harmful drugs by decreasing their systemic levels, and increasing the drug availability at the target site. Also, they may help to stabilize the compound to be delivered and increase their half-life by protecting the therapeutic molecule from hydrolysis or breakdown, solubilize certain therapeutics for intravascular administration, and may also allow for controlled delivery [53,54]. Nanoparticles may carry the therapeutic compound by dissolving, encapsulating or entrapping it within the nanoparticles, and on the other hand, by adsorbing or chemically attaching the therapeutic compound to its surface. The cargo being delivered may consist of drugs, peptides or proteins, or gene-based compounds [53,54].

Due to their sub-cellular sizes, nanoparticles can easily pass through the thin capillary beds into tissues, allowing delivery of the therapeutic compound to different tissues of the body [55]. As nanoparticles can be taken up by the cells, the therapeutics they deliver may have an intracellular target, such as the mitochondria, nucleus, or the cytoplasm [55]. Studies have shown that nanoparticles can be taken up by cells through different endocytic pathways. These pathways may include pinocytosis, phagocytosis or receptor-mediated endocytosis. Panyam and Labhasetwar studied the cellular uptake of Poly-(D,L-lactide-*co*-glycolide), PLGA, nanoparticles in vitro, using human vascular smooth muscle cells. They illustrated that nanoparticles are endocytosed by cells, at the earliest after 1 min. of incubation, showing an increase in uptake with incubation time of nanoparticles [56,57]. Upon removal of nanoparticles from the media, approximately 65% of the internalized nanoparticles underwent exocytosis and were expelled by the cells into the medium within 30 min., suggesting that there is a concentration-dependent

endocytic process [56]. The surface properties of the nanoparticles play a crucial role in determining the mechanism of their intracellular uptake, the cytosolic target and the release of the therapeutic cargo [58]. Followed by internalization, approximately 15% of the nanoparticles remain in the cytosol, whereas a significant amount is removed from the cell by exocytosis [58]. Within the cytosol, the nanoparticles exhibit a sustained release of the therapeutic compound; the rate of degradation of the polymer that the nanoparticles are comprised of would depend upon the nature of the polymer [56].

Cellular uptake of nanoparticles has also shown to be dependent upon the uniform distribution of particles and particle-size. It has been illustrated that the transfection efficiency of nanoparticles loaded with DNA that are smaller than 100 nm is 27 times greater than those larger (~200 nm) [28]. Similarly, Desai et al. illustrated that particles of 100 nm in size have a significantly greater number and total mass uptake by intestinal tissue as compared to bigger particles (1000 nm) [59]. Another parameter that may play a role in the cytosolic delivery of the therapeutic agent is the molecular weight of the polymer [56,57].

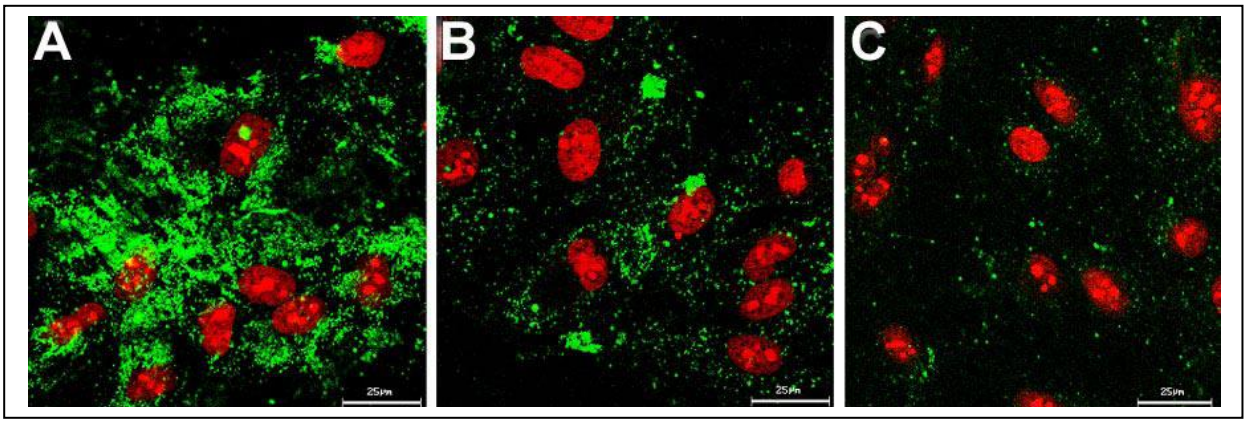

FIGURE 2.3: Cellular uptake of Human serum albumin (HSA) nanoparticles via cavaloae and clathrin-mediated endocytosis. Confocal images after HSA nanoparticles are incubated with cells for 1 hr: (A) without endocytosis inhibitor; (B) with chlorpromazime; (C) filipin [60].

Intracellular delivery of therapeutics by nanoparticles is especially important when the target of the drug, or therapeutic agent, is within the cell. The target may be present in the cytoplasm, nucleus, mitochondria or other intracellular compartments. This form of delivery protects degradation of proteins and nucleic acids by proteases and nucleases,

respectively, or other enzymatic degradation. In addition, cytosolic delivery helps overcome the problem of drug efflux from the cell by efflux transporters, such as the human multidrug-resistance gene MDR1 transporter, P-glycoprotein [61].

It is important to assess the biocompatibility and biodegradability of the polymer or material that the nanoparticles are composed of, because the remnants of the nanoparticles must be degraded and metabolized after unloading the cargo. Ideally, the nanoparticles should be broken down into non-toxic material that is easily cleared from circulation in order to avoid any toxic effects [62]. The material being used to synthesize the particles should also be chemically inert and free from impurities. Nanoparticles are cleared from circulation based upon their size. Sizes < 30 nm are removed by renal filtration and larger particles are taken up by the mononuclear phagocytic system [55].

Various polymers, including synthetic and those found naturally, may be used to make biodegradable nanoparticles. The synthetic polymers would include polylactide-polyglycolide copolymers, polyacrylates and polycaprolactones, where as albumin, gelatin, collagen and chitosan are naturally occurring polymers [63]. Synthetic polymers, in general, have an advantage over natural polymers, in being able to provide a more sustained release of the therapeutic compound from a few days till weeks in some cases. However, the synthetic polymers may be limited by the presence of organic solvents and impurities that need to be removed [64].

TABLE 2.2: Main advantages and disadvantages of various polymers used for the synthesis of nanoparticles [65,66].

Polymers used for NP	Advantages	Disadvantages
PLGA/PLA	Biodegradable, biocompatible, non-toxic	Hydrophobic polymer – unstable colloidal carrier, coating the particles is difficult and expensive.
Poly ε-caprolactone	Biodegradable, biocompatible, stable	--
Chitosan	Biocompatible, biodegradable, hydrophilic, adhesive to mucosa	Aggregation may occur during synthesis
HSA	Biodegradable, non-toxic, non-antigenic. Allows for electrostatic adsorption of positively charged species	Large-scale manufacture may be an issue

2.6 Nanoparticles can be used to enhance drug permeability and retention

Nanoparticles are particularly effective in anti-cancer drug delivery due to the Enhanced Permeability and Retention (EPR) effect [5,6]. In an active tumor, the vasculature differs from that in normal tissue as the vessels have a larger size, greater density and are more heterogenously distributed. The tumour vasculature is more leaky, irregular with large gaps or fenestrations [7]. However, normal tissue vasculature has a tight endothelium [66]. Furthermore, a poor lymphatic drainage and slow venous blood return alongside increased permeability of the tumor tissue results in an accumulation of nanoparticles and macromolecules (>50 kDa) within the tumor interstitium, as shown in Figure 4 [8]. Therefore, the EPR effect facilitates the extravasation of nanoparticles into the tumour tissue, thereby increasing the drug concentration within the tumour tissue [67,68]. Previous research has shown that nanoparticles can deliver drugs to tumor tissue with local concentrations (at least 10-fold) higher than with the same dosage of free drug administration. The drug concentrations in tumor tissue were also significantly higher than in normal tissue [67-70].

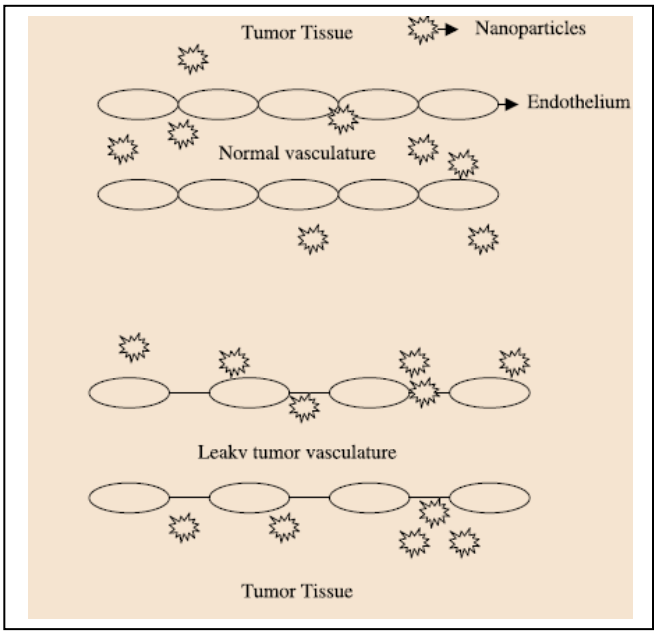

FIGURE 2.4: The top illustration depicts the lack of permeability of the normal vasculature, preventing the extravasation of nanoparticles into the tumour interstitium. The lower part shows the accumulation of nanoparticles within the tumour tissue due to large gaps in the tumour vasculature, resulting in the EPR effect [66].

2.7 Introduction to albumin-based nanoparticles

Albumin is synthesized in the liver and is released into the blood; it forms the most abundant plasma protein (35-50 grams/L human serum) [71]. Figure 2.5 illustrates the structure of Human Serum Albumin (HSA), the smallest blood plasma protein [71]. HSA acts as a carrier and solubilizing protein in blood. It binds bilirubin, the breakdown product of heme, different therapeutic drugs such as penicillin and sulphonamides, and various metal ions. Albumin is soluble in both water and ethanol, two possible solvents for intravenous delivery [72].

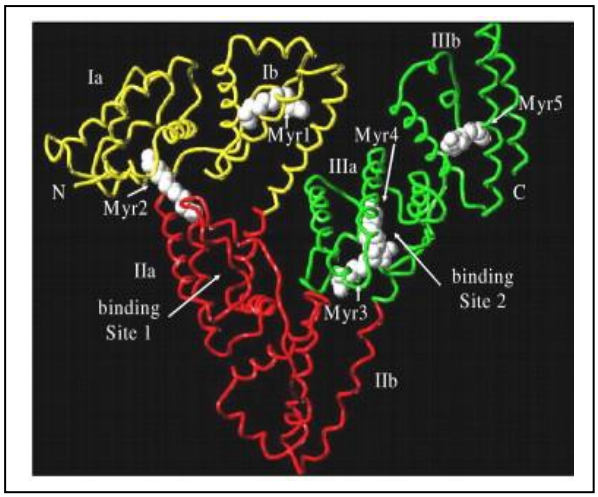

FIGURE 2.5: Three-dimensional structure of Human Serum Albumin, created by X-ray structure analysis [73].

Albumin is an acidic protein, which stays stable in pH range 4-9, and can withstand temperatures up to 60 °C. Albumin overcomes the problems of immunogenicity and toxicity that other drug delivery systems commonly face. Since albumin is found in the body naturally in such abundance, it is easily degraded and metabolized [71]. Clinical trials have suggested that Abraxane®, paclitaxel bound to a human serum albumin nanoparticle, is an effective way of delivering this drug [72].

Currently, the delivery of other taxanes using albumin nanoparticles is being studied for the treatment of hormone refractory prostate cancer [72]. Albumin binds with the albumin receptor gp60 and crosses the endothelium into extravascular space through a process known as transcytosis. Since tumour tissue has higher metabolism as compared

to normal cells, plasma proteins are more actively transported into these cells. Thus, Abraxane® is carried and accumulated within tumour tissue, making the anti-cancer drug more effective [72].

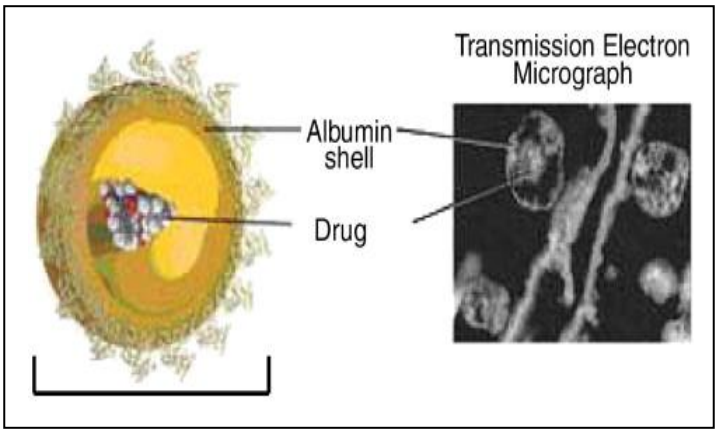

FIGURE 2.6: Model of Abraxane®, albumin-bound paclitaxel nanoparticle; Transmission electron micrograph on the right. Abraxane® is 130 nm in size [73].

2.8 Potentials of albumin-based nanoparticles

Albumin nanoparticles have a wide range of applications in the delivery of therapeutic agents. Abraxane® is a commercially available albumin-based nanoparticle with encapsulated paclitaxel, formed by passing the aqueous solution of the drug and HSA through a spray jet. This results in the formation of HSA nanoparticles in the size range of 100-200 nm, as shown in Figure 2.6. After preclinical and clinical investigation, Abraxane® was approved by FDA for the treatment of metastatic breast cancer after combination therapy has been unsuccessful [73]. Abraxane® showed higher accumulation of Paclitaxel as compared to free drug administration of the same concentration [74]. Most importantly, Abraxane® does not require the use of the hydrophobic solvent, Cremophor EL. Furthermore, hypersensitivity has not been reported after the use of Abraxane® by patients and pre-medication is not necessary [75,76]. Clinical studies have shown that the serious side-effects, such as neutropenia and neuropathy due to axonal degeneration, were lower with the use of Abraxane® than with Paclitaxel administered using Cremophor EL [75,76]. These promising advances with HSA-based nanoparticles strongly support the need for further studying and developing this technology.

Chemotherapeutic agents, doxorubicin, 5-Fluorouracil and noscapine, were encapsulated into HSA nanoparticles for drug delivery to cancer cells. Results were encouraging as they suggested an increase in drug efficacy with nanoparticle-based delivery as compared to free drug. Preclinial studies need to be carried out to examine the effect of using HSA nanoparticle-based delivery for these chemotherapeutic drugs on toxicity of healthy cells [77-79].

In addition, aspirin was also encapsulated into HSA nanoparticles. Due to their small size and biocompatibility, HSA nanoparticles can be used in sensitive regions, such as the eye, as minimal irritation will be caused. Thus, aspirin-loaded HSA nanoparticles were characterized by using the coacervation method to synthesize them for various potential applications, such as intra-articular therapy in arthritis or diabetic retinopathy [80,81].

Albumin-based nanoparticles have also been studied to deliver proteins [82]. Bovine serum albumin (BSA) was used to encapsulate the osteoinductive growth factor, bone morphogenetic protein-2 (BMP-2), which induces bone formation. The BSA nanoparticles in this study were coated with polyethylenimine (PEI), which reduced the initial burst release of BMP-2 and allowed a more prolonged and sustained availability of BMP-2 at the site of action. A more recent study modified PEI-BSA nanoparticles by attaching poly(ethylene glycol) (PEG) to PEI. PEI-PEG coated BSA nanoparticles illustrated a higher de novo bone formation in rats than PEI-coated nanoparticles [83]. More recently, the co-encapsulation of the vascular endothelial growth factor and angiopoietin-1 was carried out using HSA nanoparticles for improved mitotic and antiapoptotic effects on vascular endothelial cells [81].

HSA nanoparticles have shown potential of developing into efficient, non-toxic, non-viral vectors for gene delivery [60,81,84]. Nanoparticles have gained interest as gene carriers due to their low risk of immunogenicity, pathogenicity and oncogenicity, ease of preparation and little limitation on the size of the gene to be transferred [85]. Steinhauser et al. investigated the delivery of plasmids, expressing small hairpin RNAs designed to target polo-like kinase 1, for inhibition of cancer progression [84]. HSA-based nanoparticles have also been used as a delivery system for anti-sense oligonucleotides (ASOs). The studies show that the oligonucleotides are successfully loaded into the

nanoparticles without being degraded, and their hybridizing ability to complementary oligonucleotides is retained. The incorporation of the ASO into the nanoparticles showed to be dependent upon pH and the ionic environment of the HSA solution. Some ASO was also reported to be adsorbed at the surface, while the rest was inside the nanoparticles. The ASO at the surface was not protected from enzymatic degradation [86].

2.9 Special features of albumin-based nanoaparticles: Excellent place for surface functionalization for enhanced delivery features

Surface of nanoparticles may be modified to achieve the following objective: reduce the levels of opsonization of nanoparticles and augment the cellular uptake of nanoparticles [87]. In order to help increase the bioavailability of nanoparticles, surface modifications can be carried out by adsorbing or covalently bonding compounds. Compounds such as polyethylene oxide (PEO) or polyethylene glycol (PEG), have been employed to adsorb and coat the surface of the polymeric nanoparticles, forming a hydrophilic covering that helps decrease their rate of opsonization by the reticulo-endothelial system [88,89]. The outer layer of PEG provides steric hindrance and prevents the plasma proteins from attaching to nanoparticle, thereby disallowing the initiation of opsonization [89].

In addition, a neutrally charged surface does not show tendency of interacting with cell membranes, while charged groups found on nanoparticles are actively involved in nanomaterial-cell interaction [90]. Cho et al. found in their study of cellular internalization of gold nanoparticles that positively charged particles demonstrate greater adherence to the cell membrane and are thus taken up by the cells more than negatively and neutrally charged nanoparticles, as depicted in Figure 7 [91]. Cationic nanoparticles are shown to bind the negatively charged functional groups, such as sialic acid, found on cell surfaces and initiate transcytosis [90]. Due to the highly efficient transfection property of positively charged nanoparticles, many nanoparticle-based drug and gene delivery systems are positively charged. A variety of cationic molecules, such as poly(ethylenimine) (PEI), poly(L-lysine) and PAMAM dendrimers, have been used to form the outer layer of nanoparticles [65,90].

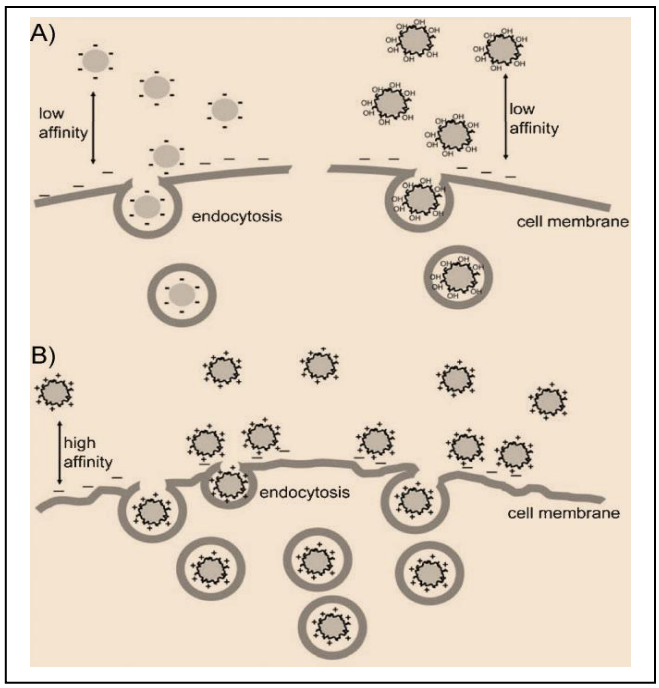

FIGURE 2.7: Schematic illustration of the effect nanoparticle surface charge has on cellular uptake [90]. (A) Negatively charged nanoparticles had a low affinity towards the cell membrane, resulting in low cellular uptake. (B) Positively charged nanoparticles adhere to the cell membrane, leading to a higher rate of endocytosis.

Ligands, such as thiamine [92] or transferrin [93] may also be conjugated with nanoparticles to enhance cellular uptake. Thiamine-conjugated nanoparticles showed that due to the addition of this ligand onto the nanoparticle surface, association of the nanoparticle with the BBB thiamine transporter was facilitated [92]. This association could then further lead to an increased transport of the nanoparticles across the BBB. Similarly, paclitaxel-loaded nanoparticles conjugated with transferrin (Tf) exhibited higher efficacy of the drug on murine models of prostate cancer [93]. The IC_{50} of paclitaxel administered with Tf-conjugated nanoparticles was approximately 5-fold lower than with unconjugated nanoparticles.

In order to facilitate the cellular uptake of nanoparticles, several coatings may be added on the nanoparticle surface. A great amount of research has been carried out to study the use of peptides that enhance cell adhesion and have the ability to penetrate eukaryotic cell plasma membrane [94]. These peptides are also known as cell penetrating peptides (CPPs) and are capable of traversing the cell membrane; thus, CPPs can be used to enhance the transport of peptides, drug molecules and genes. One such protein is the

trans-activating transcriptional activator (TAT) protein, found in HIV-I [95]. Protein transduction domains (PTDs) are the regions found within the structure of proteins and peptides that enable these molecules to easily penetrate the cell membrane by a process that is receptor, transporter and endocytosis-independent [96]. Some studies suggest that CPPs may be involved in targeting the lipid layer directly, through promoting the reorganization of the membrane lipids [96]. The PTD of the TAT protein consists of 10 residues (47-57) which include mostly basic (arginine and lysine) amino acids; the domain also conforms into an alpha helix shape [97]. TAT was conjugated onto the surface of PLGA-based nanoparticles for the delivery of Protease inhibitors across the blood brain barrier to the central nervous system [98]. Results showed a 7-fold greater PI level in the brain when administered with TAT-conjugated nanoparticles than with unconjugated nanoparticles [98].

2.10 Potential and limitations of nanoparticles: drug delivery

Various kinds of nanoparticles have been investigated for the delivery of doxorubicin, a potent anti-cancer agent, to avoid the harmful side-effects caused by it [66]. Firstly, Janes et al. showed the feasibility of using chitosan nanoparticles for the delivery of doxorubicin [99]. Results suggested that the encapsulated doxorubicin remained active. PEGylated PLGA nanoparticles seem promising as a delivery system for doxorubicin. The efficacy of doxorubicin was not decreased by its encapsulation in nanoparticles; doxorubicin delivered with nanoparticles resulted in lower pathological changes in animals as compared to free doxorubicin [100].

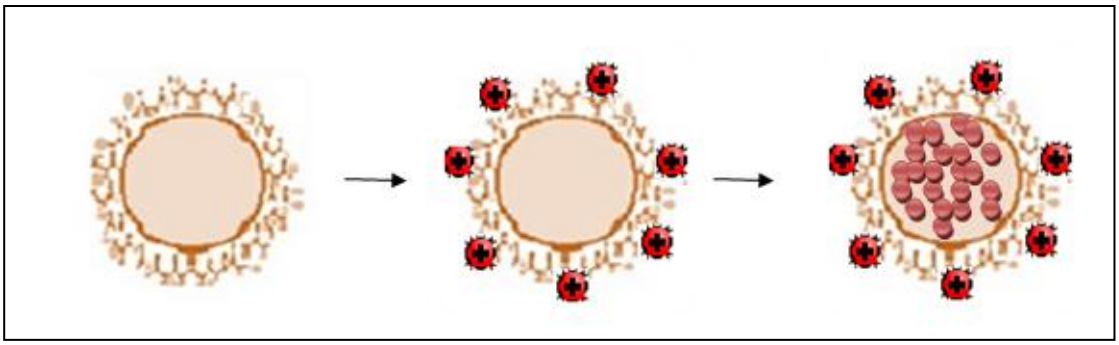

FIGURE 2.8: Encapsulation of doxorubicin inside a nanoparticle with a cationic polymer coating.

Lastly, doxorubicin was encapsulated into HSA nanoparticles and their anti-cancer effects were evaluated in vitro on two neuroblastoma cell lines (UKF-NB3; IMR 32) [101]. The drug loading of doxorubicin into HSA nanoparticles was optimized and a standard protocol was established [77]. Results showed that the IC_{50} values were significantly lower when dox was delivered with HSA nanoparticles. This also suggests that loading doxorubicin to HSA does not compromise the anti-cancer activity of doxorubicin [101]. Although studies using different kinds of nanoparticles have shown encouraging results, there is still a need for an improved biocompatible delivery system that can be made targeted to different kinds of tumours.

2.11 Potential and limitations of nanoparticles in siRNA delivery

In order to benefit from the upcoming siRNA-based gene silencing in the fight against cancer, it is imperative to design a delivery system that can both protect the siRNA and facilitate its cellular uptake. The negatively charged siRNA easily form complexes with cationic polymers that form nanoparticle-based carriers [102]. Chitosan nanoparticles have been used to deliver siRNA in vivo; results have shown effective and safe siRNA delivery via intranasal and intravenous routes [29,102,103]. PEI-based nanoparticles have also shown increased cellular uptake of siRNA. In vivo administration of siRNA using PEI-based nanooparticles resulted in 80% decrease in the target gene expression; however cytotoxicity was a concern [32]. Additionally, PLGA, PLA, dendrimers, and magnetic iron oxide nanoparticles have also been used to study the encapsulation and delivery of siRNA [29,31,39,46,102,104-106].

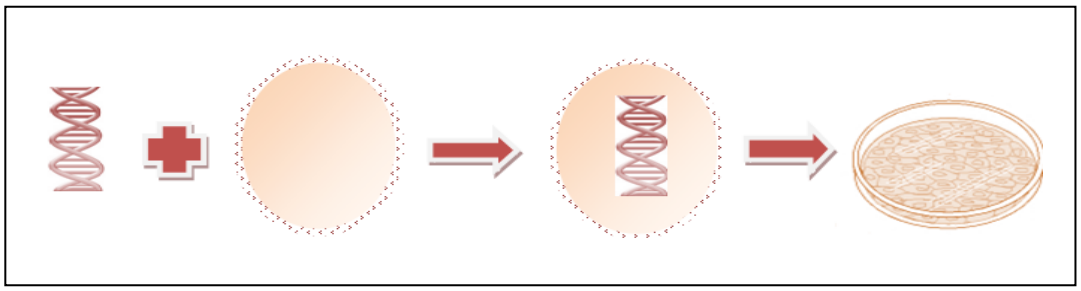

FIGURE 2.9: Schematic figure depicting the encapsulation of siRNA into a nanoparticle designed for cellular transfection.

2.12 Summary

In summary, published literature suggests that HSA nanoparticles in general hold excellent potential in breast cancer drug and siRNA delivery. However, suitable formulation is yet to be found. Designing such a formulation based on HSA nanoparticle surface modifications in breast cancer applications is the goal of this thesis.

2.13 Research Signficance

Although cancer treatments have improved a great deal over the past decades, there is still an urgent need to reduce the toxicity and related side-effects that most conventional anti-cancer drugs, such as doxorubicin cause. Secondly, upcoming anti-cancer therapeutics, such as siRNA gene-silencing, cannot be clinically used due to their unstable nature and low cellular uptake. In the current study, PEI-coated HSA nanoparticles have been prepared and characterized in vitro for the delivery of drug (doxorubicin) molecules as well as siRNA for effective anti-cancer treatment. Additionally, a novel TAT-enhanced HSA nanoparticle delivery system has been developed and characterized in vitro for increased efficacy of siRNA due to the surface adsorbed cell penetrating peptide, TAT. Using a cationic polymer (PEI) or a cell-penetrating peptide (TAT) to coat HSA nanoparticles increases the cellular uptake of HSA nanoparticles, leading to greater internalization and thus higher effectiveness of the anti-cancer therapeutic. These modified HSA-based nanoparticle delivery systems will provide a carrier for unstable anti-cancer therapeutic, such as siRNA and reduce the systemic toxicity of anti-cancer drug such as doxorubicin. The findings of this study will set a platform for further pre-clinical investigations of the suitability and benefit of the developed HSA-based nanoparticle delivery systems. In this manner, the results obtained in this study could eventually contribute towards an improved method of anti-cancer drug delivery; thereby, the quality of life of cancer patients, their survival rate and time span may be improved.

Preface for Chapters 3, 4 and 5

Chapters 3, 4 and 5 present the results obtained during this research project. Chapter 3 presents the preparation and characterization of polyethylenimine (PEI)-coated HSA nanoparticles. Furthermore, the ability of the developed nanoparticles to protect and deliver siRNA in breast cancer applications is investigated. Chapter 4 furthers the study in Chapter 3 by examining the use of PEI-coated HSA nanoparticles for anti-cancer drug (doxorubicin) delivery. The efficacy of PEI-coated HSA nanoparticle-based drug delivery is compared to free drug administration. Chapter 5 puts forward another method of enhancing the efficacy of HSA nanoparticles by developing a novel HIV-1 TAT peptide surface functionalized HSA nanoparticle delivery system for anti-cancer therapeutics. In particular, the protection and delivery of siRNA is examined.

Research Articles Presented in the Thesis Chapters 3, 4 and 5:

1) **Abbasi S**, Paul A, Prakash* S. (2011) "Investigation of siRNA-Loaded Polyethylenimine- Coated Human Serum Albumin Nanoparticle Complexes for the Treatment of Breast Cancer." Cell Biochemistry and Biophysics.

2) **Abbasi S**, Paul A, Shao W, Khan A, Prakash* S. (2011) "Cationic albumin nanoparticles for enhanced drug delivery to treat breast cancer: preparation and *in vitro* assessment." Submitted to Journal of Drug Delivery.

3) **Abbasi S**, Paul A, Khan A, Shao W, Malhotra M, Prakash* S. (2011) "HIV-1 TAT peptide surface functionalized albumin nanoparticles for improved gene delivery: optimization of *in vitro* transfection conditions to target breast cancer." 2011. To be submitted to Journal of Nanomaterials.

Contribution of Authors:

In the research articles presented in Chapters 3, 4 and 5, I am the first author and was responsible for the research design, experimental procedures, data collection and analysis. All co-authors contributed by helping me at various stages of the research work. The research project was conducted under the supervision of the Principial Investigator, Dr. Satya Prakash, who is also the corresponding author for all manuscripts and abstracts.

Contribution related to the current research, not included in the thesis:

Abstract:

Abbasi S, Arghya P, Afshan K, Prakash***** S. "Delivery Using Biodegradable Nanoparticles for Breast Cancer Therapy." TechConnect World 2011, Boston.

During the completion of M. Eng studies, the author was able to contribute to the following that are not included in the thesis.

Research Articles:

1) Khan A**,** Paul A, **Abbasi S**, Prakash* S. (2011) "Mitotic and antiapoptotic effects of nanoparticles coencapsulating human VEGF and human angiopoietin 1 on vascular endothelial cells." International Jounral of Nanomedicine.

2) Paul A, Binsalamah Z, Khan A A**, Abbasi S**, Cynthia B. Elias, Dominique Shum-Tim, Satya Prakash* (2011). A novel nanobiohybrid complex of recombinant baculovirus and Tat/DNA nanoparticles for efficient gene delivery: implication in myocardial infarction therapy using *Ang-1* transgene. Biomaterials (in press).

3) Paul A, Shao W, **Abbasi S**, Binsalamah Z, Shum-Tim D, Prakash* S. (2011) PAMAM dendrimer-baculovirus hybridized nanocomplex for adipose stem cell based gene therapy: functional assessment in myocardial therapy using PEG surface functionalized microcapsule formulation. Molecular Pharmaceutics (submitted).

4) Shao W, Paul A, **Abbasi S**, Chahal P.S., Mena J., Montes J, Kamen A, Prakash* S. (2011) Development of a novel nanovector for efficient siRNA delivery using PEI-coated Adeno Associate Viral like Particles: implications in breast cancer therapy. To be submitted to International Journal of Nanomedicine.

5) Coussa-Charley M, Rodes L, Paul A, Fakhoury M, Al-Salami H, **Abbasi S**, Khan A. A, Prakash* S. (2011) A novel continuous gut adhesion model using a packed bed bioreactor. To be submitted to *Biotechnology Research International*.

6) Coussa-Charley M, Rodes L, Paul A, Fakhoury M, Al-Salami H, **Abbasi S**, Khan A. A, Prakash* S. (2011) Investigation of the effect of *Lactobacillus* probiotic strain addition on the intestinal microflora immobilized on a novel continuous gut adhesion model. To be submitted to *Journal of Biologics: Targets and Therapy*.

Review Article:

Paul A, **Abbasi S,** Shum-Tim D, Prakash S*. (2010) "Nano- and Biotechnological Applications in Current and Future Generation of Cardiovascular Stents." Current Nanoscience.

Prakash S, Malhotra M, Shao W, Tomaro-Duchesneau C, Abbasi S. (2011) "Polymeric nanohybrids and functionalized carbon nanotubes as drug delivery carriers for cancer therapy." Advanced Drug Delivery Reviews.

Abstracts:

Abbasi S, Paul A, Shum-Tim D, Prakash S. (2010) "Stent-based Gene Therapy Using Nanoparticles to Inhibit Re-stenosis." Invited Plenary speakers Nanotech Conference 4th MPA, Portugal.

Paul A, Cantor A, **Abbasi S**, Khan A, Shum-Tim D, Prakash S. (2010) Biocompatible Polymeric Microcapsules: A Novel Delivery System for Efficient Myocardial Delivery of Human Mesenchymal Stem-cells. Canadian Cardiovascular Congress, Montreal.

CHAPTER 3

Research Article

Investigation of siRNA loaded polyethylenimine-coated human serum albumin nanoparticle complexes for the treatment of breast cancer

Sana Abbasi[1], Arghya Paul[1], Satya Prakash[1,2]*

[1]Biomedical Technology and Cell Therapy Research Laboratory, Department of Biomedical Engineering

[2]Artificial Cells and Organs Research Centre,

Faculty of Medicine, McGill University,

3775 University Street, Montreal, Quebec, H3A 2B4, Canada.

***corresponding author: Dr. Satya Prakash**

Preface:

The current chapter investigates the potential of using modified polyethylenimine (PEI)-coated HSA nanoparticles as a delivery system for siRNA for breast cancer applications. In order to characterize the PEI-coated HSA nanoparticles, various parameters were studied, such as PEI amount, HSA concentration and pH level. To ensure better scope for clinical application, cytotoxicity of the nanoparticle was optimized by using varied amounts of PEI of two different molecular weights. Results illustrating efficient transfection, retention of siRNA function and low cytotoxicity of the delivery system, it holds promise as a non-viral gene vector.

ABSTRACT

Small interfering RNA (siRNA) molecules have great potential for developing into a future therapy for breast cancer. In order to overcome the issues related to rapid degradation and low transfection of naked siRNA, polyethylenimine (PEI)-coated human serum albumin (HSA) nanoparticles have been characterized and studied here for efficient siRNA delivery to the MCF-7 breast cancer cell line. The optimized nanoparticles were ~90 nm in size, carrying a surface charge of ~+26 mV and a polydispersity index (PDI) below ~0.25. The shape and morphology of the particles was studied using electron microscopy. A cytotoxicity assessment of the nanoparticles showed no correlation of cytotoxicity with HSA concentration, while using high molecular weight PEI (MW of 70kDa against 25kDa) showed higher cytotoxicity. The optimal transfection achieved of fluorescin-tagged siRNA loaded into PEI-coated HSA nanoparticles was ~61.66 $\pm$ 6.8 %, prepared with 6.25 µg of PEI (25kDa) added per mg of HSA and 20 mg/ml HSA, indicating that this non-viral vector may serve as a promising gene delivery system.

Keywords: nanoparticles, nanomedicine, breast cancer, gene silencing, albumin, nanobiotechnology

INTRODUCTION

Deaths from cancer worldwide are projected to continue rising, with an estimated 12 million deaths in 2030 [11]. Breast cancer leads to the most number of deaths globally among women [11,107] and thus, various kinds of therapies are being devised to fight breast cancer. Small interfering RNA (siRNA) has shown potential for developing into an effective cancer therapeutic [29-32]. siRNA are about 20-25 base-pairs in length and upon entering cells, they form RNA-induced silencing complexes (RISCs) that consist of an endoribonuclease. Upon formation of the RISCs, the siRNA strands direct the complex to the target complementary strand of RNA molecules, leading to destruction of the target RNA molecule [33,34]. In this manner, the messenger RNA molecule of a particular gene can be destroyed specifically, thereby blocking protein expression of the gene. This ability of siRNA to alter gene expression is the key to employing siRNA gene-silencing in tumor cells for cancer therapy. However, therapeutic applications of siRNA are limited by their unstable nature and poor cellular uptake [36,37]. The introduction of a nanoparticle-based delivery system could overcome these problems that siRNA gene silencing therapy is currently facing.

Nanoparticle-based delivery systems can be used to provide an increased circulation period in serum and aid in cellular internalization of the siRNA [102]. Polymeric nanoparticles and liposomes can be defined as sub-cellular colloidal particles that entrap drug molecules, proteins or nucleic acids [108,109]. Polymeric nanoparticles hold an advantage over liposomal nano-carriers in terms of stability in physiological media and safety [102]. Due to the sub-cellular size of nanoparticles, they can easily pass through the thin capillary beds into tissues, allowing delivery of the therapeutic compound to different tissues of the body [110]. As nanoparticles may be taken up by the cells, the therapeutics they deliver could have an intracellular target, such as the mitochondria, nucleus, or the cytoplasm [111].

It is of vital importance to choose a biocompatible, biodegradable, non-toxic and non-immunogenic material to synthesize the nanoparticles. Colloidal nanoparticles composed of Human Serum Albumin (HSA) exhibit these properties, as albumin is found in the blood naturally in great abundance [73]. Albumin is synthesized in the liver and is

released into the blood. Albumin is an acidic protein, which stays stable in pH range 4-9, and can withstand temperatures up to 60 °C [73]. Unlike most studies that have been carried out using HSA-based nanoparticles, this study does not use glutaraldehyde as a cross-linker due to its high toxicity, which may raise a concern in vivo. Polyethylenimine (PEI), a cationic polymer, has been used to coat the HSA nanoparticles [112]. This is the first time to our knowledge that PEI-coated HSA nanoparticles are being employed to deliver siRNA.

For cancer therapy, nanoparticle-based delivery systems take advantage of the 'enhanced permeability and retention effect' (EPR), which results in an accumulation of particles within the tumor interstitium. Thus, the deposition of the therapeutic molecule within the tumor is increased. The EPR occurs due to dysfunctional lymphatic clearance and increased permeability of the tumor tissue, allowing the retention of colloidal particles or macromolecules of > 50 kDa [113,114].

In the present study, siRNA-incorporated delivery system was developed as a potential therapy for breast cancer. In order to characterize the PEI-coated HSA nanoparticles, various parameters were studied, such as PEI amount, HSA concentration and pH level. To ensure better scope for clinical application, cytotoxicity of the nanoparticle was optimized by using varied amounts of PEI of two different molecular weights. Results illustrating efficient transfection, retention of siRNA function and low cytotoxicity of the delivery system, it holds promise as a non-viral gene vector.

MATERIALS AND METHODS

Materials

Human serum albumin (HSA Fraction V, purity 96-99 %) and branched polyethylenimine (PEI) (M_W ~25,000) were purchased from Sigma Aldrich (ON, Canada). High molecular weight (MW) PEI (30% Aqueous, ~70,000 Da) was purchased from Polysciences Inc. (PA, USA). Low range DNA ladder (O'GeneRuler™), 25-700 bp and 6X Tri-track loading dye solution were purchased from Fermentas (ON, Canada). All other reagents were purchased from Fischer (ON, Canada). To maintain the cell culture, the reagents

such as fetal bovine serum, trypsin, Dulbecco's modified Eagle's Medium were obtained from Invitrogen (ON, Canada). The breast cancer cell-line, MCF-7, was purchased from ATCC (ON, Canada). RNAse A, AllStars Hs Cell Death Control siRNA and AllStars Negative Control siRNA, labeled with fluorescin were purchased from Qiagen (ON, Canada). Promega Cell-Titer 96® AQueous Non-Radioactive Cell Proliferation MTS Assay kit was purchased from Promega (WI, USA).

Preparation of HSA nanoparticles coated with PEI

HSA particles were synthesized at room temperature using a desolvation technique as depicted in the schematic illustration (Figure 3.1) with varied amounts of HSA, ranging between 10 and 100 mg [112,115]. HSA was added to 1 ml of 10 mM NaCl (aq) under constant stirring (800 rpm). The solution was stirred for 10 min. Upon complete dissolution, the solution was titrated to pH 8.5-9 with 1 N NaOH (aq) and stirred for 5 min. This aqueous phase was subjected to desolvation by the slow drop-wise addition of ethanol to the continuously stirred HSA solution until the solution became turbid. Adding an excess of ethanol caused the particles to form aggregates. Lastly, different amounts of PEI, ranging from 0.78 µg to 25 µg, were added to the newly formed particles. PEI was allowed to coat the HSA nanoparticles under constant stirring at room temperature for 2, 4 or 8 hrs. In order to synthesize siRNA-loaded HSA nanoparticles, the specified amount of siRNA was added to 1 ml of HSA solution after adjusting the pH and stirred for 30 min., followed by ethanol addition.

Purification of albumin nanoparticles

Before any purification technique was employed, the newly formed HSA nanoparticles were subjected to ultra-sonication for 10 min. (Branson 2510). Gradient centrifugation allowed impurities, PEI and ethanol to be removed from the nanoparticles. The first round of ultra-centrifugation was carried out at 16000 g for 15 min; the second round of ultra-centrifugation was of the supernatant of the first at 17000 g for 25 min. The supernatant of the second round was then ultra-centrifuged at 18000 g for 30 min. The pellets from all three rounds of centrifugation were re-dispersed in 10 mM NaCl (aq) to

the original volume and ultra-sonicated for 15 min. This cycle of ultra-centrifugation was repeated thrice to ensure complete removal of impurities.

Determination of particle size and zeta potential

The particle size, zeta potential and polydispersity index (PDI) were measured with electrophoretic laser Doppler anemometry, using a Zeta Potential Analyzer (Brookhaven Instruments Corporation, USA). The HSA nanoparticles were diluted 1:10 with double-distilled water prior to measurement.

Transmission and scanning electron microscopy

The shape and size of the nanoparticles was observed by transmission electron microscopy (TEM), using Philips CM200 200 kV TEM. The purified nanoparticles were diluted with water to allow for clearer pictures. The morphology of the HSA nanoparticles was studied by scanning electron microscopy (SEM), using a Hitachi S-4700 FE scanning microscope. The samples for SEM were prepared by ultra-centrifuging the HSA nanoparticles and washing with distilled water thrice, followed by freeze drying the samples over-night to allow complete removal of moisture.

Atomic force microscopy

Samples were prepared using the same technique as for SEM observation. Images were produced with a Nanoscope III (Digital Instruments, USA) using a silicon cantilever in tapping mode and analyzed using the nanoscope v 5.12r5 software.

Gel Retardation Assay

The gel retardation assay was performed to assess the protection PEI-coated HSA nanoparticles provide siRNA from RNAse degradation. The siRNA-nanoparticle complexes, containing the Allstar Cell death siRNA (Qiagen) were incubated with RNAse A for 30, 60 and 120 mins. The siRNA-loaded nanoparticles were then loaded onto a 4% agarose gel with 6x loading buffer. The gel electrophoresis was carried out in 0.5× Tris/Borate/EDTA (TBE) buffer at 100V for 25 minutes. The siRNA bands were visualized using an ultra violet (UV) imaging system.

Transfection of breast cancer cells with siRNA-loaded nanoparticles

MCF-7 breast cancer cells were grown in Dulbecco's modified Eagle's Medium (DMEM) with 10% Fetal Bovine Serum (FBS). Cells were cultured in a humidified incubator containing 5% CO_2 at 37˚C. Before transfection, cells were washed with Phosphate buffered saline (PBS) and replenished with fresh DMEM without FBS. The PEI-coated HSA nanoparticles were added to the cells and incubated at 37˚C. After 4 hrs of incubation of cells with the nanoparticles, the culture medium was replaced with fresh DMEM, containing 10% FBS. Under the fluorescence microscope (TE2000-U, Nikon; USA), pictures were taken to assess the levels of transfection. The percentage of transfected cells was calculated by using the average of the number of cells exhibiting fluorescence under five different fields of view. The relative fluorescence units were measured with a Victor3 Multi Label Plate Counter (Perkin Elmer, USA).

Cell viability assay

The cytotoxicity was evaluated using the Promega Cell-Titer 96® AQueous Non-Radioactive Cell Proliferation MTS Assay kit. For this, 3-(4, 5-dimethylthiazol-2-yl)-5-(3-carboxymethoxyphenyl)-2-(4-sulfophenyl)-2H-tetrazolium, (MTS) and phenazine methosulfate reagents were used. Living cells reduce MTS to form formazan, a compound soluble in tissue-culture media. The amount of formazan is thus proportional to the number of living cells and can be quantified by measuring the absorbance of formazan using 1420-040 Victor3 Multilabel Counter (Perkin Elmer, USA) at 490nm. Therefore, the intensity of the color produced by formazan reflects the viability of cells. MCF-7 cells were seeded onto a 96-well plate (10^4 cells per well) 24 hrs before treatment. Cytotoxicity was measured at the pre-determined time for each experiment using the MTS assay which was performed as per the manufacturer's protocol.

RESULTS

Characterization of PEI-coated HSA nanoparticles for siRNA delivery

The nanoparticles were synthesized using a slightly modified version of a desolvation protocol [115,116]. Nanoparticles were formed by the addition of a desolvation agent,

ethanol, to HSA. The nanoparticles were optimized based on size, zeta potential and polydispersity. Firstly, the effect of the amount of PEI added to stabilize the HSA nanoparticles was studied. Using PEI quantities of 0.78, 1.56, 3.125, 6.25, 12.5 and 25 µg added per mg of HSA, the size of the nanoparticles was observed to decrease with increasing PEI amount until 6.25 µg, after which the size remained constant (Table 3.1). 0.78 µg was not enough to allow stable particle formation, leading to precipitation of HSA (Table 3.1). The trend for zeta potential with increasing quantity of PEI added was similar to that of particle size, as the surface potential became more positive until 6.25 µg, and then stayed approximately constant (Table 3.1). The polydispersity index for nanoparticle preparations with different amounts of PEI added stayed $\leq$ 0.30. The impact of coating time on these parameters was also tested. There was little difference between the 4 and 8 hrs of coating time duration, where as 2 hrs showed particles of larger sizes (Table 3.1).

The influence of HSA concentration on the nanoparticles was also studied. At a concentration of 20 mg/ml HSA, the smallest average particle size of ~85 nm was achieved. Further increasing or decreasing the HSA concentration led to an increase in particle size (Table 3.2). Zeta potential and the polydispersity index showed no correlation with the HSA concentration.

Stirring speed of the desolvation step during the synthesis of nanoparticles also illustrated an effect on the particle size, as increasing the stirring speed from 400 to 800 rpm led to a decrease in particle size. Further increasing the stirring speed did not alter the particle size considerably (Table 3.3). Varying the pH of the aqueous HSA solution caused change in particle size and zeta potential (Table 3.3). Increasing the pH from 6.5 to 8.5 led to a great drop in the particle size, while further increasing the pH to 10.5 did not result in significant changes in particle size. As the pH became more acidic, the zeta potential resulted in more positive charge.

TEM, SEM and AFM were conducted to visualize the empty nanoparticles (Figure 3.2, 3.3). Loading siRNA into the PEI-coated HSA nanoparticles did not bring about any change in the resulting nanoparticles. A comparison of TEM and SEM images of siRNA-loaded nanoparticles with images of empty particles shows that the shape, size and

morphology remained largely unchanged (Figure 3.7). Both preparations were made using HSA concentration of 20 mg/ml, with and without loading siRNA, resulting in well-dispersed nanoparticles of $\leq$ 100 nm with an irregular shape.

Optimizing the nanoparticle dosage for minimum cytotoxic effects on MCF-7 cells

The MTS assay was used to determine the cytotoxic effect of empty PEI-coated HSA nanoparticles. MCF-7 cells (10^4 cells per well) were cultured in a 96 well-plate and incubated with 100 µl of the PEI-coated HSA nanoparticle preparations for 48 hrs. Untreated cells incubated with pure cell-culture media, DMEM, were considered as the control treatment. Firstly, cytotoxicity was measured for nanoparticles prepared using different HSA concentrations: 20, 60 and 100 mg/ml (Table 3.4). Secondly, cytotoxicity was assessed for nanoparticles prepared with PEI of molecular weights, 25 kDa and 70 kDa, and at PEI amounts of 0.78, 1.56, 3.125, 6.25, 12.5 and 25 µg of PEI added per mg of HSA (Figure 3.4). Variations in HSA concentration of the nanoparticle preparation did not show any significant change in the percentage of cell viability (Table 3.4). However, increasing the volume of the nanoparticle preparation that the cells are incubated with did result in higher cytotoxicity levels. Using higher molecular weight PEI (70 kDa) for coating the HSA nanoparticles resulted in higher cytotoxicity than lower molecular weight PEI (25 kDa). As the amount (µg) of PEI added per mg of HSA was increased, a decline in cell viability was observed. This decline seemed to be more evident with the higher molecular weight PEI (70 kDa) (Figure 3.4). For the lower molecular weight PEI (25 kDa), no significant decline in cell viability was observed until 6.25 µg of PEI per mg of HSA; however, further increasing the PEI quantity led to a steep increase in the cytotoxic effect.

Nanoparticles provide RNase protection to siRNA

Untreated siRNA and naked siRNA degraded with RNase A for 30 min. were loaded in lanes 1 and 6, respectively (Figure 3.5). Lane 1 shows a band at ~20 bp, indicating that siRNA without added RNase A remained intact. No band is observed in lane 6, as the naked siRNA was completely degraded in the presence of RNase A. Nanoparticles containing Allstar Cell death siRNA, incubated with RNase A for 30 min. were loaded in lanes 2 and 3, containing nanoparticles prepared with 1.56 and 6.25 µg of PEI added per

mg of HSA, respectively. Lane 2 shows a faint band only at the starting point of the well, while Lane 3 shows a clear band at the well. As siRNA was trapped inside the HSA nanoparticles in Lane 2 and 3, it remained protected from RNase degradation and was thus unable to travel through the gel and form a band as in the case of naked siRNA in lane 1. Lanes 4 and 5 showed no band, indicating complete degradation of siRNA.

Efficient nanoparticle-mediated transfection in breast cancer cells

Fluorescein-labeled AllStar siRNA was incorporated into PEI-coated HSA nanoparticles to determine the transfection efficiency of the siRNA-loaded nanoparticles with a fluorescence microscope and a Victor3 Multi Label Plate Counter (Perkin Elmer, USA). Transfection efficiency was measured at varying HSA concentrations: 20, 60 and 100 mg/ml. For each HSA concentration, three different PEI amounts were used to coat the particles: 1.56, 6.25 and 25 µg of PEI per mg of HSA. MCF-7 cells (10^4 cells per well) were cultured in a 96 well-plate and incubated for 4 hrs with 100 µl of the nanoparticles re-suspended in DMEM, containing 20 ng of the labeled AllStar control siRNA (Qiagen). The data representing the manually counted percentage of transfected cells (Figure 3.6 a) and the normalized fluorescence measured by the Plate Counter (Figure 3.6 b) show the same trends. With each HSA concentration, highest transfection resulted by coating the nanoparticles with 6.25 µg of PEI per mg of HSA. However, the lowest transfection percentage was observed when the nanoparticles were coated with 25 µg of PEI per mg of HSA. All three PEI amounts added for coating particles prepared with 20 mg/ml HSA show higher transfection efficiency than 60 and 100 mg/ml HSA (Figure 3.6). Similarly, fluorescence microscope images show a greater number of cells transfected using 6.25 µg of PEI per mg of HSA and 20 mg/ml HSA.

Induction of cell death in breast cancer cells by siRNA-loaded nanoparticles

For transfecting MCF-7 cells, PEI-coated HSA nanoparticles synthesized with 20 mg/ml HSA, 6.25 µg of PEI per mg of HSA, pH 8.5 under constant stirring at 800 rpm, were loaded with AllStars cell death siRNA, as observed in TEM and SEM images (Figure 3.7). 1, 2 or 4 µg of the AllStars cell death siRNA was added to 1 ml of 20 mg/ml HSA to form the nanoparticles, which were then purified and re-suspended in 5 ml of DMEM. MCF-7 cells were grown in a 96 well-plate and incubated with 100 µl of the nanoparticle

preparation, containing ~40 ng of the AllStars cell death siRNA. Nanoparticles loaded with the AllStars Cell death siRNA were incubated with MCF-7 at 37 ºC for 4 hrs to allow for transfection. The gene silencing function of AllStars Cell death siRNA was assessed by measuring cell death after 72 hrs using the MTS assay (Figure 3.8). HiPerfect transfecting reagent, a cationic lipid preparation developed by Qiagen that is shown to carry out efficient siRNA delivery inside cells, was used to deliver the AllStars Cell death siRNA as a positive control. Untreated cells and cells incubated with free siRNA and empty nanoparticles were taken as negative controls. AllStars Cell death siRNA resulted in a decrease in cell viability when delivered with PEI-coated HSA nanoparticles as compared to the negative controls. Cell viability using PEI-coated HSA nanoparticles, carrying 2 µg of siRNA, was the lowest, while nanoparticles loaded with 1 µg of siRNA showed highest cell viability. Cell viability using the HiPerfect reagent in the positive control was lower than observed using the PEI-coated HSA nanoparticles.

DISCUSSION

Using siRNA to silence the expression of genes to enhance tumour suppression is coming forth as a promising strategy to treat cancer. Due to the unstable and rapidly degrading nature of siRNA, it is imperative to put in place a delivery system that can carry siRNA to the target tissues and cells [29,33]. It is thus essential to deliver siRNA in a manner that prevents its breakdown and also allows for the siRNA to be taken up by the cells. In the current study, siRNA is delivered to MCF-7 breast cancer cells using albumin-based PEI-coated nanoparticles.

Non-viral delivery systems have attracted immense attention in order to overcome the shortcomings of viral vectors. Adeno- or retroviruses may be used, however, risks related to immunogenicity and potential pathogenicity form a serious concern [117-119]. This severely restricts the potential of using viral vectors for clinical applications. Non-viral nano-vectors also possess other favorable characteristics, including biocompatibility, easy administration and a potential for targeted delivery [118].

Human serum albumin (HSA) is a protein well-suited for synthesizing nanoparticle delivery systems. HSA is found in great abundance naturally in blood, as it acts as a carrier and solubilizing protein [73]. As HSA is one of the main constituents of blood, when used in nanoparticles, it is unlikely to cause any undesired interaction with other serum proteins. Albumin-based nanoparticles have been studied as a delivery system for anti-sense therapy, using anti-sense oligonucleotides [86]. However, these studies have largely been conducted using glutaraldehyde as the cross-linking agent. Glutaraldehyde cross-links with the amines on HSA and stabilizes the nanoparticles [120]. An alternative to glutaraldehyde was needed, as along with being cytotoxic, it is reported to hinder the release of the cargo therapeutic being delivered [121,122]. In this study, Polyethylenimine (PEI), a cationic polymer, has been used to replace glutaraldehyde to form HSA-based nanoparticles. PEI has been previously used to coat HSA nanoparticles, however, siRNA is being delivered using these nanoparticles for the first time [112,123]. On the other hand, a group has also studied the co-encapsulation of PEI with cargo DNA as a stabilizing agent in order to help increase the rate of transfection of cells [124].

The size and charge of PEI-coated HSA nanoparticles were optimized according to various parameters, including PEI amount, HSA concentration, pH of the HSA solution before desolvation, and stirring speed. An optimal nanoparticle needs to be synthesized as size and a positive surface charge of the nanoparticles are factors that determine cellular uptake of these particles. Previous studies have shown that there is an indirectly proportional relation between particle size and levels of cellular uptake of the nanoparticle, as smaller sized nanoparticles are more easily taken up by cells [28,125]. The exact size range of nanoparticles that is most efficient for cellular uptake has not been laid out in literature; thus, indicating that the type of nanoparticle and what it is composed of may play a role. The smallest size of approximately 85 nm was achieved with 6.25 µg per mg HSA of PEI and 20 mg/ml of HSA. Similarly, the optimal pH level and the stirring speed, resulting in the smallest particle size was 8.5 and 800 rpm, respectively.

For the clinical application of a therapeutic delivery system, it is of extreme importance to minimize its toxicity. PEI has been reported to have some toxic effects on cells at high

concentrations, possibly due to its ability to make cell membranes permeable [126]. According to results achieved in this study, the lower M.W. (25 kDa) should be used for nanoparticle preparation as cytotoxicity was greater for the higher M.W. PEI (70 kDa). Amounts $\leq$ than 6.25 µg per mg HSA of 25 kDa PEI showed similar cytotoxicity levels. Furthermore, Zhang et al. have carried out in vivo experiments using PEI-coated HSA nanoparticles, illustrating the stability of the particles in vivo [123].

The gel retardation assay was carried out to show that the PEI-coated HSA nanoparticles provide siRNA with protection from enzymatic degradation. The presence of a band around the well, where the samples were loaded, indicates that siRNA was not degraded by the RNase A and was retained within the nanoparticles. This retention of siRNA at the well of the agarose gel for Lane 2 and 3 confirms successful siRNA-loading of the nanoparticles. Lane 2 shows a faint band at the well, while lane 3 shows a clear band (Figure 3.6). This indicates that the nanoparticles provide protection from RNase A degradation for 30 min. As nanoparticles prepared with a very low concentration of PEI (1.56 µg) were loaded in lane 2, lesser amount of siRNA was retained at the well, resulting in a fainter band. A higher retention of siRNA in nanoparticles prepared with a greater amount of PEI (6.25 µg) suggests that PEI provides the nanoparticles with more strength, preventing the degradation of the therapeutic molecules being carried as cargo.

In order to confirm siRNA-loading of the nanoparticles and establish the conditions that yield maximum cellular uptake of the nanoparticles, control FITC-tagged siRNA was transfected into MCF-7 cells by the PEI-coated HSA nanoparticles (Figure 3.7). The presence of fluorescence suggests that the siRNA was successfully loaded into the nanoparticles and protected. The transfection efficiency of the nanoparticles was assessed based upon HSA concentration and PEI amount. The combination of 6.25 µg per mg HSA of 25 kDa PEI and 20 mg/ml of HSA showed maximum transfection. As PEI is a cationic polymer, increasing its amount makes the surface potential more positive, which would augment cellular uptake of the particle. However, further increasing the PEI amount to 12.5 µg showed lower transfection efficiency, which can be due to higher toxicity and consequent cell death. Changing the HSA concentration affects the size of

the nanoparticles, thereby influencing transfection efficiency as smaller sized nanoparticles are more easily internalized by cells [59,127].

Using optimal conditions for transfection, the efficacy of these nanoparticles was assessed by checking whether the siRNA delivered can carry out its silencing function. Cell death siRNA (Qiagen) is designed to induce cell death, and was delivered using the PEI-coated HSA nanoparticles to MCF-7 cells. The results show that the Cell death siRNA remains functional as it induces cell death; this indicates that the procedure applied to synthesize these nanoparticles does not lead to degradation of the siRNA.

Acknowledgements

This work is supported by research grant to S.P. from Natural Sciences and Engineering Research Council (NSERC), Canada. S.A. is supported by the McGill Faculty of Medicine Internal Studentship - G. G. Harris Fellowship. A.P. acknowledges the financial support from NSERC Alexander Graham Bell Canada Graduate Scholarship**.** The authors are grateful for the assistance provided for TEM imaging by Dr. Xue-Dong Liu, McGill, Department of Physics.

FIGURES

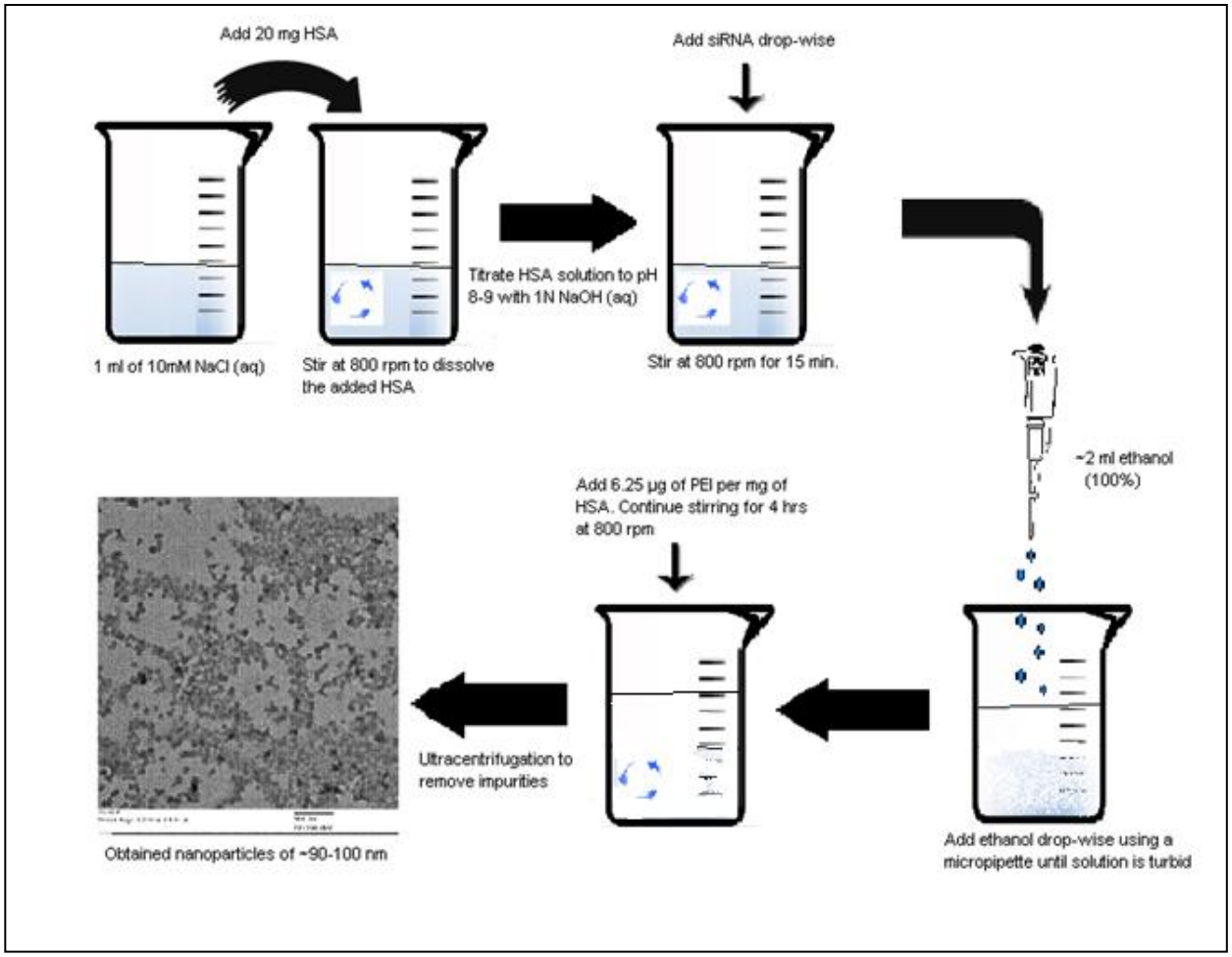

FIGURE 3.1: Schematic illustration of the method used for preparing PEI-coated HSA nanoparticles that are loaded with siRNA.

TABLE 3.1: Effect of the quantity of PEI (MW 25 kDa) added on the physical characteristics of PEI-coated HSA nanoparticles prepared at pH 8.5, 20 mg/ml HSA (mean ± S.D., n=3).

Amount of PEI (µg) added per mg of HSA	Time of incubation with PEI (hrs)	Particle Size (nm)	Zeta Potential (mV)	Polydispersity Index
0.78	2	--	- 21.1 ± 0.74	N/A
	4	--	-21.6 ± 0.47	N/A
	8	--	- 20.4 ± 1.6	N/A
1.56	2	438.1 ± 4.2	+ 3.3 ± 0.3	0.30 ± 0.008
	4	351.2 ±7.3	+ 3.6 ± 0.2	0.30 ± 0.004
	8	362.5 ± 2.1	+ 7.4 ± 0.5	0.28 ± 0.01
3.125	2	315.2 ± 5.5	+ 10.2 ± 1.2	0.275 ± 0.01
	4	279.8 ± 1.2	+ 14.8 ± 0.7	0.268 ± 0.001
	8	280.2 ± 1.1	+ 15.7 ± 1.5	0.265 ± 0.008
6.25	2	102.7 ± 1.5	+ 22.8 ± 1.1	0.241 ± 0.002
	4	90.1 ± 1.9	+ 26.4 ± 0.7	0.174 ± 0.009
	8	88.2 ± 2.4	+ 26.1 ± 0.4	0.171 ± 0.004
12.5	2	115.3 ± 2.2	+ 26.6 ± 0.3	0.205 ± 0.01
	4	83.7 ± 1.4	+ 25.7 ± 0.5	0.179 ± 0.001
	8	82.9 ± 1.2	+ 25.3 ± 2.1	0.169 ± 0.008
25	2	110.5 ± 3.2	+ 26.5 ± 0.6	0.210 ± 0.01
	4	89.5 ± 1.1	+ 26.6 ± 0.2	0.172 ± 0.005
	8	90.6 ± 2.1	+ 26.2 ± 2.5	0.178 ± 0.02

TABLE 3.2: Effect of HSA concentration on the physical characteristics of PEI-coated HSA nanoparticles prepared at pH 8.5, 6.25 µg of PEI (MW 25 kDa) added per mg of HSA (mean ± S.D., n=3).

HSA concentration (mg/ml)	Particle Size (nm)	Zeta Potential (mV)	Polydispersity Index
10	144.9 ± 5.1	+ 18.23 ± 0.15	0.194 ± 0.003
20	82.4 ± 0.8	+ 17.41 ± 0.1	0.185 ± 0.02
40	116.1 ± 2.3	+ 19.02 ± 0.31	0.25 ± 0.008
60	229.7 ± 4.4	+ 17.31 ± 0.25	0.214 ± 0.01
80	301.4 ± 3.5	+ 18.06 ± 1.2	0.201 ± 0.005
100	336.8 ± 5.9	+ 16.54 ± 0.7	0.195 ± 0.003

TABLE 3.3: Effect of stirring speed and pH during the desolvation step on the physical characteristics of PEI-coated HSA nanoparticles, prepared with 20 mg/ml HSA and 6.25 µg of PEI (MW 25 kDa) added per mg of HSA (mean ± S.D., n=3).

Stirring speed (rpm)	pH of the HSA solution	Particle Size (nm)	Zeta Potential (mV)
400	6.5	550.2 ± 4.1	+ 29.5 ± 0.3
	8.5	211.5 ± 2.3	+ 18.2 ± 1.2
	10.5	209.1 ± 1.5	+ 5.3 ± 0.2
600	6.5	420.1 ± 9.1	+ 30.1 ± 2.3
	8.5	135.4 ± 7.6	+ 20.4 ± 0.7
	10.5	140.7 ± 2.5	+ 7.8 ± 0.05
800	6.5	380.2 ± 11.2	+ 26.3 ± 3.4
	8.5	89.6 ± 3.4	+ 22.6 ± 0.9
	10.5	91.5 ± 2.4	+ 8.1 ± 0.04
1000	6.5	400.9 ± 14.2	+ 31.5 ± 4.5
	8.5	91.3 ± 3.5	+ 17.3 ± 2.6
	10.5	100.1 ± 4.9	+ 10.5 ± 1.8

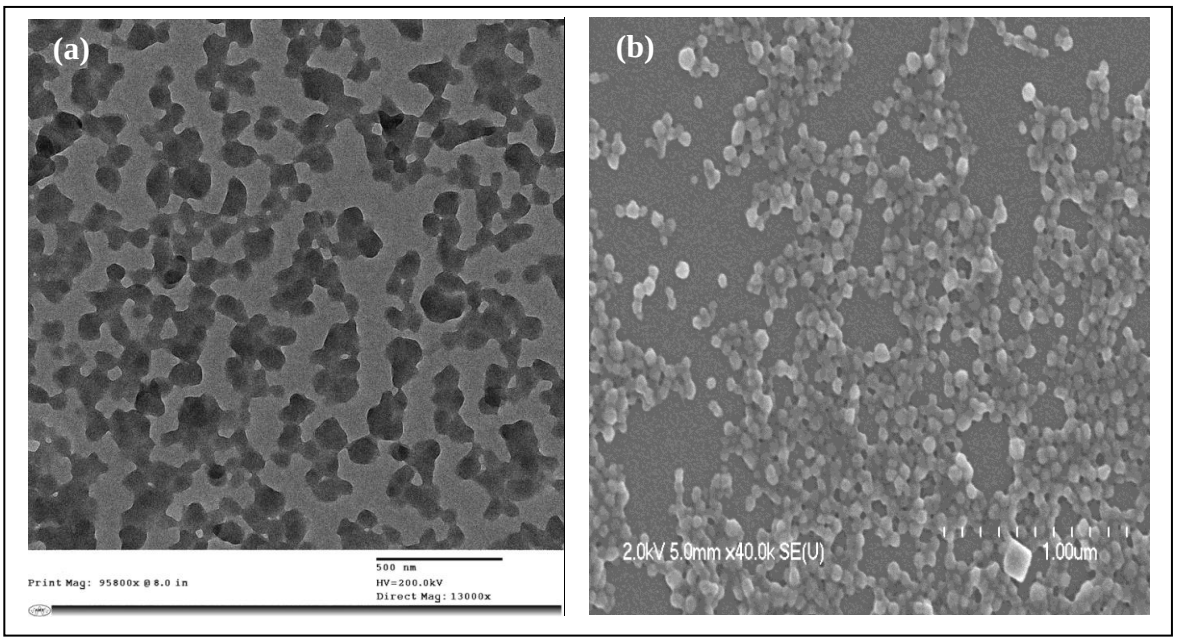

FIGURE 3.2: (a) Transmission electron microscope image. **(b)** Scanning electron microscope image of empty PEI-coated HSA nanoparticles, synthesized with 20 mg/ml HSA, pH 8.5, 6.25 µg of PEI (MW 25 kDa) added per mg of HSA under constant stirring of 800 rpm.

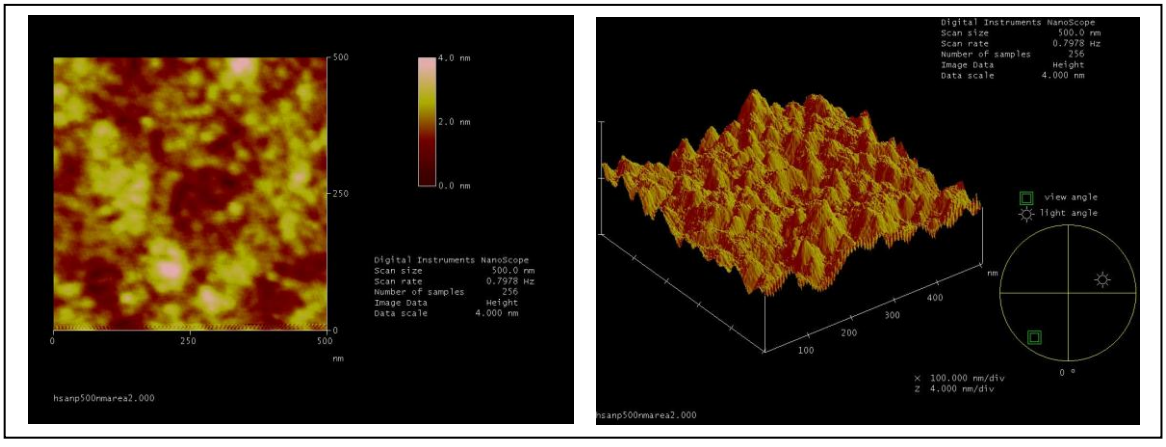

FIGURE 3.3: Atomic force microscopy image of empty PEI-coated HSA nanoparticles, synthesized with 20 mg/ml HSA, pH 8.5, 6.25 µg of PEI (MW 25kDa) added per mg of HSA under constant stirring of 800 rpm.

TABLE 3.4: Cytotoxicity of empty PEI-coated HSA nanoparticles formed using different concentrations of HSA, pH 8.5, 6.25 µg of PEI (MW 25 kDa) added per mg of HSA on MCF-7 cells after an incubation period of 48 hrs (mean ± S.D., n=3).

	Cell viability (%)		
HSA Concentration (mg/ml)	100 µl	150 µl	200 µl
-ve ctrl	100	100	100
20	94.1 ± 2.9	87.1 ± 0.5	75.8 ± 2.3
60	95.2 ± 4.0	83.8 ± 1.6	73.1 ± 0.9
100	94.6 ± 2.4	83.2 ± 4.2	76.4 ± 1.7

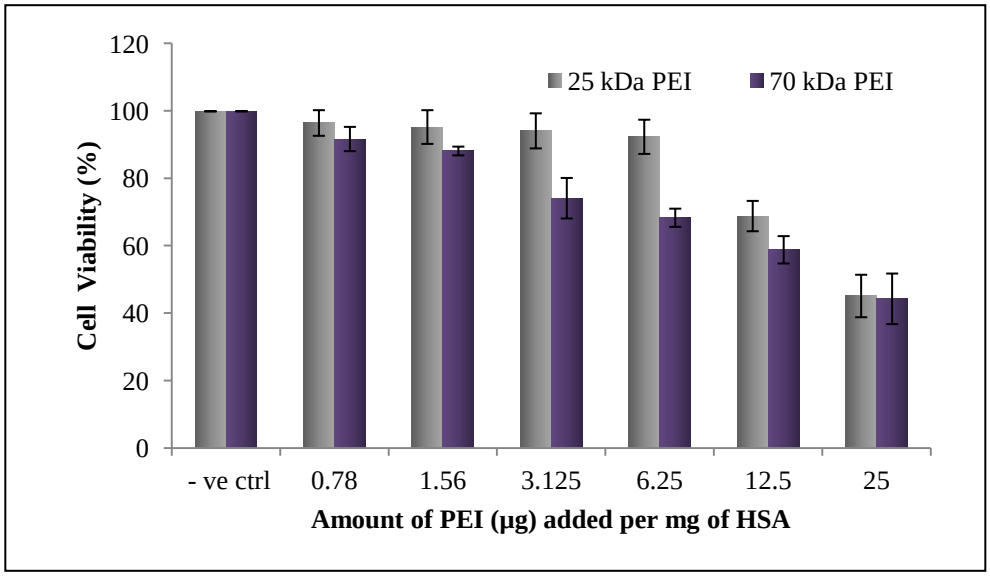

FIGURE 3.4: Cytotoxicity of empty PEI-coated HSA nanoparticles prepared with different amounts of PEI of two molecular weights (mean ± S.D., n=3). PEI-coated HSA nanoparticles were formed with either 25 kDa or 70 kDa M.W. of PEI with 0.78, 1.56, 3.125, 6.25, 12.5 and 25 µg of PEI added per mg of HSA. 100 µl of the nanoparticle preparation, suspended in DMEM, were added to MCF-7 cells that were cultured in a 96 well-plate at 10^4 cells and incubated for 48 hrs.

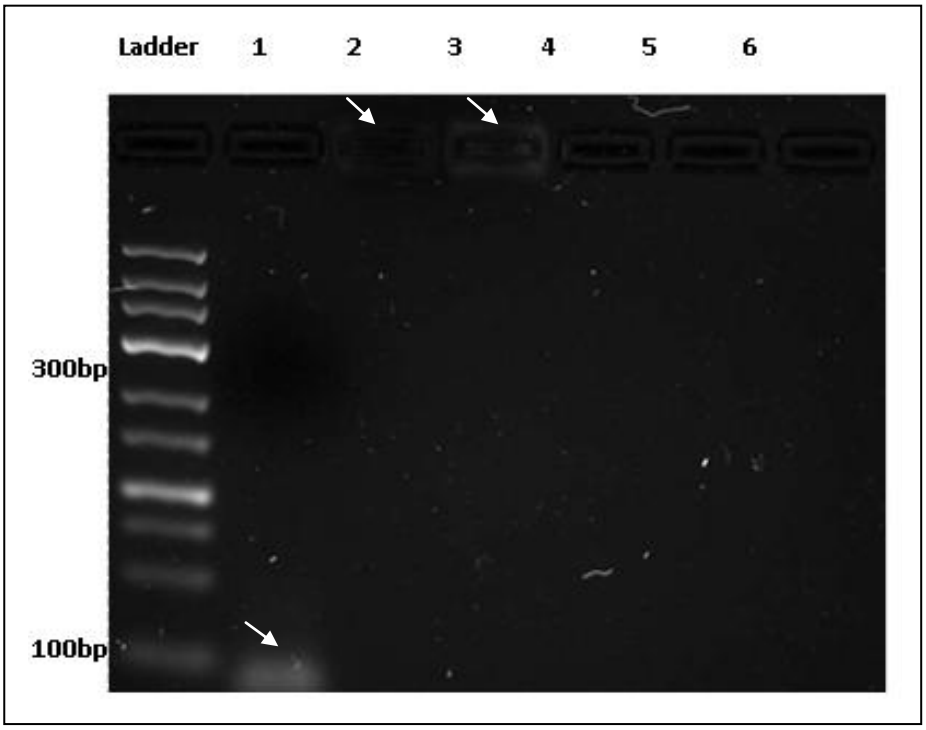

FIGURE 3.5: Gel electrophoresis of siRNA-loaded PEI-coated HSA nanoparticles. Nanoparticles containing Allstar Cell death siRNA, incubated with RNase A for 30 min were loaded in lanes 2 and 3, containing nanoparticles prepared with 1.56 and 6.25 µg of PEI (MW 25kDa) added per mg of HSA, respectively. Nanoparticles containing Allstar Cell death siRNA, incubated with RNAse A for 60 and 120 min. were loaded in lanes 4 and 5, respectively. Lane 1 was with control untreated naked siRNA while lane 6 was with naked siRNA treated with RNase A for 30min. White arrow pointing towards lane 3 shows the faint band at the well, illustrating the protected siRNA inside the nanoparticles (with high PEI conc.). lane 2 has a fainter band, which indicates lesser protection of entrapped siRNA by the nanoparticle formulation (with low PEI conc.).

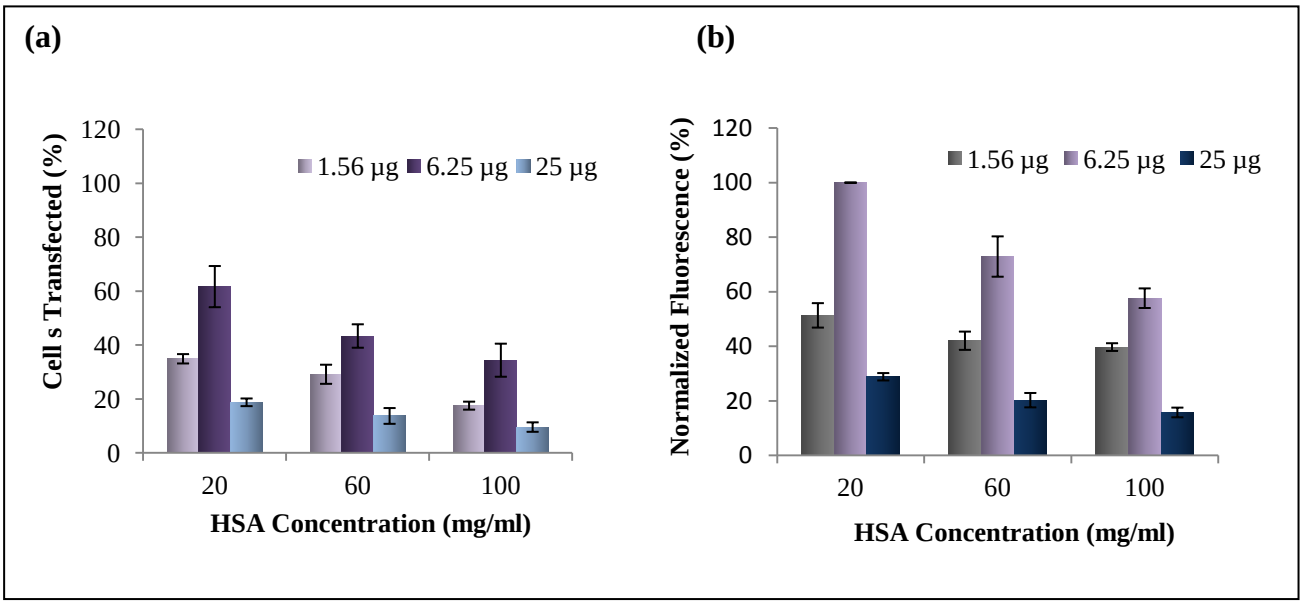

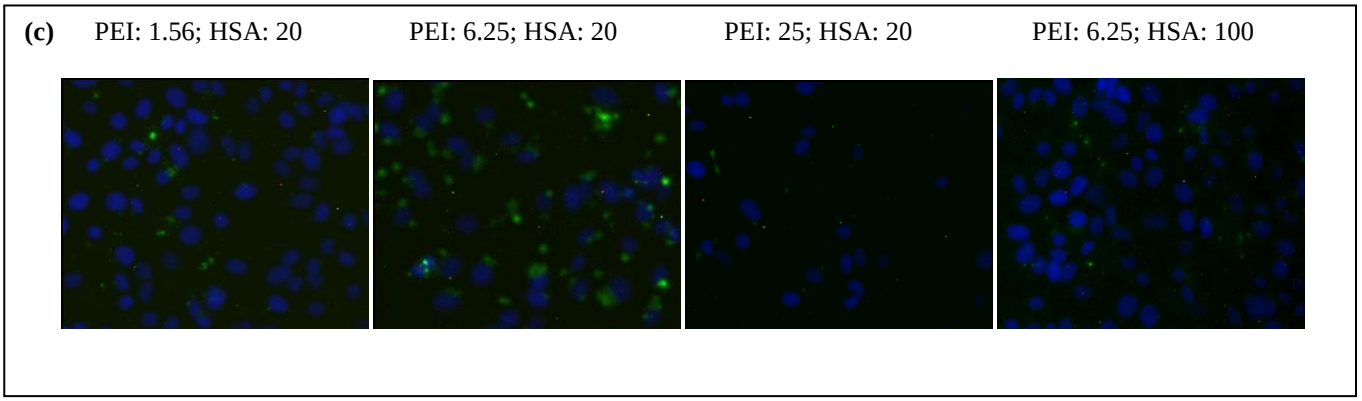

FIGURE 3.6: Transfection efficiency was measured at varying HSA concentrations: 20, 60 and 100 mg/ml. For each HSA concentration, three different PEI amounts were used to coat the particles: 1.56, 6.25 and 25 µg of PEI (MW 25kDa) per mg of HSA. 10 µg of the non-silencing Allstars negative control siRNA tagged with fluorescein was added to 20 mg/ml HSA. Upon purification, it was re-suspended in 5 ml cell-culture media. MCF-7 cells were cultured in a 96 well-plate and incubated for 4 hrs at 37 ºC with 100 µl of the nanoparticles re-suspended in DMEM. Transfection was measured by **(a)** manually counting the percentage of cells showing fluorescence different fields of view, and **(b)** a plate reader at 410 nm, expressed as normalized fluorescence expression (%), (mean $\pm$ S.D., n=3). **(c)** Fluorescence microscope images of the transfected MCF-7 cells by nanoparticles synthesized at different HSA concentrations (mg/ml) and PEI amounts (µg per mg of HSA).

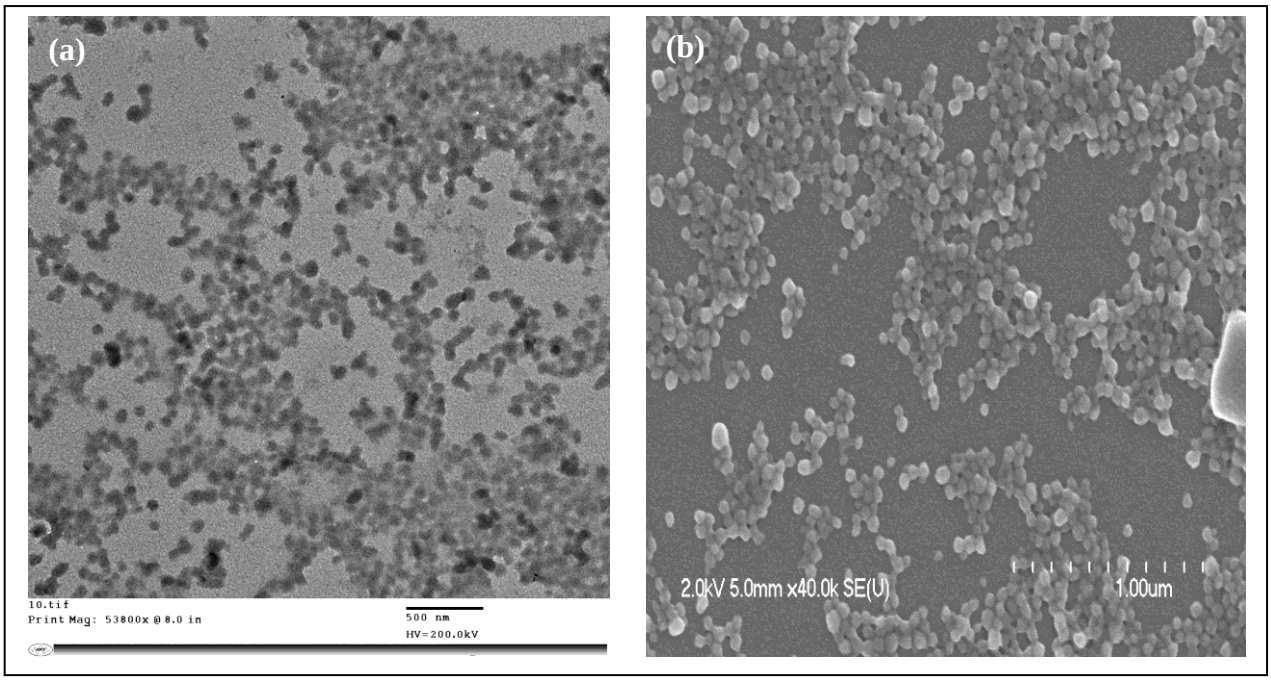

FIGURE 3.7: (a) Transmission electron microscope image. (**b)** Scanning electron microscope image of siRNA-loaded PEI-coated HSA nanoparticles, synthesized with 20 mg/ml HSA, pH 8.5, 6.25 µg of PEI (MW 25 kDa) added per mg of HSA under constant stirring of 800 rpm.

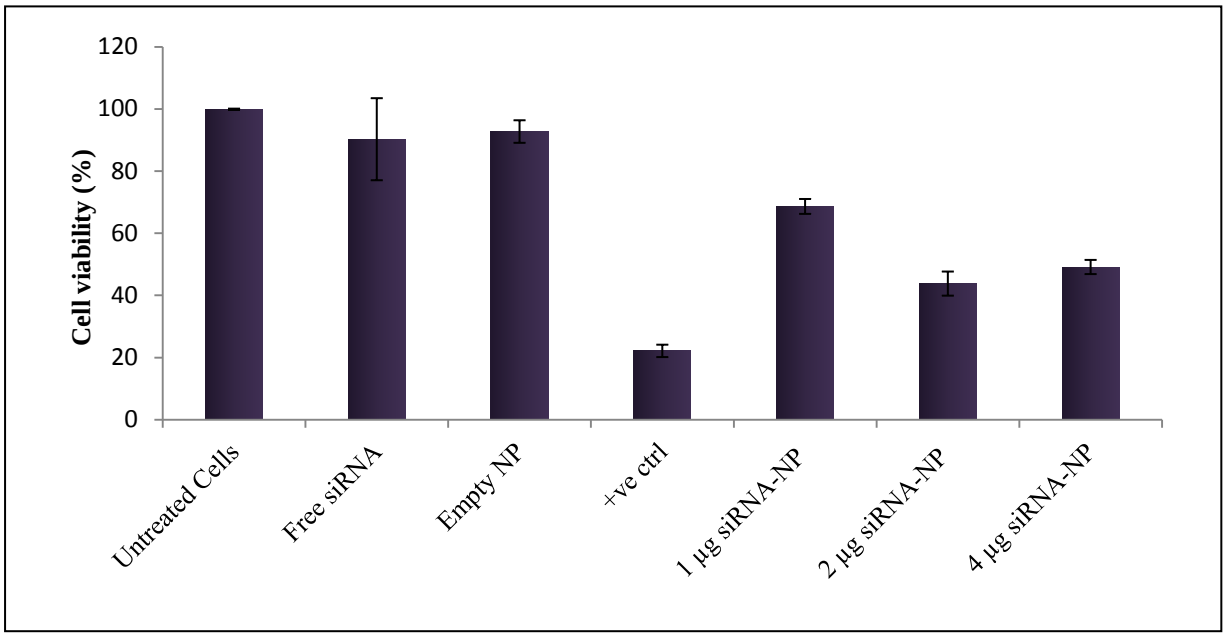

FIGURE 3.8: Assessing the functionality of siRNA delivered using PEI-coated HSA nanoparticles. 1, 2 or 4 µg of the Allstars Cell Death siRNA was added to 20 mg/ml HSA. The nanoparticles were synthesized as per the optimized parameters and re-suspended in 5 ml cell-culture media. MCF-7 cells (10^4 cells per well) were grown in a 96-well plate and incubated for 4 hrs at 37 ºC with 100 µl of the nanoparticles re-suspended in DMEM. The induction of cell death was measured after 72 hrs using the MTS assay (mean $\pm$ S.D., n=3). HiPerfect transfection reagent was used to deliver the AllStars Cell death siRNA as a positive control. Untreated cells, cells incubated with free siRNA and cells incubated with empty nanoparticles were taken as negative controls.

CHAPTER 4

Research Article

Cationic albumin nanoparticles for enhanced drug delivery to treat breast cancer: preparation and *in vitro* assessment

Sana Abbasi[1], Arghya Paul[1], Afshan Afsar Khan[1], Satya Prakash[1,2]*

[1]Biomedical Technology and Cell Therapy Research Laboratory, Department of Biomedical Engineering

[2]Artificial Cells and Organs Research Centre,

Faculty of Medicine, McGill University,

3775 University Street, Montreal, Quebec, H3A 2B4, Canada.

***corresponding author: Dr. Satya Prakash**

Preface:

In the previous chapter, polyethylenimine (PEI)-enhanced HSA nanoparticles were developed and characterized for siRNA delivery to breast cancer cells. The current chapter expands the application of PEI-coated HSA nanoparticles by investigating the delivery of a potent anti-cancer drug (doxorubicin) to MCF-7 breast cancer cells. The drug-loaded PEI-coated HSA nanoparticles are prepared using the same method as siRNA-loaded nanoparticles and characterized by measuring particle size, surface zeta potential and transfection efficiency [128-130]. The cytotoxicity of the developed dox-loaded nanoparticles was assessed in comparison to free dox at varying drug concentrations over different time points. Results suggest that PEI-coated HSA nanoparticles can also be used to deliver drugs (doxorubicin) to treat breast cancer.

ABSTRACT

Most anti-cancer drugs are greatly limited by the serious side-effects that they cause. Doxorubicin (dox) is an antineoplastic agent, commonly used against breast cancer. However, it may lead to irreversible cardiotoxicity, which could even result in congestive heart failure. In order to avoid these harmful side-effects to the patients and to improve the therapeutic efficacy of doxorubicin, we developed dox-loaded polyethylenimine (PEI)-enhanced Human Serum Albumin (HSA) nanoparticles. The formed nanoparticles were ~ 137 nm in size with a surface zeta potential of ~ +15 mV, prepared using 20 µg of PEI added per-mg-of-HSA. Cytotoxicity was not observed with empty PEI-enhanced HSA nanoparticles, formed with low-molecular weight (25 kDa) PEI, indicating biocompatibility and safety of the nanoparticle formulation. Under optimized transfection conditions, approximately 80% of cells were transfected with HSA nanoparticles containing tetramethylrhodamine-conjugated Bovine serum albumin. Conclusively, PEI-enhanced HSA nanoparticles show potential for developing into an effective carrier for anti-cancer drugs.

Keywords: Nanoparticles, nanomedicine, biotechnology, breast cancer, doxorubicin

INTRODUCTION

Doxorubicin (Adriamycin) is a commonly used anti-cancer drug. It is most often used against breast and esophageal carcinomas, osteosarcoma and soft-tissue sarcomas, Hodgkin's and non-Hodgkin's lymphomas [131]. The effectiveness of doxorubicin (dox) in treating various types of cancers is greatly limited by the serious side-effects caused by the drug. The initial side-effects caused as a result of dox administration include less serious symptoms, such as nausea, vomiting, myelosuppression and arrhythmia, which are usually reversible [131]. However, dox-associated cardiomyopathy and congestive heart failure have raised grave concern among health practitioners [132]. A widely researched approach of increasing the efficacy, while lowering the deleterious side-effects caused by anti-cancer agents such as doxorubicin, is of developing nanoparticle-based drug delivery systems [2,133,134].

Various kinds of nanoparticles have been studied for the delivery of dox, which include poly(butylcyanoacrylate) [135], poly(isohexylcyanoacrylate) [136], poly(lactic-co-glycolic acid [100], chitosan [99], gelatine [137] and liposomes [138]. In addition, Dreis et al. employed Human serum albumin (HSA) nanoparticles of a size range between 150-500 nm to deliver dox to a neuroblastoma cell line [133]. These nanoparticles showed a loading efficiency of 70-95% and an increased anti-cancer effect as compared to free dox. The endogenous HSA serves as a suitable material for nanoparticle formation as albumin is naturally found in the blood and is thus easily degraded, non-toxic and non-immunogenic [139]. Albumin is an acidic protein, and remains stable between pH range 4-9 and temperatures up to 60 °C. In addition, clinical studies carried out with HSA particle formulations, Albunex [140] and Abraxane [141], have shown that albumin-based nanoparticles do not have any adverse effects on the body.

Furthermore, albumin-based nanoparticle delivery systems are easily accumulated in tumor tissue due to the Enhanced Permeability and Retention (EPR) effect [6-8]. The vasculature in an active tumor is different from the vessels found in normal tissue. The distinctive tumor vasculature has the following properties: hypervasculature, poorly developed vascular architecture, a defective lymphatic drainage and slow venous blood return [7,8]. These characteristics lead to the preferential accumulation and retention of

macromolecules and nanoparticles in the tumor tissue. Therefore, using a nanoparticle delivery system to deliver low molecular weight anti-cancer drugs will be passively targeted to the tumour tissue through the EPR effect [6]. In addition, studies have also suggested that accumulation of albumin-based nanoparticles within the tumor tissue is also because of transcytosis, which occurs by the binding of albumin to 60-kDa glycoprotein (gp60) receptor, which then results in the binding of gp60 with caveolin-1 and the consequent formation of transcytotic vesicles [74,139]. Overall, HSA would form a suitable material to use for nanoparticle synthesis.

The surface properties of nanoparticles play a vital role in the cellular internalization of the particles. A neutrally charged surface does not show tendency of interacting with cell membranes, while charged groups found on nanoparticles are actively involved in nanomaterial-cell interaction [90]. Cho et al. found in their study of cellular internalization of gold nanoparticles that positively charged particles demonstrate greater adherence to the cell membrane and are thus taken up by the cells more than negatively and neutrally charged nanoparticles [91]. Cationic nanoparticles are shown to bind the negatively charged functional groups, such as sialic acid, found on cell surfaces and initiate translocation [90]. Due to the highly efficient transfection property of positively charged nanoparticles, many nanoparticle-based drug and gene delivery systems are positively charged. In this study, poly(ethylenimine) (PEI), a cationic polymer, has been used to coat the HSA nanoparticles in order to add stability and a positive surface charge to the nanoparticles. PEI may possess a linear or branched structure, with molecular weight ranging between 1-1000 kDa [142]. Typically, branched low molecular weight PEI (<25 kDa) has been observed to result in higher cellular uptake. As shown in our previous study, higher molecular weight PEI (70 kDa) leads to more cytotoxicity than lower molecular weight PEI (25 kDa) [143]. The most commonly used stabilizing agent for the preparation of HSA nanoparticles, glutaraldehyde, has been reported to interfere with the release of the encapsulated material [121,122]. Thus, PEI is being employed as an alternative to glutaraldehyde in the current study. PEI has been previously used to stabilize HSA nanoparticles; however, to our best knowledge, PEI-coated HSA nanoparticles are being used to delivery drugs for the first time [112,123].

In this research study, the effectiveness of dox-loaded polyethylenimine (PEI)-enhanced HSA nanoparticles used against MCF-7 breast cancer cells was investigated. The nanoparticles we prepared using an ethanol desolvation method and characterized by measuring particle size, surface zeta potential and cellular uptake [128-130]. The cytotoxicity of the developed dox-loaded nanoparticles was assessed in comparison to free dox at varying drug concentrations over different time points. Results were promising and suggest that the study needs to be followed up with an in vivo investigation of the dox-loaded PEI-enhanced HSA nanoparticles.

MATERIALS AND METHODS

Materials

Human serum albumin (HSA Fraction V, purity 96-99 %), 8% glutaraldehyde, and branched polyethylenimine (PEI) (M_W ~25,000) were purchased from Sigma Aldrich (ON, Canada). Doxorubicin hydrochloride was purchased from Calbiochem (Gibbstown, U.S.A). All other reagents were purchased from Fischer (ON, Canada). Tetramethylrhodamine conjugated Bovine serum albumin (BSA) was purchased from Invitrogen (ON, Canada). To maintain the cell culture, the reagents such as fetal bovine serum, trypsin, Dulbecco's modified Eagle's Medium and Opti-MEM I Reduced Serum Medium were obtained from Invitrogen (ON, Canada). The breast cancer cell-line, MCF-7, was purchased from ATCC (ON, Canada). Promega Cell-Titer 96® AQueous Non-Radioactive Cell Proliferation MTS Assay kit and were purchased from Promega (WI, USA).

Cell culture

MCF-7 cells were cultured on tissue culture plates as per the manufacturer's instructions. MCF-7 cells were grown in Dulbecco's modified Eagle's Medium (Invitrogen) supplemented with 10% (v/v) fetal bovine serum and placed in an incubator with 5% CO_2 at 37°C. The cells used in the experiments were obtained from passages 5-6.

Preparation of dox-loaded PEI-enhanced HSA nanoparticles

PEI-coated HSA nanoparticles were prepared at room temperature using an ethanol desolvation technique, as illustrated in Figure 4.1 [128-130,144]. In brief, 20 mg of HSA was added to 1 ml of 10 mM NaCl (aq) under constant stirring (800 rpm) at room temperature. The solution was stirred for 10 min. After total dissolution, the solution was titrated to pH 8.5 with 1 N NaOH (aq) and stirred for 5 min. This aqueous phase of HSA solution was desolvated by the drop-wise addition of ethanol under constant stirring. Ethanol was added until the HSA solution became turbid (~1-2 ml). Cross-linking agent, 8 % glutaraldehyde, was added to form stable HSA particles. The obtained nanoparticles were centrifuged three times and washed with deionized water (dH_20), followed by resuspension in an equal volume of Phosphate Buffer Saline (PBS). PEI dissolved in dH_20 was added to the nanoparticle preparation to allow PEI to form an outer coating due to electrostatic binding. For the preparation of drug-loaded HSA nanoparticles, doxorubicin was added to 1 ml HSA solution after pH adjustment and allowed to stir for 4hrs, followed by ethanol addition.

Purification of PEI-enhanced HSA nanoparticles

PEI-coated HSA nanoparticles were ultra-centrifuged (16500 g) for 12 min and added to 10 mM NaCl (aq) by vortexing and ultrasonication (Branson 2510). This method was repeated thrice to ensure complete removal of impurities.

Determining particle size and surface zeta potential

The particle size and zeta potential were measured by electrophoretic laser Doppler anemometry, using a Zeta Potential Analyzer (Brookhaven Instruments Corporation, USA). The nanoparticles were diluted with distilled water before measurement [129].

Surface characterization of PEI-enhanced HSA nanoparticles

The size and shape of the HSA nanoparticles were observed by transmission electron microscopy (TEM), using Philips CM200 200 kV TEM (Markham, Canada). The morphology of the HSA nanoparticles was studied using scanning electron microscopy (SEM), Hitachi S-4700 FE scanning microscope (Hitachi, Oakville, Canada). The

samples for SEM were prepared by ultra-centrifuging the nanoparticles and washing with distilled water, followed by air-drying the samples overnight to allow removal of moisture. Samples for atomic force microscopy (AFM) were diluted in distilled water after purification of the nanoparticles. 2.0 µl of the sample was dropped onto the surface of the disc. Images were produced with Nanoscope III (Digital Instruments, Palo Alto, USA) using a silicon cantilever in tapping mode and analyzed using the Nanoscope software (version 5.12r5; Digital instruments) [128,129,144].

Cellular Uptake of breast cancer cells with PEI-enhanced HSA nanoparticles

Prior to incubation with nanoparticles, cells were washed with Phosphate buffered saline (PBS) and replenished with fresh serum-free DMEM. The PEI-coated HSA nanoparticles were prepared using 5% of tetramethylrhodamine-conjugated Bovine serum albumin (BSA). The nanoparticles were purified and added to the cells. After 8 hrs of incubation of cells at 37˚C with the nanoparticles, the culture medium was replaced with fresh DMEM, containing 10% FBS. Under the fluorescence microscope (TE2000-U, Nikon; USA), pictures were taken to assess the levels of cellular uptake. The percentage of cellular uptake was calculated by using the average of the number of cells exhibiting fluorescence under five different fields of view.

Cell viability Assay

The number of surviving cells was assessed using the Promega Cell-Titer 96® AQueous Non-Radioactive Cell Proliferation MTS Assay kit. 3-(4, 5-dimethylthiazol-2-yl)-5-(3-carboxymethoxyphenyl)-2-(4-sulfophenyl)-2H-tetrazolium, (MTS) and phenazine methosulfate reagents were used. Live cells reduce MTS to form formazan, a compound soluble in tissue-culture media. The amount of formazan is proportional to the number of living cells and can be quantified by measuring the absorbance of formazan, using 1420-040 Victor3 Multilabel Counter (Perkin Elmer, USA) at 490 nm. The intensity of the color produced by formazan indicates the viability of cells. MCF-7 cells were seeded onto a 96-well plate (10^4 cells per well) 24 hrs before treatment. Cell viability was measured at the pre-determined time for each experiment using the MTS assay, performed as per the manufacturer's protocol.

TUNEL Assay

Terminal Deoxynucleotidyl Transferase (TdT) enzyme adds a biotinylated nucleotide at the 3´-OH ends of DNA; the biotinylated nucleotides are conjugated with horseradish-peroxidase-labelled streptavidin. The peroxidase is then detected using its substrate, hydrogen peroxide and the chromogen, diaminobenzidine (DAB). Following the manufacturer's protocol, the nuclei of apoptotic cells are stained brown.

RESULTS & DISCUSSION

Optimization of cationic dox-loaded PEI-enhanced HSA nanoparticles

The desolvation technique, as depicted in the schematic illustration in Figure 4.1, used to prepare the HSA nanoparticles [128,129,145] is simple to perform; the synthesized particles are consistent in size, surface zeta potential and morphology. The desolvation technique involves a liquid-liquid phase separation of an aqueous homogenous albumin solution, leading to the formation of a colloidal (or coacervate) phase that contains the nanoparticles [146]. In addition, the size of the nanoparticles formed by this technique can be altered based upon the various parameters of the technique, such as concentration and pH of HSA solution, volume and rate of ethanol addition [128,144,147]. In our previous research article, we presented that the smallest nanoparticle size was achieved with 20 mg/ml HSA at pH 8.5, ~1-2 ml of 100% ethanol added for desolvation of the HSA solution [128]. These parameters were kept unchanged in this study as well. Glutaraldehyde cross-linking was carried out to stabilize the formed HSA nanoparticles before PEI surface coating; this also increases the drug entrapment ability of the HSA nanoparticles [77].

In the current study, PEI-enhanced HSA nanoparticles were prepared by coating the HSA nanoparticles with electrostatic binding to the PEI molecules. As HSA is an acidic protein, it carries a negative zeta potential in ~ pH 8.5 and thus allows the positive PEI to bind to HSA nanoparticles [97,139,148]. The amount of PEI used for surface coating of the nanoparticles was optimized. Table 4.1 shows that as the amount of PEI was increased, a slight increase in the particle size was observed and the surface zeta potential became positive. This increase in size was gradual and could be attributed to the addition

of the PEI surface coating or slight aggregation of the particles. The surface zeta potential increased from approximately -47 to +18 mV, clearly indicating that the PEI was successfully adsorbed to the nanoparticle surface. Furthermore, results presented in Table 4.2 show that 8 hrs of incubation at a stirring speed of 1000 rpm resulted in the smallest particle size and maximum zeta potential. Conditions were optimized to attain the smallest particle size and maximum zeta potential in order to achieve the highest cellular uptake [90]. Size-dependence of cellular uptake has been studied previously [149]. For instance, Prabha et al. showed that smaller nanoparticles (~70 nm) experienced a 27-fold greater transfection than larger nanoparticles in COS-7 cell line, with all other parameters kept constant [149]. Similarly, surface charge of nanoparticles plays an important role in determining their transfection efficiency [90]. Harush-Frenkel et al. found that cationic nanoparticles resulted in rapid internalization through a clathrin-mediated pathway, while nanoparticles with a negative surface charge showed less efficient cellular uptake [150]. The TEM images shown in Figure 4.2 illustrate roughly spherical shape of the formed HSA nanoparticles of approximately 100 nm of size.

Increased cellular uptake of PEI-enhanced HSA nanoparticles

The cellular internalization of PEI-enhanced HSA nanoparticles was assessed by incubating MCF-7 breast cancer cells with nanoparticles prepared with tetramethylrhodamine-conjugated BSA. As shown in Figure 3, images were taken using a fluorescence microscope (TE2000-U, Nikon; USA). Cellular uptake was measured with respect to the amount of PEI added to coat the nanoparticles. It is essential to optimize the amount of PEI used for coating the nanoparticles as this helps determine how much of the polymer is required to reach the maximum adsorption capacity of the surface of the nanoparticles. Firstly, the lowest percentage of cellular uptake was observed with uncoated nanoparticles, which can be attributed to the negative surface zeta potential of the uncoated HSA nanoparticles. Based on Figure 4.3 (a), it can be concluded that increasing the amount of PEI, up to 20 µg of PEI per mg of HSA, used for coating the nanoparticles leads to an increasing in cellular uptake. Further increasing the amount of PEI used for coating the nanoparticles did not translate into higher cellular uptake. This observation could be explained by reaching the maximum capacity of PEI

binding with the surface of HSA nanoparticles. Figure 4.3 (b-d) show corresponding fluorescence images of cellular uptake of PEI-enhanced HSA nanoparticles. The increase in cellular uptake due to coating the nanoparticles with PEI is in agreement with previously published results. Cationic nanoparticles are shown to bind the negatively charged functional groups, such as sialic acid, found on cell surfaces and initiate transcytosis [90]. Previously, PEI-based nanoparticles have shown increased cellular uptake of siRNA. In vivo administration of siRNA delivered using PEI-based nanoparticles resulted in 80% decrease in the target gene expression, indicating that PEI-based nanoparticles remain effective in vivo [151,152]. Therefore, a reasonable conclusion to draw from the results of the cellular uptake experiment would be that the PEI adsorbed to the surface of the nanoparticles aids in the internalization of the particles.

Dox delivery with PEI-enhanced HSA nanoparticles to kill breast cancer cells

The efficacy of anti-cancer chemotherapy is limited by the cytotoxic effect on healthy cells due to a lack of selectivity of the drugs and poor uptake of the therapeutics by the tumor cells [3,22,90]. Doxorubicin, a strong antineoplastic agent, has been shown to cause irreversible cardiomyopathy, which could also lead to congestive heart failure [3,90,153]. In order to overcome this issue, many researchers have tried delivering dox by nanoparticles, reducing the amount of drug reaching cardiac tissue while increasing the accumulation of the drug-loaded nanoparticles in the tumor tissue [14,52,61,99,136]. Furthermore, by incorporating a layer of PEI on the surface of the HSA nanoparticles, we aimed to increase the cellular uptake of dox in the tumor tissue. Previously, uncoated HSA nanoparticles were studied for the delivery of dox to neuroblastoma cell lines. Results obtained by this group suggested that dox delivered using nanoparticles was more cytotoxic against cancer cells as compared to free dox. In our study, we observed that the cytotoxicity of dox-loaded nanoparticles and free dox against MCF-7 breast cancer cells was about the same after 48 hrs as the dox concentration was increased, shown in Figure 4.4 (a). However, assessing the cytotoxicity at different time points in Figure 4.4 (b) showed that dox-loaded nanoparticles led to a greater decrease in cell viability as compared to free dox after 144 hrs. This observation can be explained by the slow release of dox from the nanoparticles. These results would be more effective in vivo as the free drug would diffuse out of the tumor tissue, while the nanoparticles would

accumulate within the tumor tissue due to the EPR effect and release the drug over time. Images of treated cells after TUNEL staining in Figure 4.5 (a-c) confirm that the cytotoxic effect of dox-loaded nanoparticles was comparable to free dox. Figure 4.5 (c) shows that the cells remained healthy after the addition of empty PEI-enhanced HSA nanoparticles, suggesting that the nanoparticle formulation does not have cytotoxic effects. It is important for the nanoparticle delivery system to be non-toxic for any future clinical application.

CONCLUSION

In our current study, we used modified HSA nanoparticles by adding an outer coating of the polyethylenimine (PEI) to improve the therapeutic index of doxorubicin against MCF-7 breast cancer cells. The nanoparticles prepared were characterized based upon size and surface charge with respect to the amount of PEI used for coating. A rise in the surface zeta potential of the nanoparticles confirms the electrostatic binding of PEI with the surface of HSA nanoparticles. Different microscopic techniques were employed to observe the shape, dispersion and morphology of the nanoparticles. PEI-enhanced HSA nanoparticles resulted in a higher percentage of cellular uptake, indicating that the addition of the layer of cationic polymer did improve cell penetration of the particles. PEI-enhanced HSA nanoparticles illustrated a more potent cytotoxic effect on MCF-7 breast cancer cells over longer time duration. The results shown in this study are promising and set a platform for further examining the suitability of this PEI-enhanced delivery system in vivo.

Acknowledgements

This work is supported by a research grant to S.P. from Canadian Institutes of Health Research (CIHR) (MOP 93641). S.A. is supported by the McGill Faculty of Medicine Internal Studentship - G. G. Harris Fellowship and the Ontario-Quebec Exchange Fellowship. A.P. acknowledges the financial support from NSERC Alexander Graham Bell Canada Graduate Scholarship**.** The authors are grateful for the assistance provided for TEM imaging by Dr. Xue-Dong Liu, McGill, Department of Physics.

FIGURES

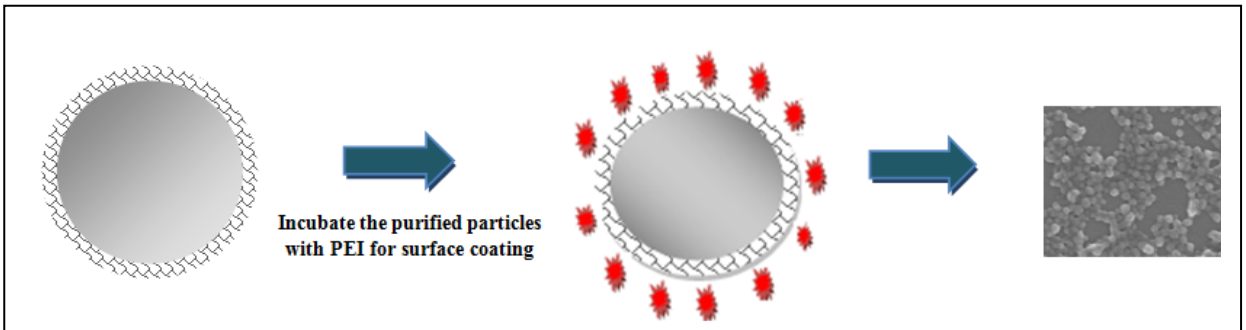
Incubate the purified particles
with PEI for surface coating

FIGURE 4.1: Schematic representation of the preparation of drug loaded polyethylenimine (PEI)-enhanced HSA nanoparticles using a desolvation technique [115,143].

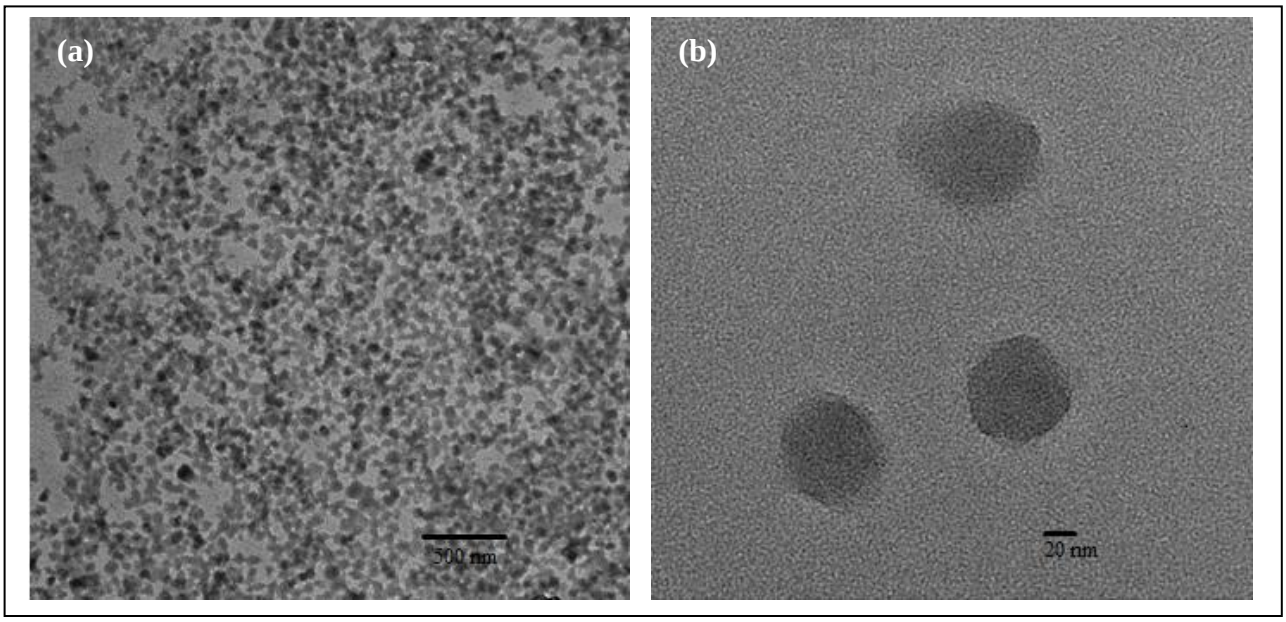

FIGURE 4.2: **(a)** Transmission electron microscope images of drug-loaded PEI-enhanced HSA nanoparticles, **(b)** Higher magnification image of nanoparticles.

TABLE 4.1: Effect of the amount of PEI added (µg per mg of HSA) on the physical characteristics of drug loaded PEI-enhanced HSA nanoparticles prepared at pH 8.5, 20 mg/ml HSA (mean $\pm$ S.D., n=3).

Amount of PEI (µg)	Particle Size (nm)	Zeta Potential

added per mg of HSA		(mV)
0	99.63±6.01	-46.9±5.06
10	105.6±8.07	+6.14±1.11
20	121.7±2.78	+12.3±0.18
30	137.2±8.20	+17.92±1.04
40	135.5±4.27	+18.38±3.7

TABLE 4.2: Effect of incubation time for PEI coating and stirring speed during the desolvation step on the physical characteristics of drug loaded PEI-enhanced HSA nanoparticles, prepared with 20 mg/ml HSA and 30 µg of PEI added per mg of HSA (mean ± S.D., n=3).

Time of incubation with PEI (hrs)	Stirring speed (rpm)	Particle Size (nm)	Zeta Potential (mV)
4	250	412.76±12.7	8.94±0.12
	500	248.43±1.7	7.20±0.19
	1000	130.47±11.3	4.24±0.08
8	250	362.77±0.65	17.4±0.36
	500	218.57±15.9	19.14±0.51
	1000	100.73±3.93	18.39±0.27
12	250	332.67±16.2	16.13±0.91
	500	205.17±8.16	10.99±0.71
	1000	111.53±4.72	13.73±0.36

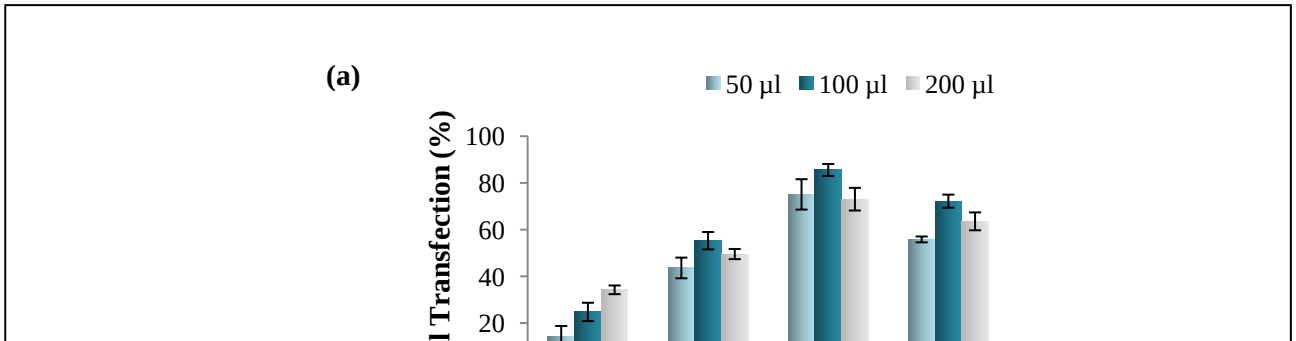

FIGURE 4.3: Cellular uptake percentage of PEI-enhanced nanoparticles was assessed with respect to different amounts of PEI used for coating (mean $\pm$ S.D., n=3). PEI-enhanced HSA nanoparticles were prepared using an ethanol desolvation technique with 20 mg/ml HSA. The nanoparticles were composed of 5% tetramethylrhodamine-conjugated BSA, and the celllular uptake was observed under a fluorescence microscope (TE2000-U, Nikon; USA). **(a)** Percentage of cellular uptake with nanoparticles prepared using: 0, 10, 20, and 30 µg of PEI per mg of HSA. Varying quantities of nanoparticle preparations were added to the cells: 50, 100 and 200 µl. Fluorescence images of cellular uptake of different HSA nanoparticle preparations, consisting of tetramethylrhodamine-conjugated BSA are shown: **(b)** uncoated HSA nanoparticles, **(c)** 10 µg and **(d)** 30 µg of PEI added per mg of HSA to form PEI-enhanced HSA nanoparticles. Corresponding bright field images are illustrated below **(b', c' and d')**.

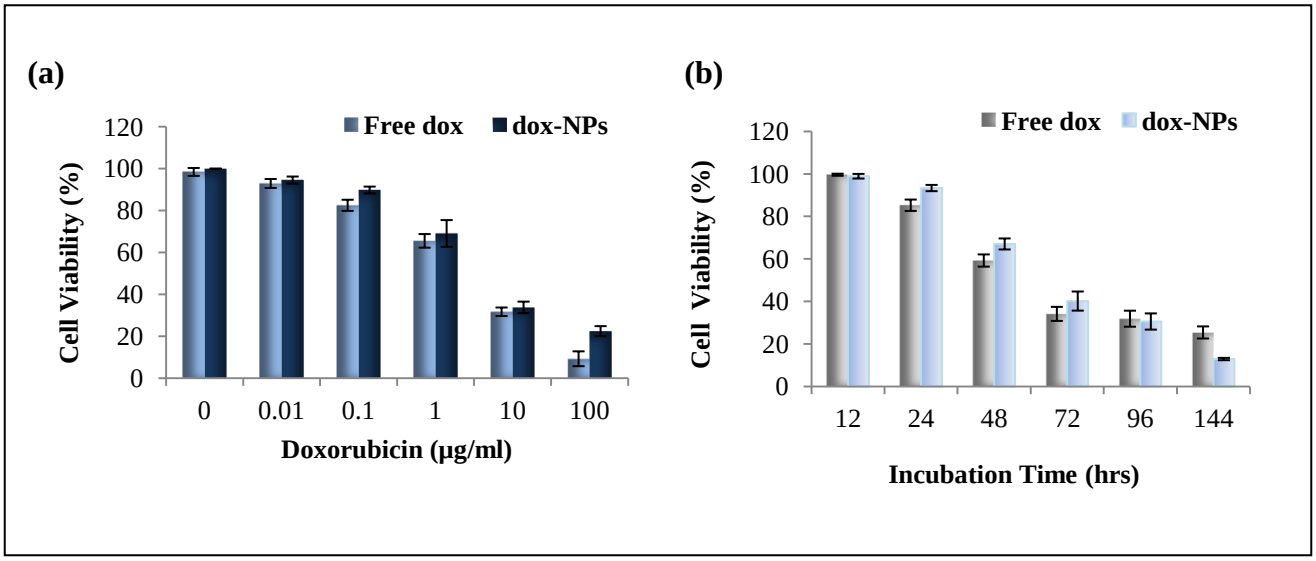

FIGURE 4.4: **(a)** Cytotoxicity of dox-loaded PEI-enhanced HSA nanoparticles as compared to free dox administered to MCF-7 breast cancer cells in log-phase culture after 48 hrs of treatment with different concentrations of dox. **(b)** Cytotoxicity resulting from dox-loaded PEI-enhanced HSA nanoparticles versus free dox over 144 hrs was measured. The concentration of dox administered was 1 µg/ml to MCF-7 breast cancer cells. Percentage of viable cells was assessed by an MTS assay and then compared to untreated cells in the control wells (mean ± S.D., n=3).

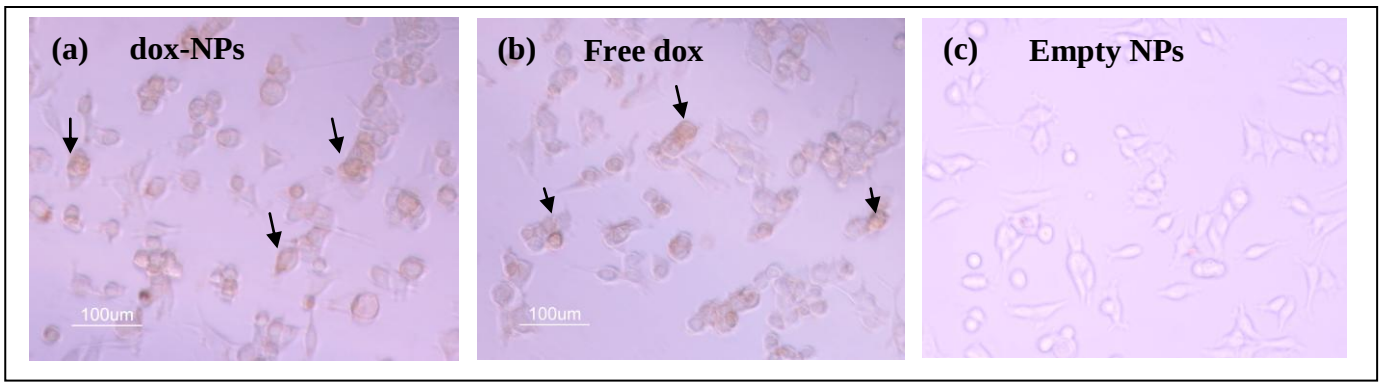

FIGURE 4.5: TUNEL assay to confirm cell death after dox administration: **(a)** dox-loaded PEI-enhanced HSA nanoparticles, **(b)** free dox and **(c)** empty PEI-enhanced HSA nanoparticles. The concentration of dox administered was 1 µg/ml to MCF-7 breast

cancer cells grown in a 96 well-plate (24 hrs). The black arrows point towards cells showing TUNEL staining.

CHAPTER 5

Research Article

HIV-1 TAT peptide surface functionalized albumin nanoparticles for improved gene delivery: optimization of *in vitro* transfection conditions to target breast cancer

Sana Abbasi[1], Arghya Paul[1], Afshan Afsar Khan[1], Wei Shao[1], Meenakhsi Malhotra[1], Satya Prakash[1,2]*

[1]Biomedical Technology and Cell Therapy Research Laboratory,
Department of Biomedical Engineering

[2]Artificial Cells and Organs Research Centre,

Faculty of Medicine, McGill University,

3775 University Street, Montreal, Quebec, H3A 2B4, Canada.

*corresponding author: Dr. Satya Prakash

Preface:

In the previous chapters, we used the polyethylenimine (PEI) as a surface coating for HSA nanoparticles to deliver siRNA and doxorubicin. In the current chapter, we designed and investigated the use of a novel TAT-coated HSA nanoparticle delivery system for carrying siRNA into MCF-7 breast cancer cells. In Chapter 5, we have modified the outer coating of the HSA nanoparticles studied in Chapters 3 and 4 by adding a cell penetrating peptide, TAT, to enhance the cellular uptake of the nanoparticles. The TAT-coated HSA nanoparticles have been characterized by size, surface charge and morphology. In addition, the transfection conditions were optimized and the functionality of siRNA delivered using the developed nanoparticles was assessed.

ABSTRACT

The clinical application of gene-silencing using siRNA-based therapy is limited by the rapid degradation of siRNA in circulation. Biodegradable nanocomplexes coated with a cell-penetrating peptide, the transactivating-transcriptional-factor (TAT) domain from HIV-1, have been developed and characterized in this study to deliver siRNA to MCF-7 breast cancer cells. The nanocomplexes are well-dispersed spherical particles, ~120-140 nm in size. The surface charge of the nanoparticles showed a rise with increasing amounts of TAT, reaching a plateau at ~+15mV. The empty nanocomplexes showed low cytotoxicity, promising scope for clinical application. Under the optimized transfection conditions, approximately 65-70% of cells showed presence of fluorescence, suggesting efficient cellular uptake of TAT-coated nanoparticles. The structural and functional

integrity of siRNA inside the nanoparticles was protected against RNase degradation. Thus, the novel TAT-coated HSA nanoparticles characterized in this study has potential of developing into a safe non-viral delivery system for future clinical application.

Keywords: Nanomedicine, gene-silencing, breast cancer, nanoparticles, biotechnology

INTRODUCTION

Nanobiotechnology is an increasingly progressive field that promises innovative avenues for the treatment of numerous diseases. It has been estimated that approximately 12.7 million new cancer cases and 7.6 million deaths from cancer occurred in 2008. Breast cancer is considered the second most commonly diagnosed type of cancer across the world [1]. After the diagnosis of cancer, the common modes of treatment include surgery, radiotherapy and chemotherapy [2].

One of the main focuses of nanobiotechnology research is to develop novel drug delivery systems that improve the drug efficacy and also limit harmful side effects of various cancer drugs. Nanoparticles are colloidal carriers with nano-dimensions that are being studied as a means of delivering drugs. Polymeric nanoparticles are often defined as

"sub-cellular colloidal entities, composed of natural or synthetic polymers" [134]. The size of the nanoparticles allows them to cross the capillary beds and enter the target tissue [110]. Nano-carriers are helpful particularly in anti-cancer drug delivery due to the Enhanced Permeability and Retention (EPR) effect [5,6]. In an active tumor, the vasculature differs from that in normal tissue as it is leaky, irregular with large gaps or fenestrations [7]. Furthermore, a poor lymphatic drainage and slow venous blood return alongside increased permeability of the tumor tissue results in an accumulation of nanoparticles and macromolecules (>50 kDa) within the tumor interstitium [8]. Previous research has shown that nanoparticles can deliver drugs to tumor tissue with local concentrations higher than with free drug administration. The drug concentrations in tumor tissue were also significantly higher than in normal tissue [5].

Considerable efforts have been channeled towards developing a bio-compatible and degradable nanoparticle-based delivery system for cancer therapeutics. The nanoparticles should be composed of a polymer that is chemically inert, free of impurities and easily degrades into a non-toxic material that does not harm the body and is rapidly removed from circulation. Human serum albumin (HSA) is an acidic protein, retains stability over a pH range of 4-9, suitable for nanoparticle synthesis as it is the most abundant plasma protein, thus easily metabolized and does not have a toxic impact on the body [139].

One of the major benefits of a nanoparticle-based delivery system is to allow the cargo therapeutics such as siRNA to remain stable in circulation over a longer period of time [102,106]. Small interfering RNA (siRNA)-based therapy has shown the potential of developing into a potent cancer treatment; however, its application is limited by its rapidly degradable nature of siRNA. siRNA-mediated gene silencing, also known as RNA interference (RNAi), involves post-transcriptional silencing of specific genes [154]. siRNAs are composed of double-stranded RNA, approximately 21-22 nucleotides in length, and are processed by a RNase III enzyme [154]. siRNA interacts with a protein complex, known as RNA-induced silencing complex (RISC), and activates it. Upon activation, the RISC is directed to the target complementary strand of mRNA molecules, leading to sequence-specific cleavage of the target transcript [33]. By incorporating

siRNA into nanoparticles, the gene silencing function of siRNA can be exploited to target cancer.

In order to facilitate the cellular uptake of nanoparticles, several coatings may be added on the nanoparticle surface. A great amount of research has been carried out to study the use of peptides that have the ability to enhance cell adhesion and internalization of eukaryotic plasma membranes [94]. These peptides are also known as cell penetrating peptides (CPPs) and are capable of penetrating the cell membrane and can be used to enhance the transport of peptides, drug molecules and genes. One such protein is the *trans*-activating transcriptional activator (TAT) protein, found in HIV-I [95]. Protein transduction domains (PTDs) are the regions found within the structure of proteins and peptides that enable these molecules to easily traverse the cell membrane through a process that is receptor, transporter and endocytosis-independent [96]. Some studies suggest that CPPs may be involved in targeting the lipid layer directly, through promoting the reorganization of the membrane lipids [96]. The PTD of the TAT protein consists of 10 residues (47-57) which include mostly basic (arginine and lysine) amino acids; the domain conforms into an alpha helix shape [97].

In this study, we investigate the use of a novel TAT-coated HSA nanoparticle delivery system for carrying siRNA into MCF-7 breast cancer cells. In order to characterize the developed nanoparticles, the amount of TAT added to coat the surface was optimized, based upon particle size, surface zeta potential and transfection efficiency. In addition, the efficacy of siRNA delivery using TAT-coated HSA nanoparticles was assessed. Results showing low cytotoxicity of the nanoparticles, high cellular transfection and preservation of siRNA structure and function suggest that the developed nanoparticle system may serve as a promising vector for siRNA delivery.

MATERIALS AND METHODS

Materials

Human serum albumin (HSA Fraction V, purity 96-99 %), 8% glutaraldehyde and fluorescein isothiocyanate (FITC)-tagged HSA were purchased from Sigma Aldrich (ON, Canada). TAT (GRKKRRQRRRPQ) and scrambled-TAT (GRKRKQRPRRRQ) (s-TAT) were purchased from Sheldon Biotechnology Centre (QC, Canada) [95]. All other reagents were purchased from Fischer (ON, Canada). To maintain the cell culture, the reagents such as fetal bovine serum, trypsin, Dulbecco's modified Eagle's Medium and Opti-MEM I Reduced Serum Medium were obtained from Invitrogen (ON, Canada). The breast cancer cell-line, MCF-7, was purchased from ATCC (ON, Canada). RNase A, HiPerfect Transfection Reagent, AllStars Hs Cell Death Control siRNA and AllStars Alexa Fluor-488 conugated negative control siRNA were purchased from Qiagen (ON, Canada). Promega Cell-Titer 96® AQueous Non-Radioactive Cell Proliferation MTS Assay kit was purchased from Promega (WI, USA).

Cell culture

MCF-7 cells were cultured and grown on tissue culture plates according to the manufacturer's instructions. They were grown in Dulbecco's modified Eagle's Medium (Invitrogen) supplemented with 10% (v/v) fetal bovine serum and placed in an incubator with 5% CO_2 at 37°C. The cells used in this study were obtained from passages 5-6.

Preparation of TAT-coated HSA nanoparticles

TAT-coated HSA nanoparticles were prepared at room temperature using a desolvation technique, as shown in Figure 5.1 [128-130,144]. Briefly, 20 mg of HSA was added to 1 ml of 10 mM NaCl (aq) under constant stirring (800 rpm) at room temperature. The solution was stirred for 10 min. Upon complete dissolution, the solution was titrated to pH 7.5-8.0 with 1 N NaOH (aq) and stirred for 5 min. This aqueous phase was subjected to desolvation by the slow addition of ethanol to the HSA solution under constant stirring. Ethanol was added drop-wise using a micropipette until the solution became turbid (~1-2 ml). Adding an excess of ethanol caused the particles to form aggregates. Cross-linking

agent, 8 % glutaraldehyde, was added to stabilize the HSA particles. The formed nanoparticles were centrifuged three times and washed with deionized water (dH_20), followed by resuspension in an equal volume of Phosphate Buffer Saline (PBS). TAT dissolved in dH_20 was added to the nanoparticle preparation to allow TAT to form an outer coating due to electrostatic binding. For the preparation of siRNA-loaded HSA nanoparticles, siRNA was added to the 1 ml HSA solution after pH adjustment and allowed to stir for 30 min, followed by ethanol addition.

Purification of TAT-coated HSA nanoparticles

TAT-coated HSA nanoparticles were ultra-centrifuged at 16000 g for 15 min and re-suspended in 10 mM NaCl (aq) by vortexing, followed by ultrasonication (Branson 2510) for 10 min. This method was repeated thrice to ensure complete removal of free TAT, ethanol and other impurities.

Determining particle size and surface zeta potential

The particle size, zeta potential and polydispersity index (PDI) were measured by electrophoretic laser Doppler anemometry, using a Zeta Potential Analyzer (Brookhaven Instruments Corporation, USA). The HSA nanoparticles were diluted 1:10 with double-distilled water prior to measurement [129].

Surface characterization of TAT-coated HSA nanoparticles

The size and shape of the HSA nanoparticles were observed by transmission electron microscopy (TEM), using Philips CM200 200 kV TEM (Markham, Canada). Samples for atomic force microscopy (AFM) were prepared using the same technique as described above for SEM observation. 1 µl of the sample was dropped onto the surface of the disc. Images were produced with Nanoscope III (Digital Instruments, Palo Alto, USA) using a silicon cantilever in tapping mode and analyzed using the Nanoscope software (version 5.12r5; Digital instruments) [128,129,144].

Gel Retardation Assay

The gel retardation assay was performed to assess the protection TAT-coated HSA nanoparticles can provide siRNA from RNAse degradation. The siRNA-nanoparticle

complexes, containing the Allstar Cell death siRNA (Qiagen) were incubated with RNAse A for 30 or 60 minutes. The siRNA-loaded nanoparticles were then loaded onto a 4% agarose gel with 6x loading buffer. The gel electrophoresis was carried out in 0.5× Tris/Borate/EDTA (TBE) buffer at 100 V for 25 minutes. The siRNA bands were visualized using an ultra violet (UV) imaging system [155].

Transfection of breast cancer cells with siRNA containing nanoparticles

Prior to transfection, MCF-7 cells were washed with Phosphate buffered saline (PBS) and replenished with fresh serum-free Opti-MEM I. The TAT-coated HSA nanoparticles were added to the cells and incubated at 37˚C for the specified duration. Upon incubating cells with the nanoparticles, the culture medium was replaced with fresh DMEM, containing 10% FBS. Under the fluorescence microscope (TE2000-U, Nikon; USA), pictures were taken to assess the transfection efficiency of the nanoparticles. The percentage of transfected cells was calculated by using the average of the number of cells exhibiting fluorescence under five different fields of view [128,155].

Cell viability assay

Cell viability was evaluated using the Promega Cell-Titer 96® AQueous Non-Radioactive Cell Proliferation MTS Assay kit. For this, 3-(4, 5-dimethylthiazol-2-yl)-5-(3-carboxymethoxyphenyl)-2-(4-sulfophenyl)-2H-tetrazolium, (MTS) and phenazine methosulfate reagents were used. Living cells reduce MTS to form formazan, a compound soluble in tissue-culture media. The amount of formazan is thus proportional to the number of living cells and can be quantified by measuring the absorbance of formazan using 1420-040 Victor3 Multilabel Counter (Perkin Elmer, USA) at 490 nm. MCF-7 cells were seeded onto a 96-well plate (10^4 cells per well) 24 hrs before treatment. Cytotoxicity was measured at the pre-determined time for each experiment using the MTS assay as per the manufacturer's protocol [128,129].

RESULTS

Characterization of TAT-coated HSA nanoparticles for siRNA delivery

The nanoparticles were prepared using a modified version of a desolvation protocol as shown in a schematic illustration in Figure 5.1 [130,144]. Nanoparticles were formed by the addition of a desolvation agent, ethanol, to 20 mg/ml of HSA solution that was titrated to pH 8.5-9. As shown in Figures 5.2 and 5.3, the TEM, SEM and AFM micrographs of the TAT-coated HSA nanoparticles were obtained to visualize empty nanoparticles. The micrographs in Figure 5.2 (a,b) show well-dispersed particles, roughly spherical shaped. Figure 5.2 shows an AFM image that provides a three-dimensional view of the nanoparticles.

As illustrated in Figures 5.4 and 5.5, the nanoparticles were optimized based on the effect of amount of TAT added on size and surface zeta potential. Using TAT quantities of 0, 200, 400, 600 and 1200 µg added to nanoparticles formed from 20 mg/ml of HSA solution, the size of the nanoparticles was observed to increase slightly as the amount of TAT was increased to 400 µg of TAT, as shown in Figure 5.4. However, further increasing the amount of TAT did not show a significant increment in the particle size. Figure 5.5 shows the surface zeta potential measurements using increasing quantities of TAT. Coating the negatively charged surface of HSA nanoparticles with increasing amount of TAT resulted in a positive surface zeta potential. Without TAT coating, the surface charge of the nanoparticles was observed to be ~ -43 mV. With 200 µg of TAT, the surface zeta potential increased to ~ +7 mV, and further increasing to ~ +15 mV with 600 µg of TAT. Adding more TAT did not result in additional increase of surface charge.

Optimizing the amount of TAT for minimum cytotoxic effects on breast cancer cells

The MTS assay was employed to determine the cytotoxic effect of empty TAT-coated HSA nanoparticles. MCF-7 cells (10^4 cells per well) were cultured in a 96 well-plate and incubated with 100 µl of the TAT-coated HSA nanoparticle preparations for 48 hrs. Untreated cells were incubated with pure cell culture media, DMEM, and considered as the control treatment. Figure 5.7 shows that adding 400 µg or lower amounts of TAT for coating the HSA nanoparticles resulted in only a negligible decrease in cell viability. Adding 600 or 1200 µg of TAT resulted in successive decrease in cell viability to 80 % and 70 %, respectively.

Protection from siRNA degradation by nanoparticles

Untreated naked siRNA degraded with RNase A for 30 min. was loaded in lane 1, as shown in Figure 5.8. Lane 1 is empty and does not show any band, indicating that naked siRNA was rapidly degraded by added RNase A. Nanoparticles containing Allstar Cell death siRNA, incubated with RNase A for 30 minutes and 60 minutes were loaded in lanes 2 and 3, respectively. A clear band can be observed at the starting point of the well in Lane 2, while Lane 3 shows a fainter band at the well. As siRNA was trapped inside the HSA nanoparticles in Lane 2 and 3, it remained protected from RNase degradation and was thus unable to travel through the gel.

Efficient nanoparticle-mediated transfection in breast cancer cells

Cellular uptake of empty TAT-coated HSA nanoparticles was shown by transfecting MCF-7 cells with nanoparticles synthesized using fluorescein isothiocyanate (FITC)-tagged HSA in the nanoparticles, as presented in Figure 5.6. The presence of fluorescence within the cells suggests that considerable cellular uptake of the nanoparticles took place. In addition, Allstar Alexa Fluor-488 conjugated negative control siRNA was incorporated into TAT-coated HSA nanoparticles to determine the transfection efficiency of the siRNA-loaded nanoparticles as illustrated in Figures 5.9 and 5.10. Transfection efficiency was measured for varying amounts of TAT added to coat the HSA nanoparticles: 200, 400 and 600 µg. MCF-7 cells (10^4 cells per well) were cultured in a 96 well-plate and incubated with 100 µl of the nanoparticles, containing 20 ng of the labeled AllStar control siRNA (Qiagen) that were re-suspended in Opti-MEM I transfection medium. Results in Figure 5.9 show an increase in transfection efficiency with respect to incubation time. Transfection efficiency approximately increases by 3 times as the incubation time is increased from 0.5 to 6 hrs. Further increasing the incubation time from 6 to 12 hrs does not lead to an increment in transfection efficiency; however, a slight decrease in the transfection efficiency was observed. In addition, the amount of TAT applied for coating the nanoparticles shows a direct relationship with the percentage of cells transfected. After an incubation period of 0.5 hr, the transfection efficiency of all nanoparticle preparations appears to be largely the same. After 2 hrs of incubation, the effect of adding an outer coating of TAT seems to be evident as the trend

shows that higher amounts of TAT yield higher transfection efficiency. After 4 hrs of incubation, the transfection efficiencies of nanoparticles prepared without TAT as compared to nanoparticles with a coating of 200 µg appear to have little difference. Although the difference between the transfection efficiency of nanoparticles prepared with 400 and 600 µg was miniscule, they are higher than the transfection efficiency observed for nanoparticles without TAT and coated with 200 µg of TAT, as evident in Figure 5.9. The highest transfection efficiency achieved across all incubation time points and nanoparticle preparations was with 400 µg of TAT coating after 6 hrs of incubation. Transfection efficiency of nanoparticles prepared with 600 µg of TAT coating was lower than that of nanoparticles with 400 µg of TAT coating after 6 hrs of incubation. At 12 hrs of incubation, the transfection efficiency of all nanoparticle preparations, except for nanoparticles prepared without TAT, was lower than at an incubation of 6 hrs, as shown in Figure 5.9.

Figure 5.10 illustrates the effect of other parameters on transfection efficiency of TAT-coated HSA nanoparticles. Firstly, transfection was carried out in MCF-7 cells using different transfection media. Results from Figure 5.10 (a) suggest that transfection was lowest for cells that were transfected using Phosphate buffered saline (PBS) (pH 7.2 1X) as the transfection medium. An increase in the cell transfection was observed when serum-free DMEM (no FBS) was used as the transfection medium instead of PBS. However, adding 10% Fetal bovine serum (FBS) to DMEM showed a decrease in cell transfection as compared to using only DMEM (no added FBS). The highest transfection was observed when OPTI-MEM (Reduced Serum Medium) was used as the transfection medium.

Secondly, the cell confluence and amount of nanoparticles added to the cells were simultaneously optimized to achieve the highest transfection level, as shown in Figure 5.10 (b). Adding 50 µl of the nanoparticle preparation to the MCF-7 cells resulted in the lowest cell transfection across the three variations of cell confluence. There appears to be little difference in the percentage of transfected cells achieved with 100 and 150 µl. A trend of decreasing cell transfection with increase in cell confluence is evident. Lowest

transfection for all three volumes of nanoparticle preparation added was obtained at a cell confluence of $1x10^5$ cells per well of a 96-well plate.

Thirdly, Figure 5.10 (c) shows the effect of adding an outer TAT coating on cell transfection of the nanoparticles which was tested using two HSA concentrations, 10 and 20 mg/ml. For all three nanoparticle preparations, using 10 mg/ml of HSA concentration to form the nanoparticles resulted in lower cell transfection than 20 mg/ml of HSA. TAT-coated nanoparticles showed the highest percentage of cell transfection, while the lowest percentage of transfection was observed with nanoparticles with no TAT-coating. Using scrambled-TAT (s-TAT) to coat the nanoparticles resulted in slightly lower cell transfection than the percentage achieved with TAT-coated nanoparticles. Images illustrating fluorescence inside cells due to the incorporated Allstar Alexa Fluor-488 conjugated negative control siRNA also support the assertion that TAT-coated HSA nanoparticles have increased transfection efficiency, as observed in Figure 5.10 (d, e, f).

Using TAT-coated HSA nanoparticles to induce cell death in breast cancer cells

TAT-coated HSA nanoparticles, synthesized with 20 mg/ml HSA, 400 µg of TAT as an outer coating, were loaded with AllStars cell death siRNA. 2, 4 or 8 µg of the AllStars cell death siRNA was added to 1 ml of 20 mg/ml HSA to form the nanoparticles that were purified and re-suspended in 5 ml of DMEM. MCF-7 cells were grown in a 96 well-plate and incubated with 100 µl of the nanoparticle preparation. Nanoparticles loaded with the AllStars cell death siRNA were incubated with MCF-7 at 37 ºC for 4 hrs to allow for transfection. The gene silencing ability of the AllStar cell death siRNA, delivered by TAT-coated HSA nanoparticles, was assessed by using the MTS assay to measure cell death after 72 hrs of treatment, as shown in Figure 5.11. A cationic lipid preparation that is shown to conduct efficient siRNA transfection, HiPerfect transfecting reagent (Qiagen), was used to deliver AllStars cell death siRNA as a positive control in order to compare the performance of the newly developed nanoparticles. Untreated cells and cells incubated with free siRNA and empty nanoparticles were used as the negative controls for the experiment. All the TAT-coated HSA nanoparticle preparations containing AllStars cell death siRNA showed significant decrease in cell viability as compared to the negative controls. TAT-coated HSA nanoparticles carrying 4 and 8 µg of siRNA showed

a greater decrease in cell viability than the nanoparticles carrying 2 µg of AllStars cell death siRNA.

DISCUSSION

Over the past few years, nanoparticle-based delivery systems for cancer therapeutics have been of great interest to researchers across the world. The benefits of prolonged stability and bioavailability of the cargo molecule, tumor accumulation of nanoparticles due to the EPR effect of the tumor tissue and decreased systemic concentration are the main reasons for developing a nanoparticle-based delivery system for cancer drugs [2,10,148,156]. For upcoming gene-silencing therapies that hold considerable promise for cancer treatment, such as siRNA, a non-toxic biodegradable and biocompatible nanoparticle-based delivery system would increase the chances of their clinical application. In the current study, novel TAT-coated HSA nanoparticles have been developed and characterized for the delivery of siRNA to MCF-7 breast cancer cells.

The novel TAT-coated HSA nanoparticles were formulated using an ethanol desolvation technique, as shown in Figure 5.1 [130,144,157]. As shown in Figures 5.2 and 5.3, the formed particles were visualized using three different microscopic techniques: TEM, SEM and AFM. Results indicated the formation of well-dispersed, irregular spherical shaped nanoparticles, approximately 110$\pm$20 nm in size. Figure 4 shows a slight increase in particle size observed as higher amounts of TAT were used to coat the surface of HSA nanoparticles. This change in particle size could suggest that coating of the nanoparticle surface with TAT was successful. A large increase in surface zeta potential confirms that TAT was coated onto the surface of the HSA nanoparticles, as observed in Figure 5.5. The cationic TAT PTD, consisting of basic residues, is expected to electrostatically bind to the anionic surface of HSA nanoparticles at the experimental pH of 7.5-8 [158]. These results are in agreement with results published by Singh et al.; they studied the electrostatic coating of Poly-(L)-Lysine on the surface of HSA nanoparticles [148]. TAT adsorption onto the surface of HSA nanoparticles was assessed as a function of the amount of TAT added to the nanoparticles. The surface zeta potential reached a plateau

when 600 µg of TAT was added to 1 mg of HSA nanoparticles, indicating that the surface area of the HSA nanoparticles was saturated with adsorbed TAT molecules.

The successful cellular uptake of TAT-coated HSA nanoparticles was confirmed by visualizing fluorescence inside MCF-7 cells after incubating them with nanoparticles, composed of 5 % FITC-tagged HSA, as presented in Figure 5.6. Internalization of the siRNA-loaded nanoparticles is important for siRNA therapy as the negatively charged siRNA molecules do not easily penetrate the lipid cell membrane and need to be facilitated by a carrier system to access the intracellular action site [156]. Taking clinical application of this novel delivery system into consideration, the cytotoxicity of the particles was assessed. Figure 5.7 shows little toxic effect of the empty nanoparticles on MCF-7 breast cancer cells after 48 hrs of exposure. Low cytotoxicity is encouraging as the widespread clinical use of delivery systems, such as cationic liposomes, is hindered by their toxicity risk [159-162]. Cytotoxicity has been reported for cationic lipids in vitro and in vivo. More recently, cationic liposomal formulations have also resulted in activating non-specific gene expression [162] and play a role in increasing siRNA immunogenicity [163].

It is essential to ensure that protection from degradation is provided to the siRNA cargo by the carrier nanoparticles until the siRNA is released inside the cell where it can carry out its gene-silencing function. Results from the gel retardation assay, shown in Figure 5.8, suggest that the TAT-coated HSA nanoparticles successfully protect siRNA from rapid breakdown. The presence of a clear band at the loading well of lane-2 indicates that siRNA was protected from degradation by RNase A and was also retained inside the nanoparticles. The band observed at the loading well of lane-3 is fainter because of a longer exposure time of the siRNA-loaded nanoparticles to RNase A. Lane-1 shows the negative control. There is no band observed, confirming that naked siRNA was completely degraded by RNase A. These results suggest that siRNA remains protected from RNase degradation by encapsulating it into nanoparticles.

The transfection efficiency of the TAT-coated HSA nanoparticles was assessed by incorporating AllStars Alexa Fluor-488 conjugated negative control siRNA into the nanoparticles. The transfection efficiency of the nanoparticles increased as higher

amounts of TAT were used to coat the surface of the particles, as illustrated in Figure 5.9. 4-6 hrs of incubation time seemed optimal to allow for maximum transfection of nanoparticles. Figure 5.10 (a, b) shows that transfection efficiency was highest with serum-free Opti-MEM I, low cell confluence ($1x10^4$), incubated with 100-150 µl of the nanoparticle preparation. In addition, nanoparticles coated with TAT showed higher transfection as compared to nanoparticles coated with s-TAT or uncoated nanoparticles as observed in Figure 5.10 (c), suggesting that TAT does play a role in facilitating better cellular uptake of the nanoparticles. The fact that TAT-coated nanoparticles resulted in higher transfection than s-TAT-coated nanoparticles suggests that TAT helps in the internalization of nanoparticles in a sequence-specific manner; thus the primary and secondary structures of the TAT PTD are important [97,158]. These findings are in coherence with previously published results which show improved transfection of lipofectin by mixing TAT with the particle preparation, without a covalent linkage [164]. A higher transfection efficiency of nanoparticles coated with s-TAT as compared to uncoated nanoparticles shows that the positive charge of the s-TAT also contributes to the cellular uptake of the particles. The fluorescence microscope images shown in Figure 5.10 (d, e, f) confirm these findings and illustrate that the greatest density of AllStars Alexa Fluor-488 conjugated negative control siRNA was observed using TAT-coated HSA nanoparticles, followed by s-TAT-coated nanoparticles. The lowest transfection was observed with uncoated nanoparticles.

Lastly, results in Figure 5.11 show that the novel TAT-coated HSA nanoparticles succeeded in protecting the functionality of the cargo siRNA. AllStars Cell death siRNA, designed to induce cell death in various cancer cell-lines, was delivered using the developed nanoparticles. The increase in cell death after the delivery of the AllStars Cell death siRNA suggests that the siRNA being carried by the nanoparticles retains its gene silencing function. It can also be concluded that the procedure of nanoparticle preparation does not compromise the structure or function of the siRNA. Empty TAT-coated HSA nanoparticles and naked siRNA serve as negative controls and showed negligible cell death. These results can be compared with our previous study involving the delivery of siRNA using polyethylenimine-coated HSA nanoparticles [128]. The TAT-coated HSA nanoparticles appear to be more effective in protecting the

encapsulated siRNA and delivering it to cells. There was a greater percentage of cell death when AllStars Cell death positive control siRNA was delivered using TAT-coated HSA nanoparticles instead of polyethylenimine-coated HSA nanoparticles. These results also suggest that the positive charge of TAT is not the only factor helping cellular uptake of siRNA loaded nanocomplexes, and that the sequence of the TAT peptide plays a role.

The clinical use of viral delivery systems is limited by the safety risks, such as severe immunogenicity and pathogenicity, associated with them [165]. In this current study, we have developed an enhanced albumin-based nanoparticle delivery system, exploiting the cell penetrating ability of the TAT peptide from HIV-1. The delivery system has very low cytotoxicity, sufficient cell transfection efficiency and would therefore serve as a suitable non-viral gene delivery system.

CONCLUSION

The present study developed a novel TAT-coated HSA nanoparticles for the efficient delivery of siRNA to MCF-7 breast cancer cells. A narrow range of particle size was observed and the morphology was studied using various microscopic techniques, illustrating roughly spherically shaped well-dispersed nanoparticles. An increase in the surface zeta potential charge of the HSA nanoparticles upon TAT coating was observed with increasing amounts of TAT. The developed nanoparticles resulted in very low cytotoxicity to MCF-7 cells, although sufficient cellular uptake was observed. The positive surface charge of TAT and its primary amino acid sequence seem to play a role in the internalization of the TAT-coated nanoparticles. siRNA encapsulated inside TAT-coated HSA nanoparticles was shown to remain intact and retain its functional integrity. The promising results found in this study suggest that the novel TAT-coated HSA nanoparticles have great potential for developing into an effective delivery system for cancer therapeutics.

Acknowledgements

This work is supported by a research grant to S.P. from Canadian Institutes of Health Research (CIHR), MOP # 93641. S.A. is supported by the McGill Faculty of Medicine Internal Studentship - G. G. Harris Fellowship and the Ontario-Quebec Exchange

Fellowship. A.P. acknowledges the financial support from NSERC Alexander Graham Bell Canada Graduate Scholarship. The authors are grateful for the assistance provided for TEM imaging by Dr. Xue-Dong Liu, McGill, Department of Physics.

FIGURES

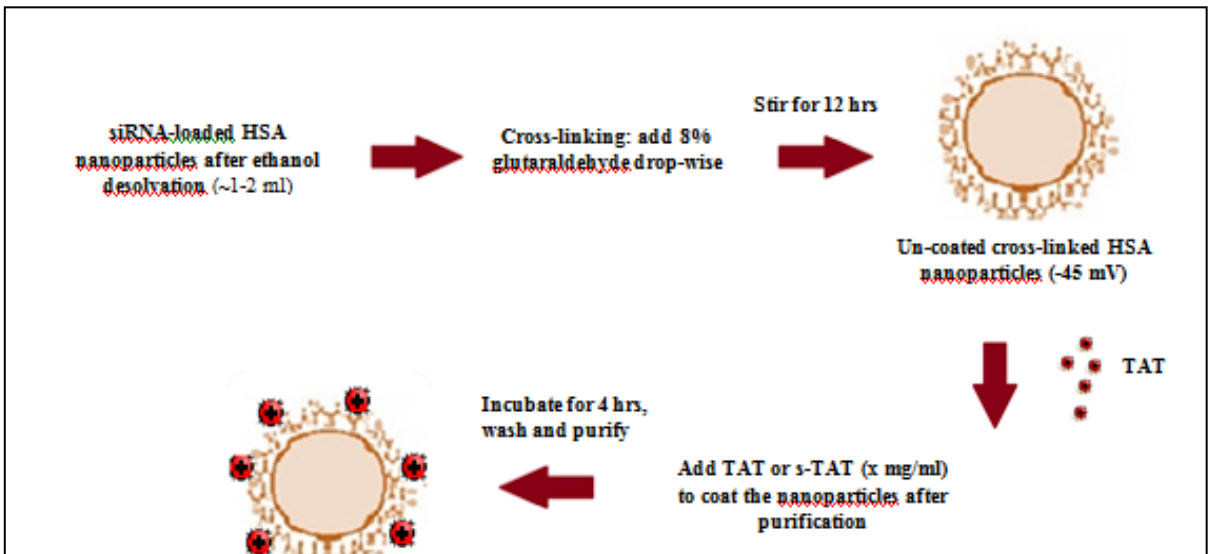

FIGURE 5.1: Schematic representation of the method employed to prepare TAT-coated HSA nanoparticles.

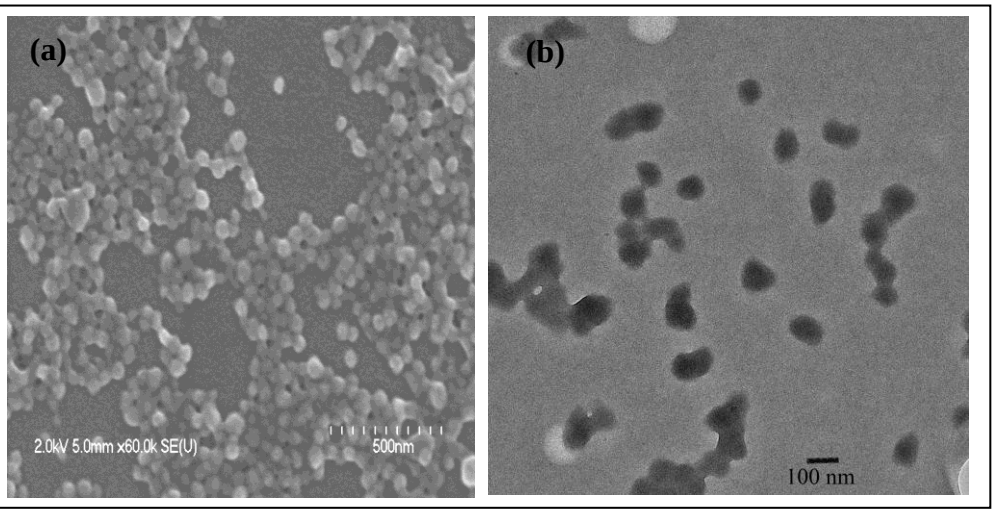

FIGURE 5.2: **(a)** Scanning electron microscope image, **(b)** Transmission electron microscope image of empty TAT-coated HSA nanoparticles. Images obtained from both techniques showed well-dispersed, roughly spherical nanoparticles, approximately 120-140 nm in size.

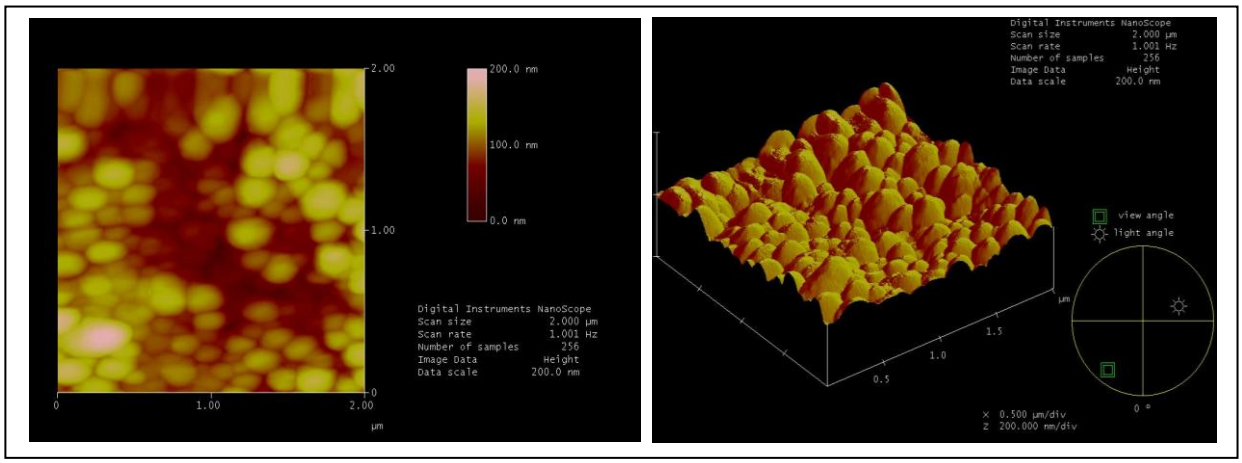

FIGURE 5.3: Atomic force microscopy image of empty TAT-coated HSA nanoparticles. The surface of the nanoparticles appeared to be smooth and spherical.

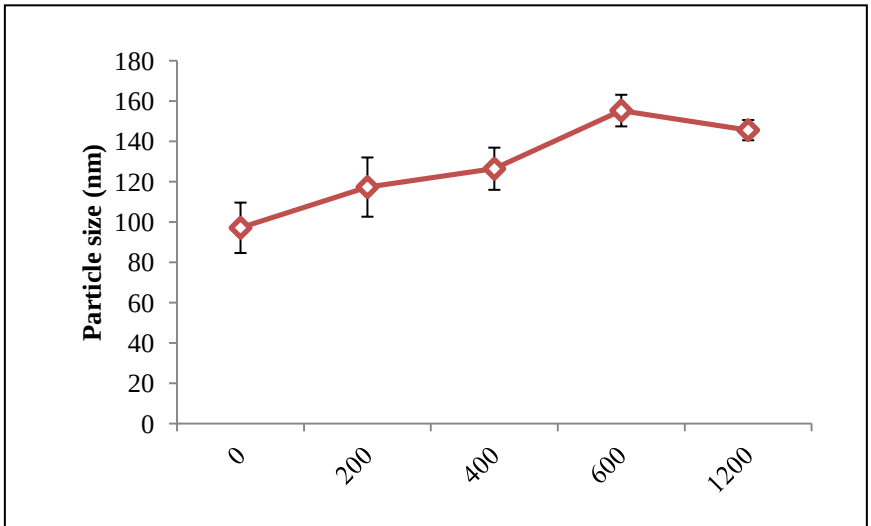

FIGURE 5.4: Effect of the amount of TAT added on the particle size (nm) of TAT-coated HSA nanoparticles (mean ± S.D., n=3). The nanoparticle size appeared to increase with higher amounts of TAT added for surface coating, until 600 µg of TAT.

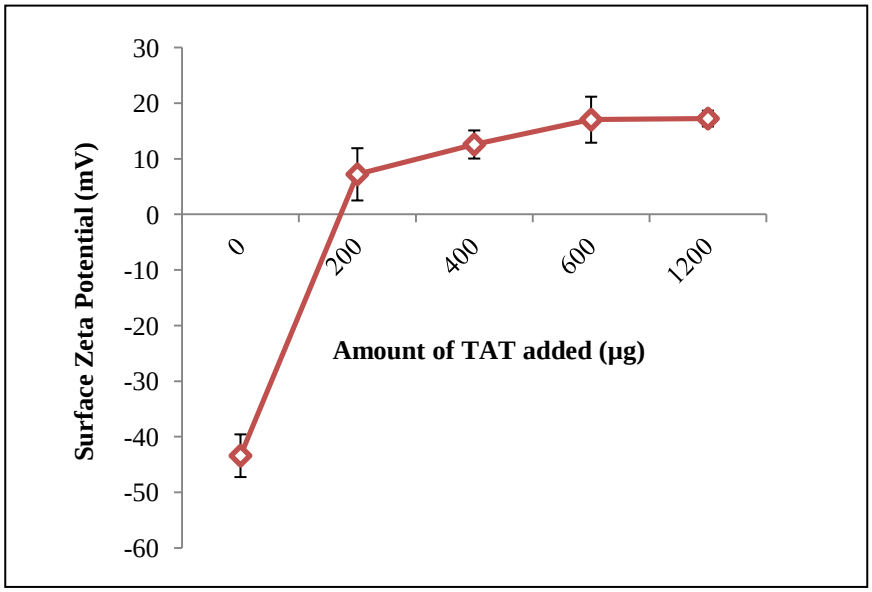

FIGURE 5.5: Effect of the amount of TAT added on the surface zeta potential (mV) of TAT-coated HSA nanoparticles (mean ± S.D., n=3). The surface zeta potential of the nanoparticles became more positive with increasing amounts of TAT added for surface coating, until 400 µg of TAT.

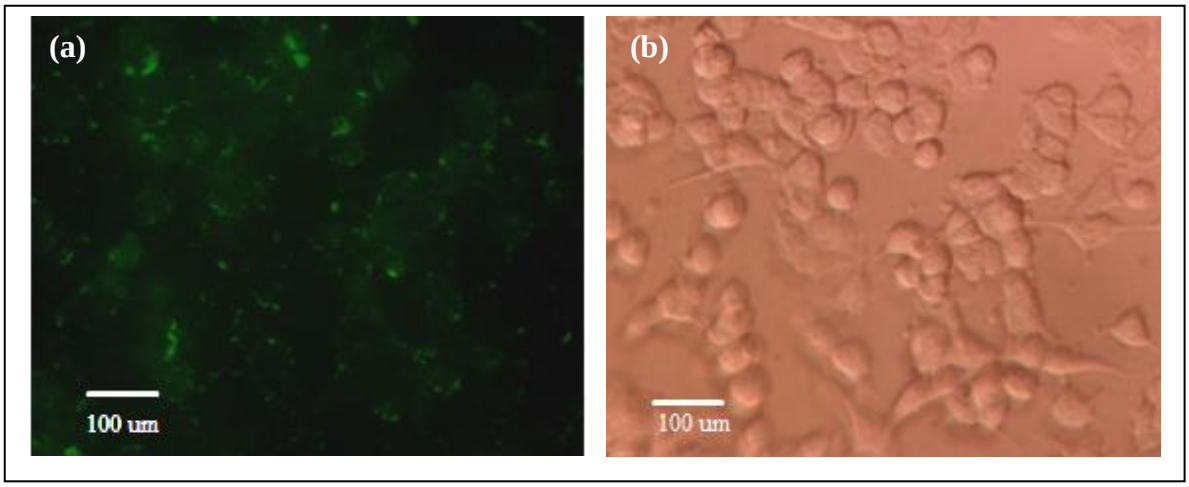

FIGURE 5.6: Cellular uptake of empty TAT-coated HSA nanoparticles. Nanoparticles were prepared using 25% FITC-tagged HSA of the total HSA. 100 µl of the nanoparticle preparation, re-suspended in serum-free Opti-MEM, were added to MCF-7 cells that were cultured in a 96 well-plate at 10^4 cells and incubated for 4 hrs. Pictures were taken under fluorescence (a) and bright field (b) to observe the transfection of nanoparticles using the fluorescence microscope (TE2000-U, Nikon; USA).

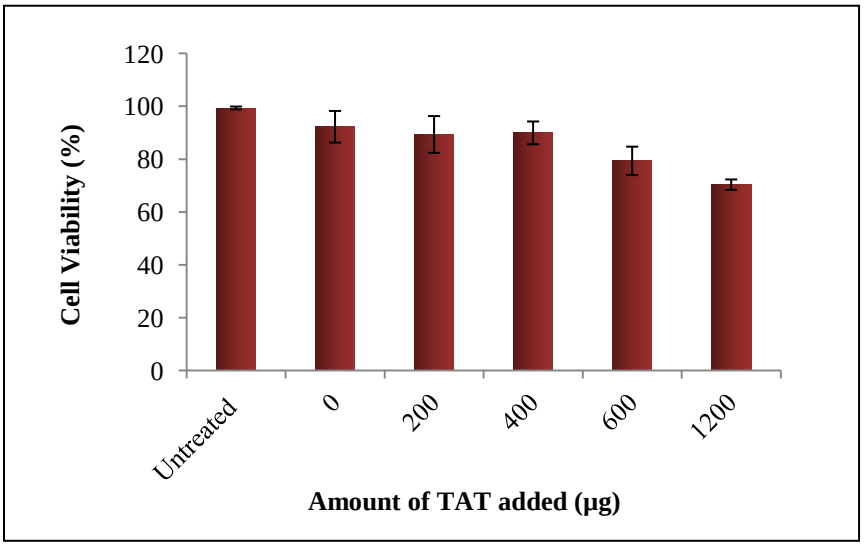

FIGURE 5.7: Cytotoxic effect of empty TAT-coated HSA nanoparticles on MCF-7 breast cancer cells. Nanoparticles were prepared with different amounts of TAT, ranging from 0-1200 µg (mean ± S.D., n=3). 100 µl of the nanoparticle preparation, suspended in DMEM, were added to MCF-7 cells that were cultured in a 96 well-plate at 10^4 cells and incubated for 48 hrs.

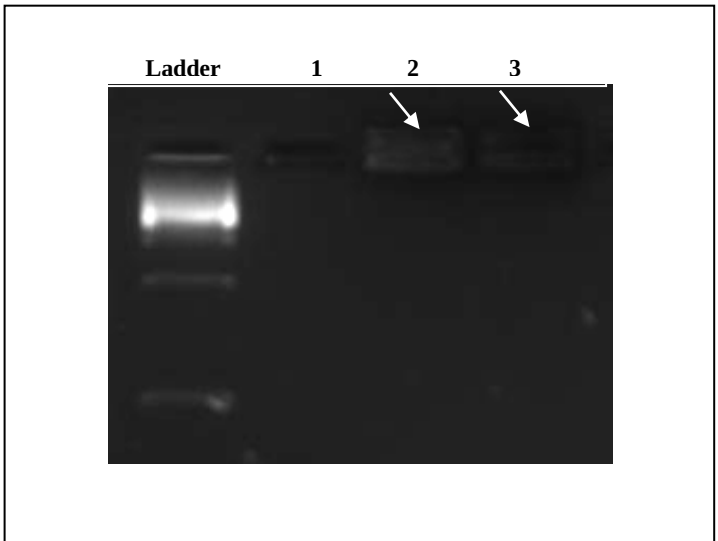

FIGURE 5.8: Effect of TAT-coated HSA nanoparticles on siRNA stability. Gel retardation assay was carried out using siRNA loaded TAT-coated HSA nanoparticles. Nanoparticles containing Allstar Cell death siRNA, incubated with RNase A for 30 and 60 minutes were loaded in lanes 2 and 3, respectively. Lane 1 was loaded with untreated naked siRNA incubated with RNase A for 30 minutes. 4 % agarose gel was used to run the samples at 100 V for 1 hr. The arrows point towards the band observed at the loading wells.

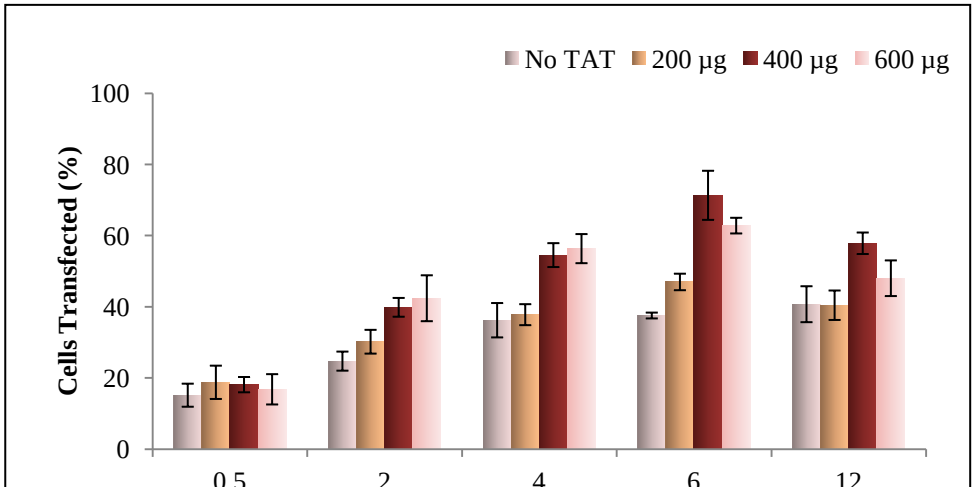

FIGURE 5.9: Transfection efficiency was measured using TAT-coated HSA nanoparticles prepared with varying amounts of TAT: 0, 200, 400 and 600 µg. Cells were incubated with each nanoparticle preparation for 0.5, 2, 4, 6 and 12 hrs. Transfection efficiency was determined by manually counting the percentage of cells showing fluorescence different fields of view (mean ± S.D., n=3). TAT-coated HSA nanoparticles were prepared by ethanol desolvation with 20 mg/ml HSA which was titrated to pH 9.0, cross-linked with glutaraldehyde and then coated with TAT. 10 µg of the non-silencing Allstars negative control siRNA tagged with Alexa 488 was added to HSA prior to ethanol addition. Upon purification, it was re-suspended in 5 ml cell-culture media. MCF-7 cells were cultured in a 96 well-plate and incubated for 4 hrs at 37 ºC with 100 µl of the nanoparticles re-suspended in serum-free Opti-MEM I.

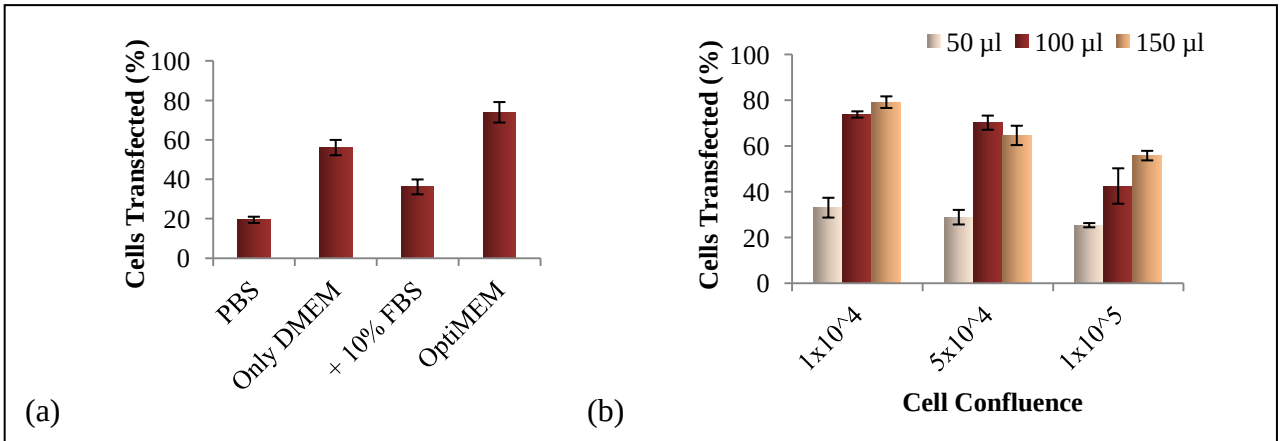

)

FIGURE 5.10: Transfection efficiency was measured using different parameters (mean ± S.D., n=3). TAT-coated HSA nanoparticles were prepared by ethanol desolvation with 20 mg/ml HSA. 10 µg of non-silencing Allstars negative control siRNA tagged with Alexa Fluor-488 was loaded into the nanoparticles. Upon purification, the nanoparticle formulation was re-suspended in 5 ml cell-culture media. MCF-7 cells were cultured in a 96 well-plate and incubated for 4 hrs at 37 ºC with 100 µl of the nanoparticles re-suspended in serum-free Opti-MEM I. The parameters that were tested include: **(a)** different transfection media, **(b)** variation of cell confluence incubated with 50, 100 and

150 µl of the nanoparticle preparation and **(c)** 10 mg/ml or 20 mg/ml of HSA to form different nanoparticle preparations, TAT-coated (TAT-np), s-TAT-coated (s-TAT-np) and without TAT (No TAT-np). s-TAT-coated nanoparticles were prepared using TAT with a scrambled primary sequence. Fluorescence microscope (TE2000-U, Nikon; USA) images of MCF-7 cells transfected with three different HSA nanoparticle preparations are illustrated: **(d)** TAT-coated HSA nanoparticles, **(e)** s-TAT-coated HSA nanoparticles, **(f)** HSA nanoparticles without coating, with corresponding bright field images **(d', e' and f').**

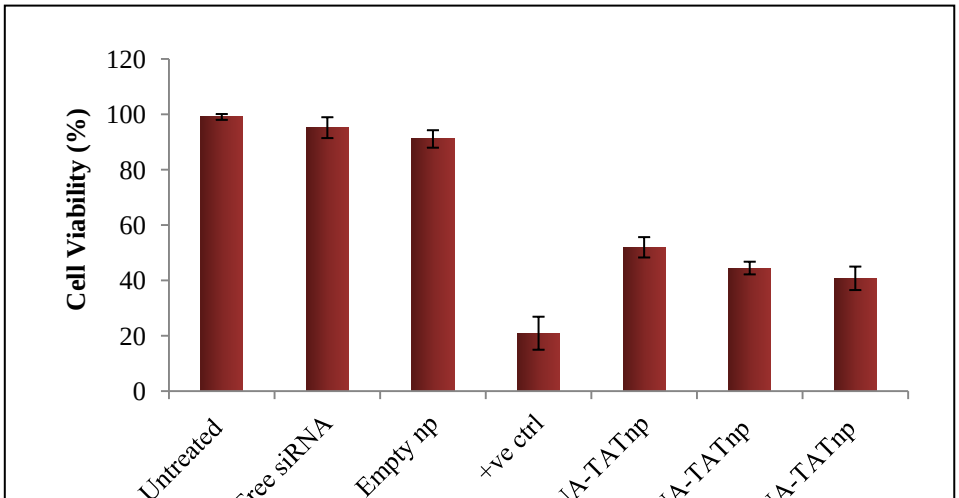

FIGURE 5.11: Assessing the functionality of siRNA delivered using TAT-coated HSA nanoparticles (TATnp). 2, 4 or 8 µg of the Allstars Cell Death siRNA was added to 20 mg/ml HSA. The nanoparticles were synthesized using the optimized parameters and re-suspended in 5 ml cell-culture media. MCF-7 cells (10^4 cells per well) were grown in a 96-well plate and incubated for 4 hrs at 37 ºC with 100 µl of the nanoparticles re-suspended in DMEM. The induction of cell death was measured after 72 hrs using the MTS assay (mean $\pm$ S.D., n=3). HiPerfect transfection reagent was used to deliver the AllStars Cell death siRNA as a positive control. Untreated cells, cells incubated with free siRNA and cells incubated with empty nanoparticles (Empty np) were taken as negative controls.

CHAPTER 6

GENERAL DISCUSSION

Scientific research advances have not proportionally translated into clinical improvisations for cancer treatments. Nanobiotechnology holds promise to ensure that potent anti-cancer drugs, such as doxorubicin, can be used more effectively to eliminate cancerous cells without adverse side-effects. Biocompatible and biodegradable delivery

systems, such as HSA nanoparticles, have potential of becoming non-toxic carriers for drug and gene therapeutics. Nanoparticle-based delivery systems exploit the Enhanced Permeability and Retention Effect of tumour tissue and allow for passive targeting of the anti-cancer therapeutic [67,68]. Encapsulating cytotoxic anti-cancer drugs will therefore reduce the side effects caused by them, due to higher accumulation of the nanoparticles within the tumour tissue and lower systemic concentration. Moreover, employing a nano-carrier will also protect siRNA molecules, used for gene-silencing anti-cancer therapy, from rapid degradation in circulation. Altogether, this research work puts forth modified cationic HSA nanoparticles as a suitable delivery system for breast cancer applications.

Firstly, the use of siRNA loaded polyethylenimine (PEI)-coated HSA nanoparticles prepared, characterized and investigated for breast cancer applications. Under the optimized conditions, PEI-coated HSA nanoparticles were observed to be ~90 nm in size, carrying a positive surface charge ~+26 mV. According to other published studies, both size and charge are favourable for cellular uptake [125,127,150,166]. A comprehensive assessment of the cytotoxicity of the nanoparticle formulation was carried out. A very low cytotoxic effect with 25 kDa PEI suggests biocompatibility of the nanoparticles and the suitability of this delivery system for clinical applications. The use of siRNA for gene-silencing therapy is limited by their inability to transfect cells; thus, our results are encouraging as ~62% cells were transfected. Furthermore, RNase treatment of siRNA-loaded PEI-coated HSA nanoparticles showed that the siRNA was resilient towards enzymatic degradation of 30 min. This also indicates that the PEI-coated HSA nanoparticles are likely to protect siRNA in circulation, allowing further exploration into siRNA gene-silencing therapy. Finally, PEI-coated HSA nanoparticles provide an appealing alternative for viral gene delivery systems. Non-viral delivery systems have attracted immense attention in order to overcome the shortcomings of viral vectors. Adeno- or retroviruses may be used, however, risks related to immunogenicity and potential pathogenicity form a serious concern [117-119]. This severely restricts the potential of using viral vectors for clinical applications. PEI-coated HSA nanoparticles also possess other favorable characteristics, including biocompatibility, easy administration and a potential for targeted delivery [118].

Secondly, polyethylenimine (PEI)-enhanced HSA nanoparticles were examined as a suitable delivery system for doxorubicin in order to minimize the systemic concentrations of the drug and to benefit from passive targeting of tumour tissue due to the Enhanced Permeability and Retention effect. Doxorubicin is a potent cytotoxic anti-cancer drug, commonly prescribed for regimes against breast cancer. The dosage and use of this drug is severely limited by its side-effects of irreversible cardiotoxicity and congestive heart failure [20,22,23]. The formed nanoparticles were ~137 nm in size with a surface zeta potential of ~+15 mV, prepared using 20 µg of PEI added per-mg-of-HSA. Cytotoxicity was not observed with empty PEI-enhanced HSA nanoparticles, formed with low-molecular weight (25 kDa) PEI, indicating biocompatibility and safety of the nanoparticle formulation. Under optimized transfection conditions, approximately 80% of cells showed cellular uptake of HSA nanoparticles. The addition of a layer of PEI showed an increase in cellular uptake and is also designed to provide further stability and protection to the structural integrity of the particles. Glutaraldehyde cross-linking was carried out to stabilize the formed HSA nanoparticles before PEI surface coating; this increases the drug entrapment ability of the HSA nanoparticles [77]. In conclusion, PEI-enhanced HSA nanoparticles show potential for developing into an effective carrier for doxorubicin. In our study, we observed that the cytotoxicity of dox-loaded nanoparticle and free dox against MCF-7 breast cancer cells was about the same after 48 hrs as the dox concentration was increased. However, assessing the cytotoxicity at different time points showed that dox-loaded nanoparticles led to a greater decrease in cell viability as compared to free dox after 144 hrs. This observation can be explained by the slow release of dox from the nanoparticles. Results were promising and suggest that the study needs to be followed up with an in vivo investigation of the dox-loaded PEI-enhanced HSA nanoparticles.

Lastly, biodegradable nanocomplexes coated with a cell-penetrating peptide, the transactivating-transcriptional-factor (TAT) domain from HIV, were proposed as efficient carriers for anti-cancer therapeutics. The clinical application of gene-silencing using siRNA-based therapy is limited by the rapid degradation of siRNA in circulation. We developed and characterized the TAT-coated HSA nanoparticles in this study to deliver siRNA to MCF-7 breast cancer cells. The nanoparticles were observed to fall within the

size range of ~120-140 nm. The surface charge of the nanoparticles showed a rise with increasing amounts of TAT, reaching a plateau at ~+15mV. This observation was important in confirming that an outer layer of TAT did form on the particle surface. The cationic TAT PTD, consisting of basic residues, was electrostatically adsorbed to the anionic surface of HSA nanoparticles [158]. Taking clinical application of this novel delivery system into consideration, the cytotoxicity of the particles was assessed. Under the optimized transfection conditions, approximately 75% of cells showed presence of fluorescence, suggesting efficient cellular uptake of TAT-coated nanoparticles consisting of fluorescein isothiocyanate (FITC)-tagged HSA. The structural and functional integrity of siRNA inside the nanoparticles was protected against RNase degradation. The novel TAT-coated HSA nanoparticles characterized in this study could be developed into a safe non-viral delivery system for future clinical application.

CHAPTER 7

SUMMARY OF OBSERVATIONS

With the general aim to design a suitable drug and siRNA nanoparticle delivery system, this research was performed. Following are the summary of observations:

1) In Chapter 3, polyethylenimine (PEI)-coated human serum albumin (HSA) nanoparticles have been characterized and studied for efficient siRNA delivery to the MCF-7 breast cancer cell line in order to overcome the issues related to rapid degradation and low transfection of naked siRNA. The size and charge of PEI-coated HSA nanoparticles were optimized according to various parameters, including PEI quantity, HSA concentration, pH of the HSA solution before desolvation, and stirring speed. The smallest size of approximately 85 nm was achieved with 6.25 µg per mg HSA of PEI and 20 mg/ml of HSA. Similarly, the optimal pH level and the stirring speed, resulting in the smallest particle size was 8.5 and 800 rpm, respectively.
2) The lower M.W. (25 kDa) should be used for nanoparticle preparation as cytotoxicity was greater for the higher M.W. PEI (70 kDa). Amounts $\leq$ than 6.25 µg per mg HSA of 25 kDa PEI showed similar cytotoxicity levels.
3) The gel retardation assay was carried out to show that the PEI-coated HSA nanoparticles provide siRNA with protection from enzymatic degradation. The presence of a band around the well, where the samples were loaded, indicates that siRNA was not degraded by the RNase A and was retained within the nanoparticles. This retention of siRNA at the well of the agarose gel for Lane 2 and 3 confirms successful siRNA-loading of the nanoparticles.
4) The combination of 6.25 µg per mg HSA of 25 kDa PEI and 20 mg/ml of HSA showed maximum transfection. As PEI is a cationic polymer, increasing its amount makes the surface potential more positive, which would augment cellular uptake of the particle. However, further increasing the PEI amount to 12.5 µg showed lower transfection efficiency, which can be due to higher toxicity and consequent cell death.
5) Results show that the Cell death siRNA remains functional as it induces cell death; this indicates that the procedure applied to synthesize these nanoparticles does not lead to degradation of the siRNA.
6) In Chapter 4, the effectiveness of dox-loaded polyethylenimine (PEI)-enhanced HSA nanoparticles used against MCF-7 breast cancer cells was investigated. The

nanoparticles were prepared using an ethanol desolvation method and characterized by measuring particle size, surface zeta potential and cellular uptake

7) As the amount of PEI was increased, a slight increase in the particle size was observed and the surface zeta potential became positive. This increase in size was gradual and could be attributed to the addition of the PEI surface coating or slight aggregation of the particles. The surface zeta potential increased from approximately -47 to +18 mV, clearly indicating that the PEI was successfully adsorbed to the nanoparticle surface.
8) Results show that 8 hrs of incubation at a stirring speed of 1000 rpm resulted in the smallest particle size and maximum zeta potential. The TEM images illustrate roughly spherical shape of the formed HSA nanoparticles of approximately 100 nm of size.
9) Firstly, the lowest percentage of cellular uptake was observed with uncoated nanoparticles, which can be attributed to the negative surface zeta potential of the uncoated HSA nanoparticles. It can be concluded that increasing the amount of PEI, up to 20 µg of PEI per mg of HSA, used for coating the nanoparticles leads to an increasing in cellular uptake. Further increasing the amount of PEI used for coating the nanoparticles did not translate into higher cellular uptake. A reasonable conclusion to draw from the results of the cellular uptake experiment would be that the PEI adsorbed to the surface of the nanoparticles aids in the internalization of the particles.
10) In our study, we observed that the cytotoxicity of dox-loaded nanoparticles and free dox against MCF-7 breast cancer cells was about the same after 48 hrs as the dox concentration was increased, shown in Figure 4.4 (a). However, assessing the cytotoxicity at different time points in Figure 4.4 (b) showed that dox-loaded nanoparticles led to a greater decrease in cell viability as compared to free dox after 144 hrs. This observation can be explained by the slow release of dox from the nanoparticles.
11) In Chapter 5, we investigate the use of a novel TAT-coated HSA nanoparticle delivery system for carrying siRNA into MCF-7 breast cancer cells. In order to characterize the developed nanoparticles, the amount of TAT added to coat the

surface was optimized, based upon particle size, surface zeta potential and transfection efficiency.

12) Nanoparticles were formed by the addition of a desolvation agent, ethanol, to 20 mg/ml of HSA solution that was titrated to pH 8.5-9. The micrographs show well-dispersed particles, roughly spherical shaped.
13) Without TAT coating, the surface charge of the nanoparticles was observed to be ~ -43 mV. With 200 µg of TAT, the surface zeta potential increased to ~ +7 mV, and further increasing to ~ +15 mV with 600 µg of TAT. Adding more TAT did not result in additional increase of surface charge.
14) Adding 400 µg or lower amounts of TAT for coating the HSA nanoparticles resulted in only a negligible decrease in cell viability. Adding 600 or 1200 µg of TAT resulted in successive decrease in cell viability to 80 % and 70 %, respectively. These results indicate that TAT-coated HSA nanoparticles are biocompatible and non-toxic.
15) The gel retardation assay was carried out to investigate the protection and stability that TAT-coated HSA nanoparticles provide to siRNA. As siRNA was trapped inside the HSA nanoparticles in Lane 2 and 3, it remained protected from RNase degradation and was thus unable to travel through the gel.
16) Conditions for transfection of siRNA-loaded TAT-coated HSA nanoparticles were optimized. Results in Figure 5.9 show an increase in transfection efficiency with respect to incubation time. The difference between the transfection efficiency of nanoparticles prepared with 400 and 600 µg was miniscule, they are higher than the transfection efficiency observed for nanoparticles without TAT and coated with 200 µg of TAT. In addition, the amount of TAT applied for coating the nanoparticles shows a direct relationship with the percentage of cells transfected. The highest transfection efficiency achieved across all incubation time points and nanoparticle preparations was with 400 µg of TAT coating after 6 hrs of incubation.
17) Furthermore, the highest transfection was observed when OPTI-MEM (Reduced Serum Medium) was used as the transfection medium. A trend of decreasing cell transfection with increase in cell confluence is evident. Using 10 mg/ml of HSA

concentration to form the nanoparticles resulted in lower cell transfection than 20 mg/ml of HSA. TAT-coated nanoparticles showed the highest percentage of cell transfection, while the lowest percentage of transfection was observed with nanoparticles with no TAT-coating. Using scrambled-TAT (s-TAT) to coat the nanoparticles resulted in slightly lower cell transfection than the percentage achieved with TAT-coated nanoparticles.

18) TAT-coated HSA nanoparticles, synthesized with 20 mg/ml HSA, 400 µg of TAT as an outer coating, were loaded with AllStars cell death siRNA. The gene silencing ability of the AllStar cell death siRNA, delivered by TAT-coated HSA nanoparticles, was assessed by using the MTS assay to measure cell death after 72 hrs of treatment. Untreated cells and cells incubated with free siRNA and empty nanoparticles were used as the negative controls for the experiment. All the TAT-coated HSA nanoparticle preparations containing AllStars cell death siRNA showed significant decrease in cell viability as compared to the negative controls.

CHAPTER 8

CONCLUSIONS

This research study was based on the general hypothesis that surface modified HSA nanoparticles enhance the therapeutic efficacy of drugs (doxorubicin) and siRNA by

increasing the stability, bioavailability and cellular uptake of the loaded therapeutics for breast cancer applications. We investigated the use of a biodegradable and biocompatible delivery system for anti-cancer drugs (doxorubicin) and siRNA. HSA nanoparticles with cationic surface properties were developed and characterized in vitro for the enhanced delivery of anti-cancer drugs and siRNA. Surface coatings were added on the HSA nanoparticles to improve the cellular uptake of the drug-loaded nanoparticles to maximize the therapeutic efficacy of the drug. Firstly, polyethylenimine, a cationic polymer, was used to coat HSA nanoparticles to improve cellular uptake and particle stability. Both drug (doxorubicin) and siRNA was used to deliver using PEI-coated HSA nanoparticles. Results illustrated efficient transfection, retention of siRNA function and low cytotoxicity of the delivery system; it holds promise as a non-viral gene vector. Secondly, HSA nanoparticles were coated with a cell-penetrating peptide, the transactivating-transcriptional-factor (TAT) domain from HIV-1. TAT-coated HSA nanoparticles were developed and characterized in this study to deliver siRNA to MCF-7 breast cancer cells. These modified HSA-based nanoparticle delivery systems provide a carrier for unstable anti-cancer therapeutic, such as siRNA and allow for the potential reduction of systemic toxicity of anti-cancer drug such as doxorubicin. The findings of this study set a platform for further pre-clinical investigations of the suitability and benefit of the developed HSA-based nanoparticle delivery systems. In this manner, the results obtained in this study may eventually contribute towards an improved method of anti-cancer drug delivery; thereby, the quality of life of cancer patients, their survival rate and time span may be improved.

CHAPTER 9

Recommendations and Future Applications

1) The encouraging results found in this research study suggest a need for further study to assess suitability of the developed and characterized surface modified HSA nanoparticles. Firstly, a preliminarly in vivo study should be carried out to assess the efficacy of the nanoparticle-based therapeutic delivery. It needs to be established whether the proposed delivery system withstands the enzymatic degradation in circulation and is not removed by the reticuloendothelial system. Although in vivo studies using HSA nanoparticles have been previously carried out, no animal studies have been done with PEI-enhanced or TAT-coated HSA nanoparticles.

2) A more elaborate in vivo study should compare the proposed modified HSA nanoparticles to uncoated HSA nanoparticles carrying the therapeutics and the commonly crosslinking agent, glutaraldehyde.

3) In order to make developed nanoparticle delivery system clinically viable, a thorough toxicological investigation needs to be carried out. The in vitro effect of the nanoparticle preparation should be observed on other human cell lines. Furthermore, a biodistribution study should be carried out in vivo to investigate whether the nanoparticles aggregate in healthy tissues.

4) The developed modified HSA nanoparticles should be further characterized for the delivery of other anti-cancer therapeutics, such as epirubicin, docetaxel, other gene vectors, and proteins. Also, these nanoparticles should be studied for oral delivery of anti-cancer drugs by encapsulating them in microcapsules, such as the alginate-poly-L-lysine-alginate (APA) microcapsules [167].

5) The presented modified HSA nanoparticles could also be made more targeted for increased tumour-based selectivity by adding ligands on antibodies to the nanoparticles [21].

References

[1] J.Ferlay, H.R.Shin, F.Bray, D.Forman, C.Mathers, D.M.Parkin, "Estimates of worldwide burden of cancer in 2008: GLOBOCAN 2008," *International Journal of Cancer,* vol. 127, no. 12, pp. 2893-2917, 2010.

[2] R.Seigneuric, L.Markey, D.S.A.Nuyten, C.Dubernet, C.T.A.Evelo, E.Finot, C.Garrido, "From Nanotechnology to Nanomedicine: Applications to Cancer Research," *Current Molecular Medicine,* vol. 10, no. 7, 2010.

[3] A.H.Partridge, H.J.Burstein, E.P.Winer, "Side Effects of Chemotherapy and Combined Chemohormonal Therapy in Women With Early-Stage Breast Cancer," *JNCI Monographs,* vol. 2001, no. 30, pp. 135-142, 2001.

[4] J.Crown, M.O'Leary, "The taxanes: an update," *The Lancet,* vol. 355, no. 9210, pp. 1176-1178, 2000.

[5] A.K.Iyer, G.Khaled, J.Fang, H.Maeda, "Exploiting the enhanced permeability and retention effect for tumor targeting," *Drug Discovery Today,* vol. 11, no. 17-18, pp. 812-818, 2006.

[6] Y.J.Son, J.S.Jang, Y.W.Cho, H.Chung, R.W.Park, I.C.Kwon, I.S.Kim, J.Y.Park, S.B.Seo, C.R.Park, S.Y.Jeong, "Biodistribution and anti-tumor efficacy of doxorubicin loaded glycol-chitosan nanoaggregates by EPR effect," *Journal of Controlled Release,* vol. 91, no. 1-2, pp. 135-145, 2003.

[7] H.Maeda, J.Wu, T.Sawa, Y.Matsumura, K.Hori, "Tumor vascular permeability and the EPR effect in macromolecular therapeutics: a review," *Journal of Controlled Release,* vol. 65, no. 1-2, pp. 271-284, 2000.

[8] H.Maeda, "Tumor-Selective Delivery of Macromolecular Drugs via the EPR Effect: Background and Future Prospects," *Bioconjugate Chemistry,* vol. 21, no. 5, pp. 797-802, 2010.

[9] J.C.Cheng, T.B.Moore, K.M.Sakamoto, "RNA interference and human disease," *Molecular Genetics and Metabolism,* vol. 80, no. 1-2, pp. 121-128, 2009.

[10] Y.Patil, J.Panyam, "Polymeric nanoparticles for siRNA delivery and gene silencing," *International Journal of Pharmaceutics,* vol. 367, no. 1-2, pp. 195-203, 2009.

[11] A.Jemal, R.Siegel, E.Ward, Y.Hao, J.Xu, T.Murray, M.J.Thun, "Cancer Statistics, 2008," *CA: A Cancer Journal for Clinicians,* vol. 58, no. 2, pp. 71-96, 2008.

[12] J.Ferlay, H.R.Shin, F.Bray, D.Forman, C.Mathers, D.M.Parkin, "Estimates of worldwide burden of cancer in 2008: GLOBOCAN 2008," *International Journal of Cancer,* vol. 127, no. 12, pp. 2893-2917, 2010.

[13] R.G.Dumitrescu, I.Cotarla, "Understanding breast cancer risk - where do we stand in 2005?," *Journal of Cellular and Molecular Medicine,* vol. 9, no. 1, pp. 208-221, 2005.

[14] L.Brannon-Peppas, J.O.Blanchette, "Nanoparticle and targeted systems for cancer therapy," *Advanced Drug Delivery Reviews,* vol. 56, no. 11, pp. 1649-1659, 2004.

[15] J.G.Elmore, K.Armstrong, C.D.Lehman, S.W.Fletcher, "Screening for Breast Cancer," *JAMA: The Journal of the American Medical Association,* vol. 293, no. 10, pp. 1245-1256, 2005.

[16] V.Vinh-Hung, C.Verschraegen, For The Breast Conserving Surgery Project, "Breast-Conserving Surgery With or Without Radiotherapy: Pooled-Analysis for Risks of Ipsilateral Breast Tumor Recurrence and Mortality," *Journal of the National Cancer Institute,* vol. 96, no. 2, pp. 115-121, 2004.

[17] D.A.Berry, K.A.Cronin, S.K.Plevritis, D.G.Fryback, L.Clarke, M.Zelen, J.S.Mandelblatt, A.Y.Yakovlev, J.D.Habbema, E.J.Feuer, "Effect of Screening and Adjuvant Therapy on Mortality from Breast Cancer," *New England Journal of Medicine,* vol. 353, no. 17, pp. 1784-1792, 2005.

[18] C.Van Poznak, A.D.Seidman, "Critical Review of Current Treatment Strategies for Advanced Hormone Insensitive Breast Cancer," *Cancer Investigation,* vol. 20, no. s2, pp. 1-14, 2002.

[19] S.Greenberg, A.Stopeck, H.S.Rugo, "Systemic treatment of early breast cancerGÇöa biological perspective," *Journal of Surgical Oncology,* vol. 103, no. 6, pp. 619-626, 2011.

[20] T.Osako, R.Horii, M.Matsuura, K.Domoto, Y.Ide, Y.Miyagi, S.Takahashi, Y.Ito, T.Iwase, F.Akiyama, "High-grade breast cancers include both highly sensitive and highly resistant subsets to cytotoxic chemotherapy," *Journal of cancer research and clinical oncology,* vol. 136, no. 9, pp. 1431-1438, 2010.

[21] M.Richter, H.Zhang, "Receptor-Targeted Cancer Therapy," *DNA and Cell Biology,* vol. 24, no. 5, pp. 271-282, 2005.

[22] K.L.Maughan, M.Lutterbie, P.S.Ham, "Treatment of Breast Cancer," *Amerian Family Physician,* vol. 81, no. 11, 2010.

[23] M.S.Ewer, S.M.Lippman, "Type II Chemotherapy-Related Cardiac Dysfunction: Time to Recognize a New Entity," *Journal of Clinical Oncology,* vol. 23, no. 13, pp. 2900-2902, 2005.

[24] N.Normanno, A.Morabito, A.De Luca, M.C.Piccirillo, M.Gallo, M.R.Maiello, F.Perrone, "Target-based therapies in breast cancer: current status and future perspectives," *Endocrine-Related Cancer,* vol. 16, no. 3, pp. 675-702, 2009.

[25] E.A.Mittendorf, G.E.Peoples, S.E.Singletary, "Breast cancer vaccines," *Cancer,* vol. 110, no. 8, pp. 1677-1686, 2007.

[26] A.l.Huang, Y.Wan, D.y.Liao, H.z.Hu, L.Wei, X.h.Wang, Y.j.Wen, J.Li, L.j.Chen, B.Kan, P.Chen, Y.s.Wang, X.Chen, X.Zhao, H.x.Deng, Y.q.Wei, "Suppression of human MDA-MB-435S tumor by U6 promoter-driven short hairpin RNAs targeting focal adhesion kinase," *Journal of cancer research and clinical oncology,* vol. 136, no. 8, pp. 1229-1242, 2010.

[27] S.Jeyarajan, J.Xavier, N.M.Rao, "Plasmid DNA delivery into MDA-MB-453 cells mediated by recombinant Her-NLS fusion protein," *International Journal of Nanomedicine,* vol. 5, no. 1, 2010.

[28] S.Prabha, W.Z.Zhou, J.Panyam, V.Labhasetwar, "Size-dependency of nanoparticle-mediated gene transfection: studies with fractionated nanoparticles," *International Journal of Pharmaceutics,* vol. 244, no. 1-2, pp. 105-115, 2002.

[29] K.A.Howard, U.L.Rahbek, X.Liu, C.K.Damgaard, S.Z.Glud, M.O.Andersen, M.B.Hovgaard, A.Schmitz, J.R.Nyengaard, F.Besenbacher, J.Kjems, "RNA Interference in Vitro and in Vivo Using a Chitosan/siRNA Nanoparticle System," *Mol Ther,* vol. 14, no. 4, pp. 476-484, 2006.

[30] X.Liu, K.A.Howard, M.Dong, M.+.Andersen, U.L.Rahbek, M.G.Johnsen, O.C.Hansen, F.Besenbacher, J.r.Kjems, "The influence of polymeric properties on chitosan/siRNA nanoparticle formulation and gene silencing," *Biomaterials,* vol. 28, no. 6, pp. 1280-1288, 2007.

[31] R.M.Schiffelers, A.Ansari, J.Xu, Q.Zhou, Q.Tang, G.Storm, G.Molema, P.Y.Lu, P.V.Scaria, M.C.Woodle, "Cancer siRNA therapy by tumor selective delivery with ligand-targeted sterically stabilized nanoparticle," *Nucleic Acids Research,* vol. 32, no. 19, pp. e149, 2004.

[32] B.Urban-Klein, S.Werth, S.Abuharbeid, F.Czubayko, A.Aigner, "RNAi-mediated gene-targeting through systemic application of polyethylenimine (PEI)-complexed siRNA in vivo," *Gene Ther,* vol. 12, no. 5, pp. 461-466, 2004.

[33] Y.Patil, J.Panyam, "Polymeric nanoparticles for siRNA delivery and gene silencing," *International Journal of Pharmaceutics,* vol. 367, no. 1-2, pp. 195-203, 2009.

[34] S.M.Elbashir, J.Harborth, W.Lendeckel, A.Yalcin, K.Weber, T.Tuschl, "Duplexes of 21-nucleotide RNAs mediate RNA interference in cultured mammalian cells," *Nature,* vol. 411, no. 6836, pp. 494-498, 2001.

[35] F.Petrocca, J.Lieberman, "Promise and Challenge of RNA InterferenceGÇôBased Therapy for Cancer," *Journal of Clinical Oncology,* vol. 29, no. 6, pp. 747-754, 2011.

[36] D.Bumcrot, M.Manoharan, V.Koteliansky, D.W.Y.Sah, "RNAi therapeutics: a potential new class of pharmaceutical drugs," *Nat Chem Biol,* vol. 2, no. 12, pp. 711-719, 2006.

[37] B.Ozpolat, A.K.Sood, G.Lopez-Berestein, "Nanomedicine based approaches for the delivery of siRNA in cancer," *Journal of Internal Medicine,* vol. 267, no. 1, pp. 44-53, 2010.

[38] A.de Fougerolles, H.P.Vornlocher, J.Maraganore, J.Lieberman, "Interfering with disease: a progress report on siRNA-based therapeutics," *Nat Rev Drug Discov,* vol. 6, no. 6, pp. 443-453, 2007.

[39] G.L.Storvold, T.I.Andersen, C.M.Perou, E.Frengen, "siRNA: A Potential Tool for Future Breast Cancer Therapy?," *Critical Reviews in Oncogenesis,* vol. 12, no. 1-2, 2006.

[40] H.Zhang, X.Xie, X.Zhu, J.Zhu, C.Hao, Q.Lu, L.Ding, Y.Liu, L.Zhou, Y.Liu, C.Huang, C.Wen, Q.Ye, "Stimulatory Cross-talk between NFAT3 and Estrogen Receptor in Breast Cancer Cells," *Journal of Biological Chemistry,* vol. 280, no. 52, pp. 43188-43197, 2005.

[41] J.M.Rae, M.D.Johnson, J.O.Scheys, K.E.Cordero, J.M.Larios, M.E.Lippman, "GREB1 is a critical regulator of hormone dependent breast cancer growth," *Breast Cancer Research and Treatment,* vol. 92, no. 2, pp. 141-149, 2005.

[42] G.Yang, K.Q.Cai, J.A.Thompson-Lanza, R.C.Bast, J.Liu, "Inhibition of Breast and Ovarian Tumor Growth through Multiple Signaling Pathways by Using Retrovirus-mediated Small Interfering RNA against Her-2/neu Gene Expression," *Journal of Biological Chemistry,* vol. 279, no. 6, pp. 4339-4345, 2004.

[43] Q.Leng, A.J.Mixson, "Small interfering RNA targeting Raf-1 inhibits tumor growth in vitro and in vivo," *Cancer Gene Ther,* vol. 12, no. 8, pp. 682-690, 2005.

[44] J.Y.Pille, C.Denoyelle, J.Varet, J.R.Bertrand, J.Soria, P.Opolon, H.Lu, L.L.Pritchard, J.P.Vannier, C.Malvy, C.Soria, H.Li, "Anti-RhoA and Anti-RhoC siRNAs Inhibit the Proliferation and Invasiveness of MDA-MB-231 Breast Cancer Cells in Vitro and in Vivo," *Mol Ther,* vol. 11, no. 2, pp. 267-274, 2005.

[45] R.T.Lima, L.M.Martins, J.E.Guimaraes, C.Sambade, M.H.Vasconcelos, "Specific downregulation of bcl-2 and xIAP by RNAi enhances the effects of chemotherapeutic agents in MCF-7 human breast cancer cells," *Cancer Gene Ther,* vol. 11, no. 5, pp. 309-316, 2004.

[46] Y.Zhang, Y.Wang, W.Gao, R.Zhang, X.Han, M.Jia, W.Guan, "Transfer of siRNA against XIAP induces apoptosis and reduces tumor cells growth potential in human breast cancer <i>in vitro</i> and <i>in

vivo</i>" *Breast Cancer Research and Treatment,* vol. 96, no. 3, pp. 267-277, 2006.

[47] D.Xu, D.McCarty, A.Fernandes, M.Fisher, R.J.Samulski, R.L.Juliano, "Delivery of MDR1 Small Interfering RNA by Self-Complementary Recombinant Adeno-Associated Virus Vector," *Mol Ther,* vol. 11, no. 4, pp. 523-530, 2005.

[48] H.Wu, W.N.Hait, J.M.Yang, "Small Interfering RNA-induced Suppression of MDR1 (P-Glycoprotein) Restores Sensitivity to Multidrug-resistant Cancer Cells," *Cancer Research,* vol. 63, no. 7, pp. 1515-1519, 2003.

[49] J.M.Atienza, R.B.Roth, C.Rosette, K.J.Smylie, S.Kammerer, J.Rehbock, J.Ekblom, M.F.Denissenko, "Suppression of RAD21 gene expression decreases cell growth and enhances cytotoxicity of etoposide and bleomycin in human breast cancer cells," *Molecular Cancer Therapeutics,* vol. 4, no. 3, pp. 361-368, 2005.

[50] E.Lipscomb, A.Dugan, I.Rabinovitz, A.Mercurio, "Use of RNA interference to inhibit integrin (+¦6+¦4)-mediated invasion and migration of breast carcinoma cells," *Clinical and Experimental Metastasis,* vol. 20, no. 6, pp. 569-576, 2003.

[51] M.Ferrari, "Cancer nanotechnology: opportunities and challenges," *Nat Rev Cancer,* vol. 5, no. 3, pp. 161-171, 2005.

[52] R.Dhankhar, S.P.Vyas, A.K.Jain, S.Arora, G.Rath, A.K.Goyal, "Advances in Novel Drug Delivery Strategies for Breast Cancer Therapy," *Artificial Cells, Blood Substitutes and Biotechnology,* vol. 38, no. 5, pp. 230-249, 2010.

[53] M.L.Hans, A.M.Lowman, "Biodegradable nanoparticles for drug delivery and targeting," *Current Opinion in Solid State and Materials Science,* vol. 6, no. 4, pp. 319-327, 2002.

[54] C.Fonseca, S.Simões, R.Gaspar, "Paclitaxel-loaded PLGA nanoparticles: preparation, physicochemical characterization and in vitro anti-tumoral activity," *Journal of Controlled Release,* vol. 83, no. 2, pp. 273-286, 2002.

[55] M.Gaumet, A.Vargas, R.Gurny, F.Delie, "Nanoparticles for drug delivery: The need for precision in reporting particle size parameters," *European Journal of Pharmaceutics and Biopharmaceutics,* vol. 69, no. 1, pp. 1-9, 2008.

[56] J.Panyam, V.Labhasetwar, "Dynamics of Endocytosis and Exocytosis of Poly(D,L-Lactide-<i>co</i>-Glycolide) Nanoparticles in Vascular Smooth Muscle Cells," *Pharmaceutical Research,* vol. 20, no. 2, pp. 212-220, 2003.

[57] J.Panyam, V.Labhasetwar, "Biodegradable nanoparticles for drug and gene delivery to cells and tissue," *Advanced Drug Delivery Reviews,* vol. 55, no. 3, pp. 329-347, 2003.

[58] J.K.Vasir, V.Labhasetwar, "Biodegradable nanoparticles for cytosolic delivery of therapeutics," *Advanced Drug Delivery Reviews,* vol. 59, no. 8, pp. 718-728, 2007.

[59] M.P.Desai, V.Labhasetwar, E.Walter, R.J.Levy, G.L.Amidon, "The Mechanism of Uptake of Biodegradable Microparticles in Caco-2 Cells Is Size Dependent," *Pharmaceutical Research,* vol. 14, no. 11, pp. 1568-1573, 1997.

[60] M.Yun, M.Barnett, D.Takemoto, "Human serum albumin nanoparticles for efficient delivery of Cu, Zn superoxide dismutase gene," *Molecular Vision,* vol. 13, no. 2007.

[61] S.Bennis, C.Chapey, J.Robert, P.Couvreur, "Enhanced cytotoxicity of doxorubicin encapsulated in polyisohexylcyanoacrylate nanospheres against multidrug-resistant tumour cells in culture," *European Journal of Cancer,* vol. 30, no. 1, pp. 89-93, 1994.

[62] Y.Malam, M.Loizidou, A.M.Seifalian, "Liposomes and nanoparticles: nanosized vehicles for drug delivery in cancer," *Trends in Pharmacological Sciences,* vol. 30, no. 11, pp. 592-599, 2009.

[63] J.Panyam, V.Labhasetwar, "Biodegradable nanoparticles for drug and gene delivery to cells and tissue," *Advanced Drug Delivery Reviews,* vol. 55, no. 3, pp. 329-347, 2003.

[64] S.Parveen, S.K.Sahoo, "Polymeric nanoparticles for cancer therapy," *Journal of Drug Targeting,* vol. 16, no. 2, pp. 108-123, 2008.

[65] S.C.De Smedt, J.Demeester, W.E.Hennink, "Cationic Polymer Based Gene Delivery Systems," *Pharmaceutical Research,* vol. 17, no. 2, pp. 113-126, 2000.

[66] S.Parveen, S.K.Sahoo, "Polymeric nanoparticles for cancer therapy," *Journal of Drug Targeting,* vol. 16, no. 2, pp. 108-123, 2008.

[67] H.Maeda, J.Wu, T.Sawa, Y.Matsumura, K.Hori, "Tumor vascular permeability and the EPR effect in macromolecular therapeutics: a review," *Journal of Controlled Release,* vol. 65, no. 1-2, pp. 271-284, 2000.

[68] H.Maeda, "Tumor-Selective Delivery of Macromolecular Drugs via the EPR Effect: Background and Future Prospects," *Bioconjugate Chemistry,* vol. 21, no. 5, pp. 797-802, 2010.

[69] J.Fang, H.Nakamura, H.Maeda, "The EPR effect: Unique features of tumor blood vessels for drug delivery, factors involved, and limitations and augmentation of the effect," *Advanced Drug Delivery Reviews,* vol. 63, no. 3, pp. 136-151, 2011.

[70] Y.J.Son, J.S.Jang, Y.W.Cho, H.Chung, R.W.Park, I.C.Kwon, I.S.Kim, J.Y.Park, S.B.Seo, C.R.Park, S.Y.Jeong, "Biodistribution and anti-tumor efficacy of doxorubicin loaded glycol-chitosan nanoaggregates by EPR effect," *Journal of Controlled Release,* vol. 91, no. 1-2, pp. 135-145, 2003.

[71] F.Kratz, "Albumin as a drug carrier: Design of prodrugs, drug conjugates and nanoparticles," *Journal of Controlled Release,* vol. 132, no. 3, pp. 171-183, 2008.

[72] Y.Malam, M.Loizidou, A.M.Seifalian, "Liposomes and nanoparticles: nanosized vehicles for drug delivery in cancer," *Trends in Pharmacological Sciences,* vol. 30, no. 11, pp. 592-599, 2009.

[73] F.Kratz, "Albumin as a drug carrier: Design of prodrugs, drug conjugates and nanoparticles," *Journal of Controlled Release,* vol. 132, no. 3, pp. 171-183, 2008.

[74] N.Desai, V.Trieu, Z.Yao, L.Louie, S.Ci, A.Yang, C.Tao, T.De, B.Beals, D.Dykes, P.Noker, R.Yao, E.Labao, M.Hawkins, P.Soon-Shiong, "Increased antitumor activity, intratumor paclitaxel concentrations, and endothelial cell transport of cremophor-free, albumin-bound paclitaxel, ABI-007, compared with cremophor-based paclitaxel," *Clinical Cancer Research,* vol. 12, no. 4, pp. 1317-1324, 2006.

[75] S.Goble, H.D.Bear, "Emerging role of taxanes in adjuvant and neoadjuvant therapy for breast cancer: the potential and the questions," *The Surgical clinics of North America,* vol. 83, no. 4, pp. 943-971, 2003.

[76] H.Gelderblom, J.Verweij, K.Nooter, A.Sparreboom, "Cremophor EL: the drawbacks and advantages of vehicle selection for drug formulation," *European Journal of Cancer,* vol. 37, no. 13, pp. 1590-1598, 2001.

[77] S.Dreis, F.Rothweiler, M.Michaelis, J.Cinatl, J.Kreuter, K.Langer, "Preparation, characterisation and maintenance of drug efficacy of doxorubicin-loaded human serum albumin (HSA) nanoparticles," *International Journal of Pharmaceutics,* vol. 341, no. 1-2, pp. 207-214, 2007.

[78] K.Santhi, S.A.Dhanaraj, V.Joseph, S.Ponnusankar, B.Suresh, "A Study on the Preparation and Anti-Tumor Efficacy of Bovine Serum Albumin Nanospheres Containing 5-Fluorouracil," *Drug Development and Industrial Pharmacy,* vol. 28, no. 9, pp. 1171-1179, 2002.

[79] S.Sebak, M.Mirzaei, M.Malhotra, A.Kulamarva, S.Prakash, "Human serum albumin nanoparticles as an efficient noscapine drug delivery system for potential use in breast cancer: preparation and in vitro analysis," *International Journal of Nanomedicine,* vol. 2010, no. 5, pp. 525-532, 10 A.D.

[80] S.Das, R.Banerjee, J.Bellare, "Aspririn loaded Albumin Nanoparticles by Coacervation: Implications in Drug Delivery," *Trends in Biomaterials & Artificial Organs,* vol. 18, no. 2011.

[81] A.Khan, A.Paul, S.Abbasi, S.Prakash, " Mitotic and antiapoptotic effects of nanoparticles coencapsulating human VEGF and human angiopoietin 1 on vascular endothelial cells," *International Jounral of Nanomedicine,* vol. 6, no. 1, 2011.

[82] S.Zhang, M.R.Doschak, H.Uludag, "Pharmacokinetics and bone formation by BMP-2 entrapped in polyethylenimine-coated albumin nanoparticles," *Biomaterials,* vol. 30, no. 28, pp. 5143-5155, 2009.

[83] S.Zhang, C.Kucharski, M.R.Doschak, W.Sebald, H.Uludag, "Polyethylenimine-PEG coated albumin nanoparticles for BMP-2 delivery," *Biomaterials,* vol. 31, no. 5, pp. 952-963, 2010.

[84] I.Steinhauser, K.Langer, K.Strebhardt, B.Sp+ñnkuch, "Uptake of plasmid-loaded nanoparticles in breast cancer cells and effect on Plk1 expression," *Journal of Drug Targeting,* vol. 17, no. 8, pp. 627-637, 2009.

[85] S.Jin, K.Ye, "Nanoparticle-Mediated Drug Delivery and Gene Therapy," *Biotechnology Progress,* vol. 23, no. 1, pp. 32-41, 2007.

[86] H.Wartlick, B.SpSnkuch-Schmitt, K.Strebhardt, J.r.Kreuter, K.Langer, "Tumour cell delivery of antisense oligonuclceotides by human serum albumin nanoparticles," *Journal of Controlled Release,* vol. 96, no. 3, pp. 483-495, 2004.

[87] J.K.Vasir, V.Labhasetwar, "Biodegradable nanoparticles for cytosolic delivery of therapeutics," *Advanced Drug Delivery Reviews,* vol. 59, no. 8, pp. 718-728, 2007.

[88] H.M.Redhead, S.S.Davis, L.Illum, "Drug delivery in poly(lactide-co-glycolide) nanoparticles surface modified with poloxamer 407 and poloxamine 908: in vitro characterisation and in vivo evaluation," *Journal of Controlled Release,* vol. 70, no. 3, pp. 353-363, 2001.

[89] C.Perez, A.Sanchez, D.Putnam, D.Ting, R.Langer, M.J.Alonso, "Poly(lactic acid)-poly(ethylene glycol) nanoparticles as new carriers for the delivery of plasmid DNA," *Journal of Controlled Release,* vol. 75, no. 1-2, pp. 211-224, 2001.

[90] A.Verma, F.Stellacci, "Effect of Surface Properties on NanoparticleGÇôCell Interactions," *Small,* vol. 6, no. 1, pp. 12-21, 2010.

[91] J.Cho, F.Caruso, "Investigation of the Interactions between Ligand-Stabilized Gold Nanoparticles and Polyelectrolyte Multilayer Films," *Chemistry of Materials,* vol. 17, no. 17, pp. 4547-4553, 2005.

[92] P.R.Lockman, M.O.Oyewumi, J.M.Koziara, K.Roder, R.J.Mumper, D.D.Allen, "Brain uptake of thiamine-coated nanoparticles," *Journal of Controlled Release,* vol. 93, no. 12, pp. 271-282, 2003.

[93] S.K.Sahoo, W.Ma, V.Labhasetwar, "Efficacy of transferrin-conjugated paclitaxel-loaded nanoparticles in a murine model of prostate cancer," *International Journal of Cancer,* vol. 112, no. 2, 2004.

[94] M.Lundberg, S.Wikstrom, M.Johansson, "Cell Surface Adherence and Endocytosis of Protein Transduction Domains," *Mol Ther,* vol. 8, no. 1, pp. 143-150, 2003.

[95] B.S.Weeks, K.Desai, P.M.Loewenstein, M.E.Klotman, P.E.Klotman, M.Green, H.K.Kleinman, "Identification of a novel cell attachment domain in the HIV-1 Tat protein and its 90-kDa cell surface binding protein," *Journal of Biological Chemistry,* vol. 268, no. 7, pp. 5279-5284, 1993.

[96] C.Plank, W.Zauner, E.Wagner, "Application of membrane-active peptides for drug and gene delivery across cellular membranes," *Advanced Drug Delivery Reviews,* vol. 34, no. 1, pp. 21-35, 1998.

[97] V.P.Torchilin, R.Rammohan, V.Weissig, T.S.Levchenko, "TAT peptide on the surface of liposomes affords their efficient intracellular delivery even at low temperature and in the presence of metabolic inhibitors," *Proceedings of the National Academy of Sciences,* vol. 98, no. 15, pp. 8786-8791, 2001.

[98] K.S.Rao, M.K.Reddy, J.L.Horning, V.Labhasetwar, "TAT-conjugated nanoparticles for the CNS delivery of anti-HIV drugs," *Biomaterials,* vol. 29, no. 33, pp. 4429-4438, 2008.

[99] K.A.Janes, M.P.Fresneau, A.Marazuela, A.Fabra, M.c.a.a.Alonso, "Chitosan nanoparticles as delivery systems for doxorubicin," *Journal of Controlled Release,* vol. 73, no. 2-3, pp. 255-267, 2001.

[100] J.Park, P.M.Fong, J.Lu, K.S.Russell, C.J.Booth, W.M.Saltzman, T.M.Fahmy. PEGylated PLGA nanoparticles for the improved delivery of doxorubicin. Nanomedicine : nanotechnology, biology, and medicine 5(4), 410-418. 1-12-2009.
Ref Type: Abstract

[101] S.Dreis, F.Rothweiler, M.Michaelis, J.Cinatl, J.Kreuter, K.Langer, "Preparation, characterisation and maintenance of drug efficacy of doxorubicin-loaded human serum albumin (HSA) nanoparticles," *International Journal of Pharmaceutics,* vol. 341, no. 1-2, pp. 207-214, 2007.

[102] S.Zhang, B.Zhao, H.Jiang, B.Wang, B.Ma, "Cationic lipids and polymers mediated vectors for delivery of siRNA," *Journal of Controlled Release,* vol. 123, no. 1, pp. 1-10, 2007.

[103] S.Mao, W.Sun, T.Kissel, "Chitosan-based formulations for delivery of DNA and siRNA," *Advanced Drug Delivery Reviews,* vol. 62, no. 1, pp. 12-27, 2010.

[104] G.R.Devi, "siRNA-based approaches in cancer therapy," *Cancer Gene Ther,* vol. 13, no. 9, pp. 819-829, 2006.

[105] S.Jin, K.Ye, "Nanoparticle-Mediated Drug Delivery and Gene Therapy," *Biotechnology Progress,* vol. 23, no. 1, pp. 32-41, 2007.

[106] D.R.S°rensen, M.Leirdal, M.Sioud, "Gene Silencing by Systemic Delivery of Synthetic siRNAs in Adult Mice," *Journal of Molecular Biology,* vol. 327, no. 4, pp. 761-766, 2003.

[107] A.Jemal, R.Siegel, J.Xu, E.Ward, "Cancer Statistics, 2010," *CA: A Cancer Journal for Clinicians,* pp. caac, 2010.

[108] M.L.Hans, A.M.Lowman, "Biodegradable nanoparticles for drug delivery and targeting," *Current Opinion in Solid State and Materials Science,* vol. 6, no. 4, pp. 319-327, 2002.

[109] N.Templeton, D.Lasic, "New directions in liposome gene delivery," *Molecular Biotechnology,* vol. 11, no. 2, pp. 175-180, 1999.

[110] M.Gaumet, A.Vargas, R.Gurny, F.Delie, "Nanoparticles for drug delivery: The need for precision in reporting particle size parameters," *European Journal of Pharmaceutics and Biopharmaceutics,* vol. 69, no. 1, pp. 1-9, 2008.

[111] Panyam and Labhasetwar, "Dynamics of Endocytosis and Exocytosis of Poly(D,L-Lactide-co-Glycolide) Nanoparticles in Vascular Smooth Muscle Cells," *Pharmaceutical Research,* vol. 20, no. 2, pp. 212-220, 2003.

[112] G.Wang, K.Siggers, S.Zhang, H.Jiang, Z.Xu, R.Zernicke, J.Matyas, H.Uluda-¦, "Preparation of BMP-2 Containing Bovine Serum Albumin (BSA) Nanoparticles Stabilized by Polymer Coating," *Pharmaceutical Research,* vol. 25, no. 12, pp. 2896-2909, 2008.

[113] J.M.L++, X.Wang, C.Marin-Muller, H.Wang, P.H.Lin, Q.Yao, C.Chen, "Current advances in research and clinical applications of PLGA-based nanotechnology," *Expert Review of Molecular Diagnostics,* vol. 9, no. 4, pp. 325-341, 2009.

[114] Y.Liu, H.Miyoshi, M.Nakamura, "Nanomedicine for drug delivery and imaging: A promising avenue for cancer therapy and diagnosis using targeted functional nanoparticles," *International Journal of Cancer,* vol. 120, no. 12, pp. 2527-2537, 2007.

[115] W.Lin, A.G.A.Coombes, M.C.Davies, S.S.Davis, L.Illum, "Preparation of Sub-100 nm Human Serum Albumin Nanospheres Using a pH-Coacervation Method," *Journal of Drug Targeting,* vol. 1, no. 3, pp. 237-243, 1993.

[116] K.Langer, S.Balthasar, V.Vogel, N.Dinauer, H.von Briesen, D.Schubert, "Optimization of the preparation process for human serum albumin (HSA) nanoparticles," *International Journal of Pharmaceutics,* vol. 257, no. 1-2, pp. 169-180, 2003.

[117] J.Douglas, "Adenoviral vectors for gene therapy," *Molecular Biotechnology,* vol. 36, no. 1, pp. 71-80, 2007.

[118] S.A.Vorburger, K.K.Hunt, "Adenoviral Gene Therapy," *The Oncologist,* vol. 7, no. 1, pp. 46-59, 2002.

[119] A.Paul, B.Jardin, A.Kulamarva, M.Malhotra, C.Elias, S.Prakash, "Recombinant Baculovirus as a Highly Potent Vector for Gene Therapy of Human Colorectal Carcinoma: Molecular Cloning, Expression, and In Vitro Characterization," *Molecular Biotechnology,* vol. 45, no. 2, pp. 129-139, 2010.

[120] R.Arshady, "Albumin microspheres and microcapsules: Methodology of manufacturing techniques," *Journal of Controlled Release,* vol. 14, no. 2, pp. 111-131, 1990.

[121] E.Leo, M.Angela Vandelli, R.Cameroni, F.Forni, "Doxorubicin-loaded gelatin nanoparticles stabilized by glutaraldehyde: Involvement of the drug in the cross-linking process," *International Journal of Pharmaceutics,* vol. 155, no. 1, pp. 75-82, 1997.

[122] S.Segura, S.Espuelas, M.a.J.s.Renedo, J.M.Irache, "Potential of Albumin Nanoparticles as Carriers for Interferon Gamma," *Drug Development and Industrial Pharmacy,* vol. 31, no. 3, pp. 271-280, 2005.

[123] S.Zhang, G.Wang, X.Lin, M.Chatzinikolaidou, H.P.Jennissen, M.Laub, H.Uluda-¦, "Polyethylenimine-coated albumin nanoparticles for BMP-2 delivery," *Biotechnology Progress,* vol. 24, no. 4, pp. 945-956, 2008.

[124] S.Rhaese, H.von Briesen, H.R³bsamen-Waigmann, J.r.Kreuter, K.Langer, "Human serum albumin-polyethylenimine nanoparticles for gene delivery," *Journal of Controlled Release,* vol. 92, no. 1-2, pp. 199-208, 2003.

[125] K.Yin Win, S.S.Feng, "Effects of particle size and surface coating on cellular uptake of polymeric nanoparticles for oral delivery of anticancer drugs," *Biomaterials,* vol. 26, no. 15, pp. 2713-2722, 2005.

[126] I.M.Helander, H.L.Alakomi, K.Latva-Kala, P.Koski, "Polyethyleneimine is an effective permeabilizer of Gram-negative bacteria," *Microbiology,* vol. 143, no. 10, pp. 3193-3199, 1997.

[127] W.Zauner, N.A.Farrow, A.M.R.Haines, "In vitro uptake of polystyrene microspheres: effect of particle size, cell line and cell density," *Journal of Controlled Release,* vol. 71, no. 1, pp. 39-51, 2001.

[128] S.Abbasi, A.Paul, S.Prakash, "Investigation of siRNA-Loaded Polyethylenimine-Coated Human Serum Albumin Nanoparticle Complexes for the Treatment of Breast Cancer," *Cell Biochemistry and Biophysics,* pp. 1-11, 2011.

[129] S.Sebak, M.Mirzaei, M.Malhotra, A.Kulamarva, S.Prakash, "Human serum albumin nanoparticles as an efficient noscapine drug delivery system for potential use in breast cancer: preparation and in vitro analysis," *International Journal of Nanomedicine,* vol. 2010, no. 5, pp. 525-532, 10 A.D.

[130] C.Weber, J.Kreuter, K.Langer, "Desolvation process and surface characteristics of HSA-nanoparticles," *International Journal of Pharmaceutics,* vol. 196, no. 2, pp. 197-200, 2000.

[131] P.K.Singal, N.Iliskovic, "Doxorubicin-Induced Cardiomyopathy," *New England Journal of Medicine,* vol. 339, no. 13, pp. 900-905, 1998.

[132] P.Singal, T.Li, D.Kumar, I.Danelisen, N.Iliskovic, "Adriamycin-induced heart failure: mechanisms and modulation," *Molecular and Cellular Biochemistry,* vol. 207, no. 1, pp. 77-86, 2000.

[133] S.Dreis, F.Rothweiler, M.Michaelis, J.Cinatl, J.Kreuter, K.Langer, "Preparation, characterisation and maintenance of drug efficacy of doxorubicin-loaded human serum albumin (HSA) nanoparticles," *International Journal of Pharmaceutics,* vol. 341, no. 1-2, pp. 207-214, 2007.

[134] M.L.Hans, A.M.Lowman, "Biodegradable nanoparticles for drug delivery and targeting," *Current Opinion in Solid State and Materials Science,* vol. 6, no. 4, pp. 319-327, 2002.

[135] A.E.Gulyaev, S.E.Gelperina, I.N.Skidan, A.S.Antropov, G.Y.Kivman, J.+.Kreuter, "Significant Transport of Doxorubicin into the Brain with Polysorbate 80-Coated Nanoparticles," *Pharmaceutical Research,* vol. 16, no. 10, pp. 1564-1569, 1999.

[136] C.Cuvier, L.Roblot-Treupel, J.M.Millot, G.Lizard, S.Chevillard, M.Manfait, P.Couvreur, M.F.Poupon, "Doxorubicin-loaded nanospheres bypass tumor cell multidrug resistance," *Biochemical Pharmacology,* vol. 44, no. 3, pp. 509-517, 1992.

[137] E.Leo, M.Angela Vandelli, R.Cameroni, F.Forni, "Doxorubicin-loaded gelatin nanoparticles stabilized by glutaraldehyde: Involvement of the drug in the cross-linking process," *International Journal of Pharmaceutics,* vol. 155, no. 1, pp. 75-82, 1997.

[138] A.N.Lukyanov, T.A.Elbayoumi, A.R.Chakilam, V.P.Torchilin, "Tumor-targeted liposomes: doxorubicin-loaded long-circulating liposomes modified with anti-cancer antibody," *Journal of Controlled Release,* vol. 100, no. 1, pp. 135-144, 2004.

[139] F.Kratz, "Albumin as a drug carrier: Design of prodrugs, drug conjugates and nanoparticles," *Journal of Controlled Release,* vol. 132, no. 3, pp. 171-183, 2008.

[140] S.B.Feinstein, J.Cheirif, F.J.Ten Cate, P.R.Silverman, P.A.Heidenreich, C.Dick, R.M.Desir, W.F.Armstrong, M.A.Quinones, P.M.Shah, "Safety and efficacy of a new transpulmonary ultrasound contrast agent: Initial multicenter clinical results," *Journal of the American College of Cardiology,* vol. 16, no. 2, pp. 316-324, 1990.

[141] N.K.Ibrahim, N.Desai, S.Legha, P.Soon-Shiong, R.L.Theriault, E.Rivera, B.Esmaeli, S.E.Ring, A.Bedikian, G.N.Hortobagyi, J.A.Ellerhorst, "Phase I and Pharmacokinetic Study of ABI-007, a Cremophor-free, Protein-stabilized, Nanoparticle Formulation of Paclitaxel," *Clinical Cancer Research,* vol. 8, no. 5, pp. 1038-1044, 2002.

[142] A.Kichler, "Gene transfer with modified polyethylenimines," *The Journal of Gene Medicine,* vol. 6, no. S1, pp. S3-S10, 2004.

[143] S.Abbasi, A.Paul, S.Prakash, "Investigation of siRNA-Loaded Polyethylenimine-Coated Human Serum Albumin Nanoparticle Complexes for the Treatment of Breast Cancer," *Cell Biochemistry and Biophysics*, pp. 1-11, 2011.

[144] K.Langer, S.Balthasar, V.Vogel, N.Dinauer, H.von Briesen, D.Schubert, "Optimization of the preparation process for human serum albumin (HSA) nanoparticles," *International Journal of Pharmaceutics,* vol. 257, no. 1-2, pp. 169-180, 2003.

[145] A.Khan, A.Paul, S.Abbasi, S.Prakash, " Mitotic and antiapoptotic effects of nanoparticles coencapsulating human VEGF and human angiopoietin 1 on vascular endothelial cells," *International Jounral of Nanomedicine,* vol. 6, no. 1, 2011.

[146] F.M.Menger, B.M.Sykes, "Anatomy of a Coacervate," *Langmuir,* vol. 14, no. 15, pp. 4131-4137, 1998.

[147] W.Lin, A.Coombes, M.Davies, S.Davis, L.Illum, "Preparation of Sub-100 nm Human Serum Albumin Nanospheres Using a pH-Coacervation Method," *Journal of Drug Targeting,* vol. 1, no. 3, pp. 237-243, 1993.

[148] H.D.Singh, G.Wang, H.Uludag, L.D.Unsworth, "Poly-l-lysine-coated albumin nanoparticles: Stability, mechanism for increasing in vitro enzymatic resilience,

and siRNA release characteristics," *Acta Biomaterialia,* vol. 6, no. 11, pp. 4277-4284, 2010.

[149] S.Prabha, W.Z.Zhou, J.Panyam, V.Labhasetwar, "Size-dependency of nanoparticle-mediated gene transfection: studies with fractionated nanoparticles," *International Journal of Pharmaceutics,* vol. 244, no. 1-2, pp. 105-115, 2002.

[150] O.Harush-Frenkel, E.Rozentur, S.Benita, Y.Altschuler, "Surface Charge of Nanoparticles Determines Their Endocytic and Transcytotic Pathway in Polarized MDCK Cells," *Biomacromolecules,* vol. 9, no. 2, pp. 435-443, 2008.

[151] A.C.Hunter, "Molecular hurdles in polyfectin design and mechanistic background to polycation induced cytotoxicity," *Advanced Drug Delivery Reviews,* vol. 58, no. 14, pp. 1523-1531, 2006.

[152] N.Tietze, J.Pelisek, A.Philipp, W.Roedl, T.Merdan, P.Tarcha, M.Ogris, E.Wagner, "Induction of Apoptosis in Murine Neuroblastoma by Systemic Delivery of Transferrin-Shielded siRNA Polyplexes for Downregulation of Ran," *Oligonucleotides,* vol. 18, no. 2, pp. 161-174, 2008.

[153] P.K.Singal, N.Iliskovic, "Doxorubicin-Induced Cardiomyopathy," *New England Journal of Medicine,* vol. 339, no. 13, pp. 900-905, 1998.

[154] J.C.Cheng, T.B.Moore, K.M.Sakamoto, "RNA interference and human disease," *Molecular Genetics and Metabolism,* vol. 80, no. 1-2, pp. 121-128, 2009.

[155] M.Malhotra, A.Kulamarva, S.Sebak, A.Paul, J.Bhathena, M.Mirzaei, S.Prakash, "Ultrafine chitosan nanoparticles as an efficient nucleic acid delivery system targeting neuronal cells," *Drug Development and Industrial Pharmacy,* vol. 35, no. 6, pp. 719-726, 2009.

[156] S.Zhang, B.Zhao, H.Jiang, B.Wang, B.Ma, "Cationic lipids and polymers mediated vectors for delivery of siRNA," *Journal of Controlled Release,* vol. 123, no. 1, pp. 1-10, 2007.

[157] W.Lin, A.Coombes, M.Davies, S.Davis, L.Illum, "Preparation of Sub-100 nm Human Serum Albumin Nanospheres Using a pH-Coacervation Method," *Journal of Drug Targeting,* vol. 1, no. 3, pp. 237-243, 1993.

[158] E.Vives, P.Brodin, B.Lebleu, "A Truncated HIV-1 Tat Protein Basic Domain Rapidly Translocates through the Plasma Membrane and Accumulates in the Cell Nucleus," *Journal of Biological Chemistry,* vol. 272, no. 25, pp. 16010-16017, 1997.

[159] S.Akhtar, "Cationic nanosystems for the delivery of small interfering ribonucleic acid therapeutics: a focus on toxicogenomics," *Expert Opinion on Drug Metabolism & Toxicology,* vol. 6, no. 11, pp. 1347-1362, 2010.

[160] S.Akhtar , I.F.Benter, "Nonviral delivery of synthetic siRNAs in vivo," *The Journal of Clinical Investigation,* vol. 117, no. 12, pp. 3623-3632, 2007.

[161] Y.Malam, M.Loizidou, A.M.Seifalian, "Liposomes and nanoparticles: nanosized vehicles for drug delivery in cancer," *Trends in Pharmacological Sciences,* vol. 30, no. 11, pp. 592-599, 2009.

[162] S.Akhtar, I.Benter, "Toxicogenomics of non-viral drug delivery systems for RNAi: Potential impact on siRNA-mediated gene silencing activity and specificity," *Advanced Drug Delivery Reviews,* vol. 59, no. 2-3, pp. 164-182, 2007.

[163] A.L.Jackson, P.S.Linsley, "Recognizing and avoiding siRNA off-target effects for target identification and therapeutic application," *Nat Rev Drug Discov,* vol. 9, no. 1, pp. 57-67, 2010.

[164] L.Hyndman, J.L.Lemoine, L.Huang, D.J.Porteous, A.C.Boyd, X.Nan, "HIV-1 Tat protein transduction domain peptide facilitates gene transfer in combination with cationic liposomes," *Journal of Controlled Release,* vol. 99, no. 3, pp. 435-444, 2004.

[165] J.Douglas, "Adenoviral vectors for gene therapy," *Molecular Biotechnology,* vol. 36, no. 1, pp. 71-80, 2007.

[166] M.Lundberg, S.Wikstrom, M.Johansson, "Cell Surface Adherence and Endocytosis of Protein Transduction Domains," *Mol Ther,* vol. 8, no. 1, pp. 143-150, 2003.

[167] H.Chen, W.Ouyang, M.Jones, T.Haque, B.Lawuyi, S.Prakash, "In-vitro analysis of APA microcapsules for oral delivery of live bacterial cells," *Journal of Microencapsulation,* vol. 22, no. 5, pp. 539-547, 2005.